Università del Piemonte Orientale "Amedeo Avogadro"

MerckSerono S.A. Ivrea, Italy

In vivo Pharmacology Department

PhD Dissertation in Molecular Medicine

by

Claudia Patrignani

"Characterization of PTPH1-KO mice in healthy and diseased conditions"

MerckSerono Supervisors: Academic Supervisor:

Maria Chiara Magnone   **Prof. Andrea Graziani**
and
Valeria Muzio

Academic Year 2009/2010

Abstract

The present study has widely investigated the protein tyrosine phosphatase H1 (PTPH1) expression pattern and impact throught the characterization of a functional PTPH1-KO mouse. We mainly focused on three topics: growth, neurological functions and immunological response.

We found that mice lacking the PTPH1 catalytic domain showed significantly enhanced growth over wild-type littermates. In addition, PTPH1 mutant animals showed enhanced plasma and liver mRNA expression of Insulin-like Growth Factor (IGF-1), as well as increased bone density and mineral content, all consistent with a natural role for PTPH1 in desensitizing GHR signaling.

In CNS, PTPH1 is known to be expressed during development and in adulthood and mainly localized in hippocampus, thalamus, cortex and cerebellum neurons. Our goal was to verify this statement and to evaluate PTPH1 potential effect on neurological functions. Therefore, PTPH1 expression pattern was evaluated by LacZ staining in the brain and PTPH1-KO and WT mice were also behaviorally tested for CNS functions. The behavioral tests performed on the PTPH1-KO mice showed an impact on working memory in male mice and an impaired learning performance at rotarod in females. These results demonstrate for the first time a neuronal expression of PTPH1, in particular mainly in GABAergic neurons, and its functionality at the level of cognition. Furthermore, superarray studies on PTPH1-KO and WT mouse cortices and hippocampi identified cholecistokinin A receptor (CCKAR) as a potential tanget of PTPH1. This gene was upregulated in the cortex of female PTPH1-KO mice compared to matched WTs, but no difference in its protein expression was detected by histological evaluation. The modulation of CCKAR gene in the cortex could be responsible for the effect on cognition of PTPH1-KO female mice, but further studies are needed to corroborate this hypothesis.

In addition, it is reported that PTPH1 is expressed in T cells and but its effect on immune response is still controversial. PTPH1 dephosphorylates TCRζ *in vitro*, inhibiting the downstream inflammatory pathway, but no immunological phenotype has been detected in primary T cells derived from PTPH1-KO mice. We challenged PTPH1-KO mice with carrageenan and LPS, two potent immunomodulatory molecules, to determine PTPH1 role in innate immune response *in vivo*. The present study shows that carrageenan induces a trend of slight increase in spontaneous pain sensitivity in PTPH1-KO mice compared to WT littermates, but no differences in cytokine release, in induced pain perception and in cellular infiltration were detected between the two genotypes.

Comparatively in the LPS model, TNFα, MCP-1 and IL10 release were significantly reduced in PTPH1-KO plasma compared to WTs after 30 and 60 minutes post challenge. The KO cytokine levels returned comparable to WTs at 180 minutes post LPS injection. In conclusion, the present study points out a slight potential role for PTPH1 in spontaneous pain sensitivity and it indicates that this phosphatase might play a role in the positive regulation of the LPS-induced cytokines release *in vivo*, in contrast to previous reports indicating PTPH1 as potential negative regulator of immune response.

In summary, the present study provides new information about how PTPH1 affects CNS functions, body growth and immune response and further helps the understanding of tyrosine phosphorylation impact on these processes, pointing out novel pathways and novel potential targets and strategies.

Aknowledgements

First, I would like to thank Maria Chiara Magnone, who gave me the chance to work and learn from her for two years. I am deeply thankful to Chiara for being an inspiring teacher, for her never-ending new ideas, optimism and encouragement: she taught me to look at my experiments with a critical view, to look beyond my results and to take advantage of my enthusiasm. Chiara also taught me what it means being a generous person. She was and remains my best role model for a scientist and mentor.

Special thanks go out to Valeria Muzio that helped me in the last two years of my PhD. Thank you Valeria for letting me free to walk thought my experiments on my own and for always being there when I needed you. I would also like to thank Béatrice Gréco for the stimulating brainstormming and for her patience in teaching me how to write my own article: now I know that *"writing is hard, editing is harder!"*. Thanks to Paola Zaratin for appreciating my enthusiasm: *"Yes, I like my project!"*. I am grateful to Fabien Richard and Mara Fortunato for teaching me all the secrets on RT-PCR. Thanks to Monique Van den Eijden for the stimulating collaboration and to Rob Hooft for his fruitful input and for critical reviewing my manuscripts.

I am very grateful to Sonia Carboni for her friendship, for the time spent together at the miscroscope, for her advices at any time, but especially during coffee break, and finally for her wonderful tartiflette. I would like to thank Daniela, Vittoria and Chiara for being the best "office neighbours" ever, and for having make immunology simple and easy to me. You'll always be my "only and reliable immunologists" and I'll miss our scientific lunch. A special thank to Patrizia Tavano, a pillar for our lab, never-ending source of precious advices from WB to CBA, always there to help and to get coffee together.

I also thank all the friends who make funny working in the lab, with their camaraderie and teamwork: Miriam Canavese, Piercesare Balestra, Elena Brini, Gabriele Dati, Roberto Ferrero, Flavio Boin, Tiziana Fraone, Lucia D'Avino, Aldo Martucci and Graziella Casu. It has been amazing working with you. Thanks to all our technicians for training me and helping me with my little animals. You have been indispensable.

I would also like to thank Prof. Andrea Graziani, for his critical input and for giving me the chance to work with his great biochemists: thank to Paolo, Federica, Nicoletta and Elena, for teaching me all the tricks of siRNA and for letting me breath the academic spirit!

A good support system is important to surviving and staying sane during the years of PhD. Thus, I would especially like to acknowledge all the friends that make my life easier and funnier

outside the lab. Thank to Patrizia, Silvia, Licia, Angelo, Simona, Pier, Ornella, Olga, Barbara, Rocco, Veronica, Marianna "Pacciani" Sabetta, Niccolò "Tutti i giorni" Chiambretti and Elena for all the past adventures and the future ones. A special thank to Tommy and Paola, for letting me discover Turin, its magic, its beauties and especially its mountains. Thank you also for letting me cuddle your little Gimba!

I would also like to thank all my friends "at home", my supporters since old times. A big hug to Francesca, Claudia, Lotty and Anto for the long phone calls and funny coffee/tea times. I'll never forget Simonetta, for coming here to far and cold Piedmont. I wish you could have stayed longer, like old times in Bologna. And I was very lucky in finding two very good friends already in high school. Thank you Sara and Fedy for all the great moments together, for letting me be part of your life even if I was faraway and thank you for being the most supportive and caring friends ever!

I especially thank my family for their support during my Ph.D. work. My grandparents, uncles and cousins for being a never-ending source of positive energy for me, you're great! My parents that have always believed in me and told me that I was capable of anything I set my mind to and that it is always worthy to do things at my best. They've been a great encouragement to me, even if my mom still thinks a "knockout mouse" is an especially fluorescent rodent. My brother Teo, who relieved my desesperation any time my pc gave me strange messages, who always took interest in my project…thank you for always being my great little brother! My sister Francesca, who is always able to make me lagh with her energy and enthusiasm for life: you got the secret darling!

And at least but not last, a special thank to my Dimi, for his love, help and patience as I've worked through these research years. Thank you for always answering my questions on dilutions and "numbers", for the rehearsal of my poster and presentations and for spending nights trying to understand what a tyrosin-phopshatase was. You have believed in me and reassured me many times when I was ready to give up. I don't know how I'd have done it without you.

Ringraziamenti

La prima persona che vorrei ringraziare è Maria Chiara Magnone per avermi scelto come compagna di viaggio e per avermi dato la possibilità di lavorare con lei per ben due anni. Chiara è una ricercatrice brillante e un mentore paziente. Mi ha insegnato ad analizzare in modo critico i miei esperimenti, a vedere oltre i miei risultati ed a sfruttare in modo proficuo i miei slanci di entusiasmo. Lavorare con Chiara mi ha insegnato tanto anche personalmente, facendomi capire cosa significa essere una persona generosa. Chiara era e rimane un esempio per me! Un grande grazie a Valeria Muzio, che mi ha seguito per gli ultimi due lunghi anni di dottorato. Grazie Vale per avermi lasciata libera di camminare con le mie gambe in laboratorio e per esserci sempre stata ogni volta che sono inciampata.

Un grazie speciale anche a Béatrice Gréco per gli stimolanti brainstorming e per la pazienza nell'insegnarmi a scrivere un articolo scientifico: ora so che *"writing is hard, editing is harder!"*. Grazie a Paola Zaratin per aver apprezzato il mio entusiasmo: *"Yes, I like my project!"*. Grazie a Fabien Richard e Mara Fortunato per avermi insegnato tutti i segreti della RT-PCR. Un ringraziamento a Monique van den Eijden per la sua collaborazione e Rob Hooft per la sua disponibilità ed anche per aver revisionato i miei articoli.

Un grande grazie anche a Sonia per l'amicizia, per il tempo passato insieme al microscopio e per i consigli dati in qualunque momento, soprattutto in pausa caffè e grazie sopratutto per la tartiflette. A Daniela, Vittoria e Chiara per essere state delle "vicine d'ufficio" fantastiche e per aver reso più semplice l'immunologia per me: sarete sempre le mie "immunologhe di fiducia" e mi mancheranno i nostri "pranzi scientifici". Un grazie particolare a Patrizia Tavano, pilastro del laboratorio e fonte inesauribile di consigli preziosi dal WB al CBA, sempre disponibile per un aiuto ed un caffè.

Un ringraziamento speciale anche a coloro che hanno reso piacevole lavorare in laboratorio: Miriam Canavese, David La Font, Elena Brini, Gabriele Dati, Roberto Ferrero, Flavio Boin, Tiziana Fraone, Lucia D'Avino, Aldo Martucci e Graziella Casu. E' stato bello lavorare a fianco a voi!Grazie anche a tutti i tecnici del laboratorio che mi hanno insegnato ed aiutato a lavorare con gli animali.

Vorrei anche ringraziare il Prof Andrea Graziani per i suoi consigli e per avermi dato la possibilità di lavorare con i suoi "biochimici": grazie a Paolo, Federica, Nicoletta ed Elena, per avermi insegnato con pazienza i trucchi del siRNA e per avermi fatto respirare aria di Università!

Ed ora un grande ringraziamento va a quelle persone che hanno reso più facile la mia vita fuori dal laboratorio, in una terra che non è la mia e che sono state la mia valvola di sfogo e la mia fonte di energia.

Grazie quindi agli amici e abitanti della Grande Sorella, di tutte le "annate". A Patrizia, per essere stata la mia fidata compagna di caffè per quasi 2 anni; a Silvia, ti voglio bene nonostante i broccoli ed il tuo nuovo accento milanese; a Barbara che sa apprezzare come me un panino con la porchetta; a Licia ed Angelo per avermi introdotto nel magico mondo della raclette e per esserci stati sempre quando la caldaia ha fatto le bizze.

Un grazie speciale anche agli amici, che hanno creduto in me ed alcuni col tempo sono diventati anche "colleghi". A Simona, che mi ha fatto scoprire ed apprezzare il canavese, che non è la Romagna, ma che ha margini di miglioramento. A Pier, per la sua risposta sempre pronta e per avermi fatto ridere sempre sia in lab che fuori. A Ornella che mi ha mostrato la vera ospitalità piemontese. A Olga, ora anche vicina di casa. A Rocco, Veronica, Marianna "Pacciani" Sabetta e Niccolò "Tutti i giorni" Chiambretti per le risate inaspettate. A Elena con cui condivido la stessa passione per lo zapping e per i reality e che mi ha introdotto nel magico mondo QA.

Un ringraziamento particolare sento di doverlo a due amici che ci sono sempre stati, che mi hanno dato ripetizioni di chimica, che mi hanno accolto di notte quando ero in lacrime per una borsa lasciata sul treno, che mi hanno fatto scoprire le magie di Torino e le bellezze dello sci, per essere compagni di camminate, concerti (forza Laura!) chiacchiere e sciate (anche se fatico a stargli dietro): grazie di tutto Paola e Tommy, anche per lasciarmi coccolare la piccola Ginevra.

Certo non sarei mai arrivata fino a qui, senza tutti gli amici che mi hanno sostenuto fin da tempi non sospetti. Grazie a tutto il nutrito gruppo di supporters romagnoli.

Grazie a Francesca per il vicendevole scambio di sfoghi davanti ad una camomilla fumante: io per il dottorato e lei per la tesi di laurea. Grazie a Claudia per riuscire a ridimensionare la mia confusione mentale, per capire i miei lunghi silenzi e per esserci sempre per me, soprattutto nei momenti difficili. Grazie a Simonetta, per essere arrivata fin quassù per sostenermi: avrei voluto potessi lasciare Riccione e trasferirti qui in onore dei vecchi tempi. Grazie a Lotty ed Anto, per le chiacchierate davanti al caffè, per le lunghe telefonate e la comune passione per "Un posto al sole": i chilometri non contano.

Un grazie particolare a Federica e Sara, per tutti i bei momenti, per lasciarmi camminare a fianco a voi anche a distanza e per essere un continuo sprono a seguire i miei sogni: vi voglio bene amiche mie, siete speciali!

Un grazie di cuore va alla mia famiglia. Ai miei nonni, zii e cugini che sono un'inesauribile fonte di energia positiva per me, siete fantastici! Ai miei genitori. Mi avete insegnato a credere in me stessa, a capire che se voglio davvero qualcosa basta solo impegnarsi per otternerlo e che quando ci si impegna in un progetto, vale sempre la pena di farlo al massimo delle proprie capacità. Mi avete sempre incoraggiato, anche se la mamma pensa ancora che il mio topo knock-out sia un topo fluorescente. A Teo, per aver placato la mia disperazione davanti a qualche strano messaggio del computer, per aver ascoltato i dettagli del mio progetto ed essere sempre il mio grande fratellino. Alla Fra, perché riesci sempre a strapparmi un sorriso con la tua energia ed il tuo entusiasmo per la vita: tu hai capito tutto sorellina! Vi voglio bene!

Un ultimo ma non meno importante abbraccio per l'aiuto ed il sostegno che mi ha dato in questi anni va a Dimi. Grazie Dimi, per aver sopportato le mie domande su diluizioni e numeri di animali, per aver ascoltato i miei poster e le mie presentazioni e per aver passato le serate cercando di capire cos'è una tirosin-fosfatasi. Grazie per avermi sostenuto e creduto in me, quando ero pronta a gettare la spugna. Non so cosa avrei fatto senza di te. Abbiamo passato tanti momenti, belli e meno belli, in questi quattro anni di dottorato. Abbiamo sbagliato molto entrambi, ma abbiamo saputo sostenerci a vicenda e sarà banale, ma ora siamo più vicini e forti.

Grazie di cuore, a Tutti.

Table of Contents

Chapter 1: Introduction

1.1. Overview of Literature

Overview on Protein Tyrosine Phosphatases

Tyrosine phosphorylation plays an important role in regulating fundamental aspects of eukaryote physiology and human diseases [1]. Although tyrosine phosphorylation accounts for only the 0.01% to 0.05% of the total protein phosphorylation[2], this process is fundamental in several signaling pathways controlling cell growth, differentiation, cell cycle, apoptosis and neuronal functions [3,4].

The phosphorylation/dephosphorylation balance is controlled by protein tyrosine kinases and phosphatases. Like PTKs, PTPs represent a large family of enzymes and can exert positive and negative effects on crucial physiological processes and can be mainly distinguished into four classes (Fig. 1).

Class I PTPs are also called classical PTPs and can be divided into transmembrane, receptor-like enzymes, and the intracellular, nonreceptor PTPs. The class II is composed by dual-specificity PTPs (Ser and Tyr phosphatases), class III includes low molecular weight PTP and class IV the Asp-based PTPs (Tyr/Ser phosphatase activity) (Fig. 1) [1].

PTPs family proteins display a high structural diversity and complexity. Besides the presence of a conserved catalytic site, a wide range of structural domains, as SH2 domains, PDZ, FERM and ligand-binding domains characterizes PTPs.

Fig. 1: Domain Structure of All PTPs from Alonso et al. [1]. Schematic view of the domain composition of all members of the four PTP families, which are in color coded areas. Abbreviations: coil, coiled-coil domain; GB, glycogen binding; mRC, mRNA capping; PBM, PDZ binding motif; pepN, N-terminal peptidase-like; PH-G, pleckstrin homology-"GRAM" domain; Pro-rich, proline-rich; Sec14, Sec14p homology (or CRAL/TRIO). In addition, a small black box signifies transmembrane stretch and a red cross over a PTP domain signifies catalytically inactive domain.
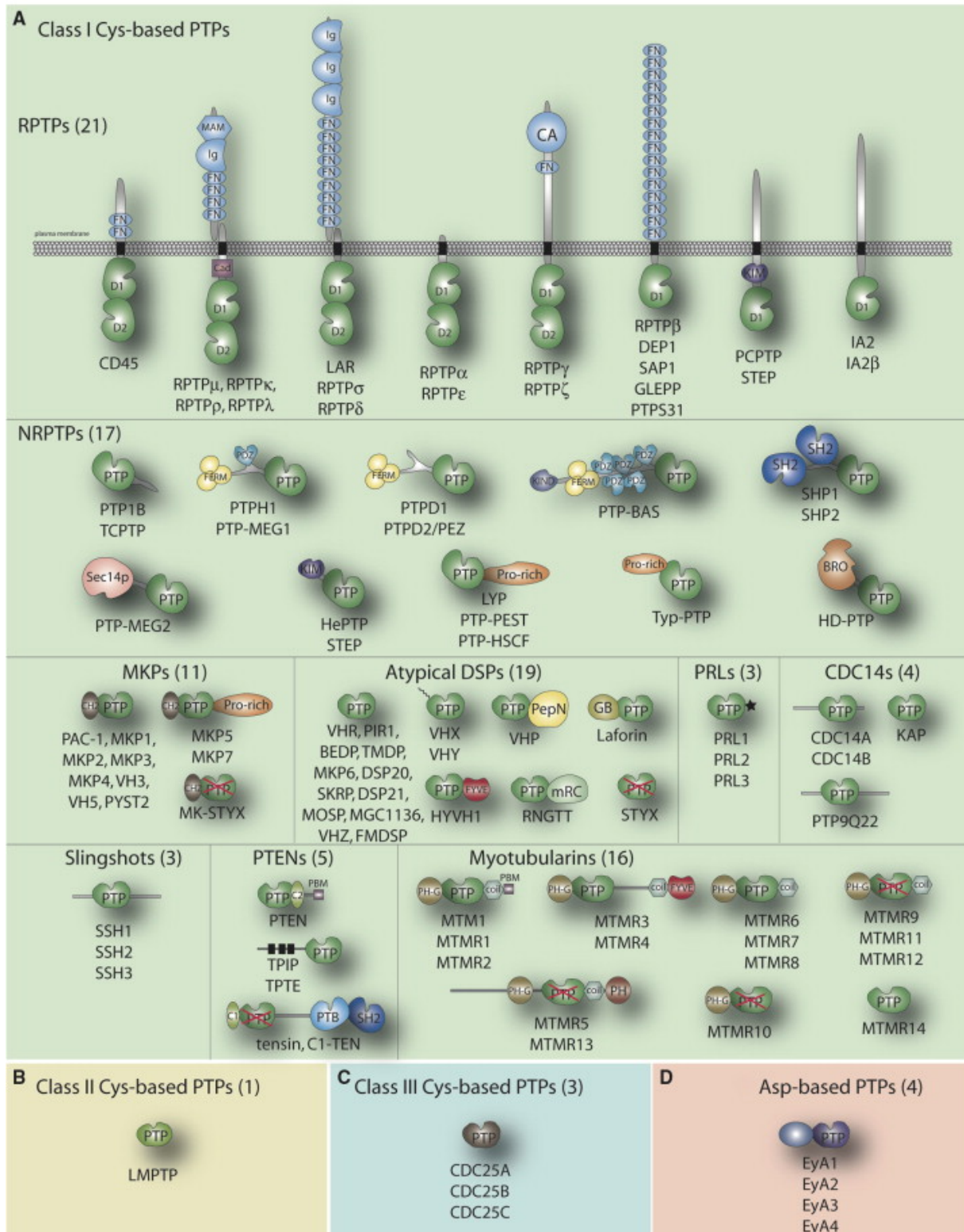
Fig. 2: Schematic representation of some of the protein-tyrosine phosphatase protein domains from Ostman et al. [5]. **a:** Nonreceptor PTPs contain one PTP domain, which is often linked to domains that mediate protein–protein interactions, such as Src-homology 2 (SH2), 4.1 Ezrin Radixin Moesin (FERM), and post-synaptic density proteindisc large-zonula occludens (PDZ) domains. **b:** Receptor-like PTPs are transmembrane proteins consisting of an extracellular part that typically contains domains implicated in cell adhesion, such as immunoglobulin-like, fibronectin-III-like repeat, and meprin/A5/µ (MAM) domains. The intracellular part consists of one catalytically active PTP domain (green) and, in some subfamiles, a PTP domain with little or no catalytic activity (grey), which is likely to have a regulatory function. In the case of tandem PTP domains, the membrane-proximal domain is designated D1, and the distal domain D2.
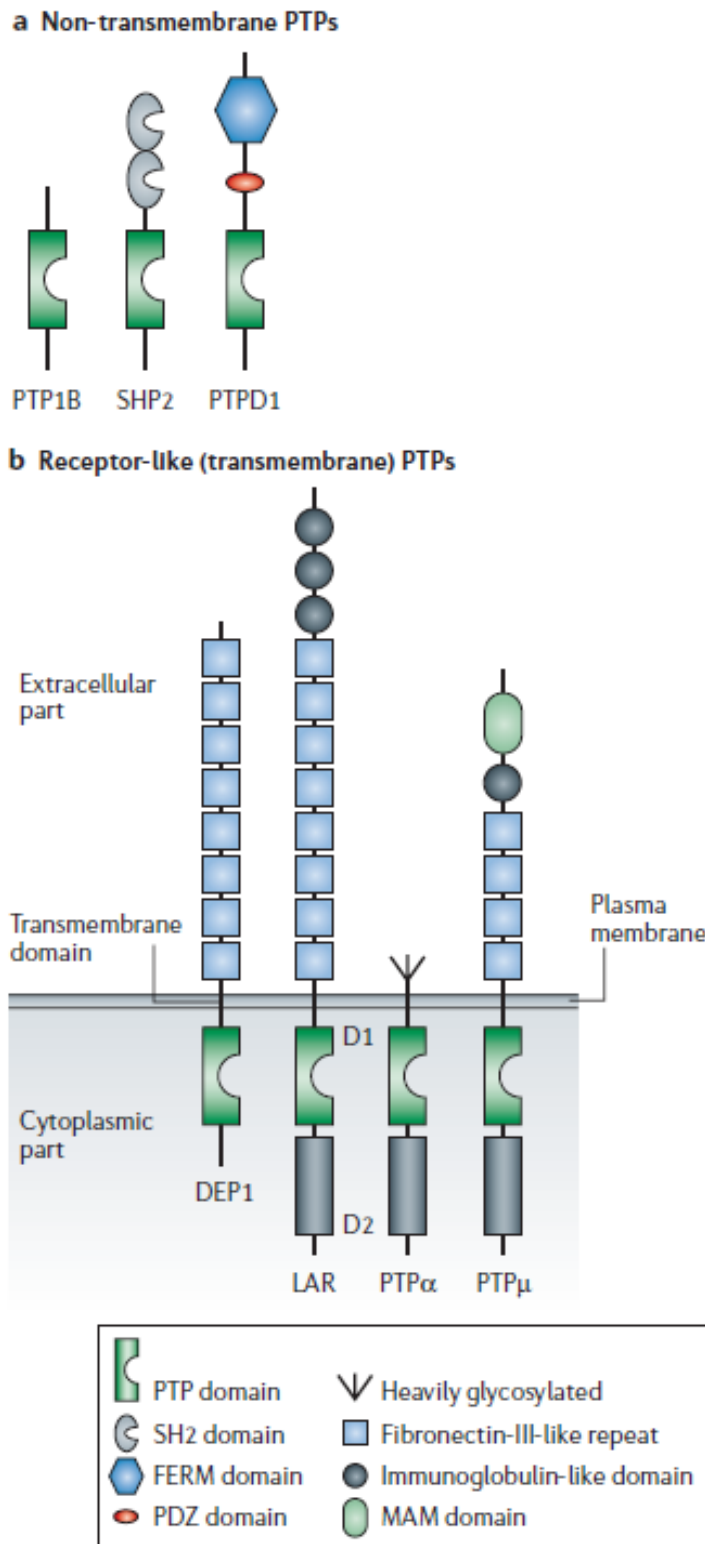
The molecular control of PTPs action is still poorly understood, but recent studies provide new insights of this phenomenon. As other proteins, PTPs can be phosphorylated on tyrosine residues, displaying binding sites for SH2-containing proteins. These domains allow the interaction among proteins, leading to the formation of signaling complexes [6]. Another mechanism of PTP activation is the post-translational proteolytic cleavage. Intracellular and extracellular cleavage of PTPs may occur, leading to activation or to targeted localization of these enzymes within the cell [7,8]. PTP ligands can also have an effect of PTP activities, as pleiotrophin for RPTPζ.

Once pleiotrophin binds to RPTPζ, it inhibits its phosphatase activity, leading to increased β-catenin phosphorylation [9]. Another well-known regulatory mechanism is dimerization. RPTPs can have a dimerized form that inhibits the catalytic activity [10] but it is still not clear whether the dimerization process is constitutive or is ligand-dependent. A recent universal regulatory mechanism has been pointed out for PTPs: oxidation. RPTKs inactivate PTPs locally and temporarily stimulating peroxide production that oxidates some cysteines present in the catalytic site [11,12].

1.1.1. Class I PTPs

Classical PTPs can be divided into two main subgroups: *i)* receptor-like and *ii)* cytosolic PTPs (Fig. 2). The receptor-like PTPs have a single transmembrane domain and variable extracellular domain. Several receptor-PTPs have a tandem of catalytic domain (D1 and D2) localized intracellularly, and D1 is mostly the site of phosphorylation activity. The extracellular domains can include immunoglobulin-like domain and fibronectin type III domain, which are involved in protein-protein interaction and in adhesion [5].

Cytosolic PTPs are characterized by a heterogeneous structural diversity, containing one or more domains responsible for interaction with other proteins, such as PDZ and SH2 domains, and for the subcellular localization, such as the FERM domain (Fig. 2). The catalytic domain is a highly conserved region with a cysteine residue that is crucial for the phosphatase activity [5].

Both receptor-like and cytosolic PTPs play a key role in several processes, but the present work will examine three topical areas of PTP action, 1) growth hormone (GH) signaling, 2) neurological and 3) immunological functions.

1.1.2. Class I PTPs in growth hormone signaling

PTP action on GH signaling has been widely investigated. There is an increasing interest in finding novel negative regulators in GH pathway due to the potential therapeutic opportunities. Several studies report that GH binds to its cell surface receptor (GHR) that associates with phosphorylated JAK2. This GHR-JAK2 complex leads to the phosphorylation of downstream transcription factors, Stat1, Stat3, and Stat5 [13]. Several phosphatases have been implicated at different level of this signaling pathway, as SHP-1 [14] and -2 (Src-Homology domain 2 containing tyrosine phosphatase-1 and –2) [15], TC-PTP [16] and PTP1B [17].

Indeed, SHP-1 associates with JAK2 activation upon GH stimulation in vitro [18]. SHP-2 has been shown to act either as a positive and negative regulator of GH signaling, depending on the concentration and cell type. SHP-2 binds to GHR and inhibits the GHR/JAK2/STAT-5-induced signaling by dephosphorylating tyrosine residues on these molecules [14]. Blocking SHP-2 binding site on GHR prolongs GH signaling, but the expression of catalytically inactive SHP-2 reduces transcriptional activity downstream GHR [15].

JAK2, STAT-5a and STAT-5b are also physiological targets for PTP-1B [19]. Ptp1b gene deletion *in vitro* leads to GH-induced hyperphosphorylation of JAK2, STAT-3 and STAT-5, whereas PTP-1B overexpression reduces GH-mediated gene expression [17].

TC-PTP is also involved in STAT inactivation, in particular it is known to dephosphorylate STAT1 [16] and STAT-5 [20]. Tc-ptp gene deletion *in vitro* leads to impaired nuclear dephosphorylation of GH-activated STAT1 and STAT-3 [16].

All these studies have been performed *in vitro*, and suggest a role of these phosphatases in GHR signaling. This hypothesis has not been fully confirmed *in vivo*, thus mice lacking functional SHP-1 [21-23], SHP-2 [24], TC-PTP [25] or PTP-1B [26,27] do not show enhanced growth or enhanced sensitivity to GH.

Further detailed studies are needed to dissect the role of these PTPs in the regulation of GH signaling pathway. It has also to be considered that other phosphatases might be involved at different levels of GH signaling and their identification and understanding their mechanism of action would lead to new possibilities as therapeutic targets for metabolic dysfunctions.

1.1.3. Class I PTPs in CNS functions

Classical PTPs have been reported to play a key role in neural functions, from development to cognitive function. RPTPs, such as PTPδ, PTPσ, LAR, and especially PTPRO, are important

players in axonal growth and guidance during development [28]. Studies on PTPσ-KO (RPTP) mice have shown involvement of this PTP in the regulation of the developing hypothalamo-pituitary axis [29,30] and in the development of the CNS architecture [31]. PTPBL-KO (non receptor like PTP- NRPTP) mice display impaired motor nerve repair in a model of sciatic nerve crush lesion [32] and PTPMEG (NRPTP) interacts with key intracellular players leading to the stimulation of the channel activity of NMDA receptors [33].

Better understanding the interplay between various phosphatases regulating CNS functions will be of importance in the future to unravel some of the complexity of CNS signaling pathways necessary for information processing.

## 1.1.4. Class I PTPs in immunological functions

The vertebrate immune response can be divided into innate and adaptive immunity. Innate immunity is the early and relatively nonspecific response to invading pathogens, while adaptive immunity is a slower and finer process, mediated by T and B cells expressing a wide range of antigen receptors [34].

The present study is mainly focused on innate immunity, and especially on its activation via the Toll-like receptors and T-cell receptors. The intensity and duration of the immune response is regulated by feedback mechanisms. Tyrosine phosphorylation is a central mechanism in the control of key signaling proteins involved in innate immunity. While the role of PTKs in this process has been widely studied, less is known on the PTPs responsible for lymphocyte physiology regulation [35]. Recent advances have been done in the identification of the phosphatases involved in immunity [36] (Fig. 3).

PTP action on immune response can be either positive or negative, promoting or inhibiting the immune system. SHP2 have a controversial effect on lymphocyte signaling. Qu and colleagues demonstrated that SHP-2 is needed for erythroid and myeloid cell differentiation [37] and missense mutation on ptpn11 gene encoding for SHP-2 is associated to various forms of leukemia [38]. SHP-2 may also have an inhibitory role in the activation of T and B lymphocytes [39] and inhibits the TRIF adaptor protein-dependent TLR4 and TLR3 signal transduction, blocking the proinflammatory cytokine production [40].

SHP-1 is mainly expressed in hematopoietic and lymphoid cells and several publications elucidate its role as key negative regulator of hematopoietic cell development and functions [41].

Fig. 3: Protein tyrosine phosphatases in lymphocytes from Mustelin et al. [36]**.** The domain architecture and the subcellular location of protein tyrosine phosphatases (PTPs) in lymphocytes are illustrated. Catalytic PTP domains are shown in green, and a green domain with a red cross denotes a catalytically inactive PTP domain. A star denotes a farnesylation motif. **Abbreviations:** BRO, baculovirus Bro homology; C2, protein-kinase-C conserved region 2; CDC, cell-division cycle; CH2, CDC25-homology region 2; Coil, coiled coil; D1, domain 1 of PTPs with two catalytic domains; D2, domain 2 of PTPs with two catalytic domains; DNA, DNA binding; ERM, ezrin, radixin and moesin; EYA, eyes absent; FN, fibronectin-like; FYVE, Fab1, YOTB, Vac1 and EEA1 homology; HDPTP, histidine-domain PTP; HEPTP, haematopoietic PTP; KAP, kinase-associated phosphatase; KIM, kinase-interaction motif; KIND, kinase amino-lobelike domain; LMPTP, low-molecular-weight PTP; LYP, lymphoid-specific PTP; MKP, mitogen-activated protein kinase (MAPK) phosphatase; mRC, mRNA capping; MTM1, myotubularin 1; MTMR, MTM-related protein; PAC1, phosphatase of activated cells 1; PBM, PDZ-binding motif; PDZ, PSD95, DLGA and ZO1 homology; PEZ, phosphatase with ezrin domain; PH, pleckstrin homology; PH-G, pleckstrin homology-GRAM (glucosyltransferases, RAB-like GTPase activators and MTMs) domain; PRL, phosphatase of regenerating liver; Pro-rich, proline rich; PTEN, phosphatase and tensin homologue; PTP-BAS, PTP basophil; PTP-HSCF, PTP haematopoietic stem-cell fraction; PTP-MEG, PTP megakaryocyte; PTP-PEST, PTP with PEST (proline-, glutamic-acid-, serine- and threonine-rich) domains; RNGTT, RNA guanylyltransferase and 5′-phosphatase; RPTP-ε, receptortype PTP-ε; Sec14, *Saccharomyces cerevisiae* phosphatidylinositol-transfer protein homology; SH2, SRC homology 2; SHP, SH2- domain-containing PTP; TCPTP-45, T-cell PTP of 45 kDa; TCPTP-48, T-cell PTP of 48 kDa; VHR, Vaccinia virus-VH1 related;VHX, Vaccinia virus-VH1-related MKP X; VHZ, Vaccinia virus-VH1-like member Z.
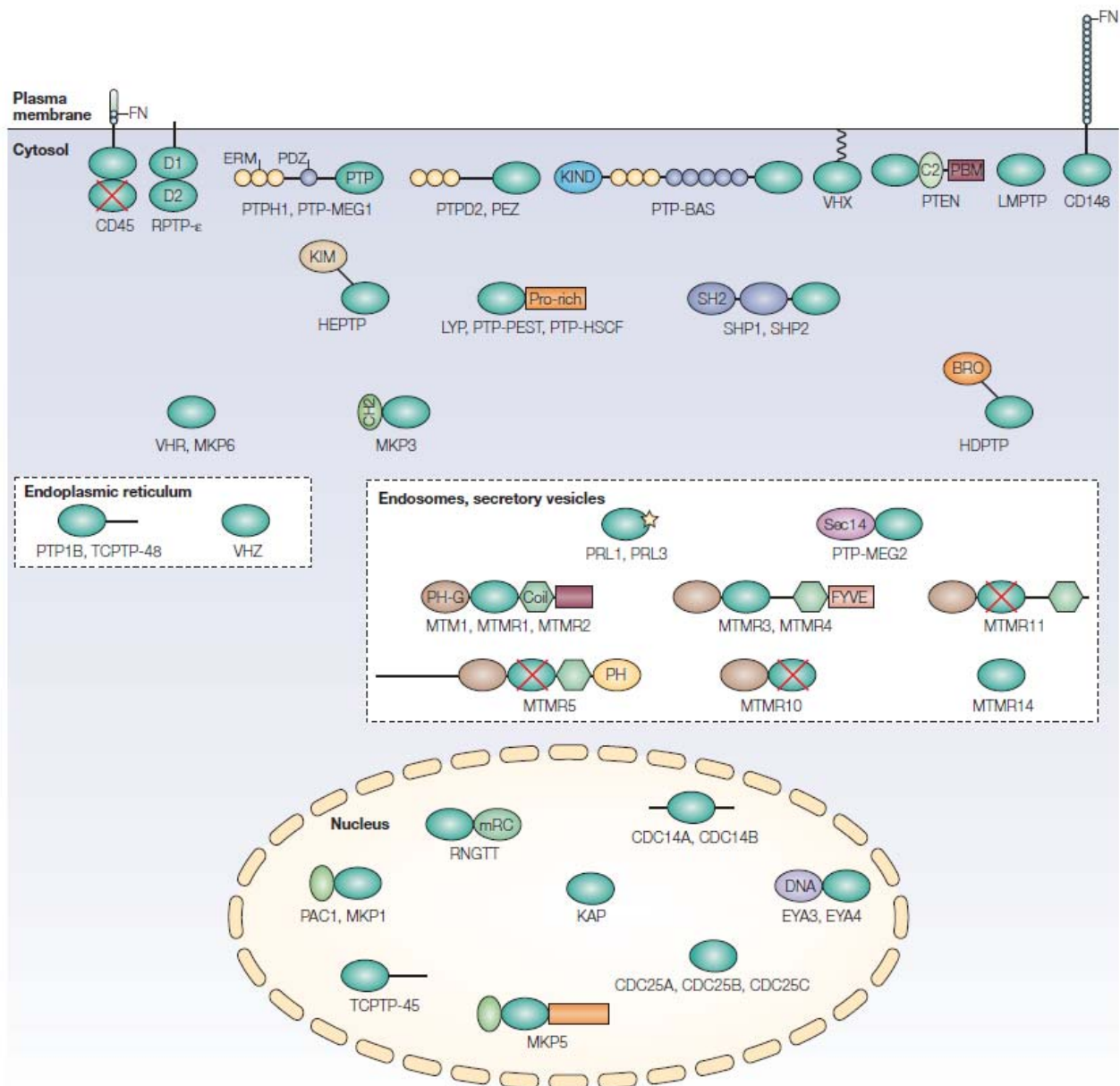
LYP and its mouse orthologue PEP are predominantly expressed in leukocytes and act as potent negative regulator of TCR signaling pathway [42]. LYP encoding gene, ptpn22, has been associated with autoimmune disease, as type1 diabetes [43] and rheumatoid arthritis [44].

Receptor-like PTP-LAR (common leukocyte antigen receptor) is highly expressed in the thymus and in a lower extent in spleen and lymph nodes. LAR expression is restricted to progenitor and T-cells, pointing out its peculiar role as T-cell specific phosphatase. However inactivating LAR phosphatase activity *in vivo* does not show any significant impact on T cell development and functions [45].

PTPMEG is a cytosolic phosphatase expressed in the thymus that is able to dephosphorylate TCRζ ITAMs *in vitro*. Trapping mutant experiments show that PTPMEG depletion leads to increased activation of NF-kB pathway [46]. However PTPMEG deletion *in vivo* does not induce TCRζ ITAMs dephosphorylation and PTPMEG-KO mice do not show an altered immunological phenotype [46].

Thus, as for GH signaling pathway (page 20), a discrepancy occurs between *in vitro* and *in vivo* studies. This incongruence might indicate a functional redundancy among PTPs in the immune response and further experiments are needed to unravel the interplay among these enzymes.

1.2. PTPH1

Protein tyrosine phosphatase PTPH1 belongs to a family of membrane-associated non-receptor PTPs characterized by containing at the N-terminus a FERM domain, that is responsible for the interaction with transmembrane proteins and/or phospholipids in the cell membrane. Indeed PTPH1 has been shown to localize close to the cell membrane in Jurkat T-cells [47]. In the central segment, PTPH1 contains a PDZ domain and possible phosphorylation sites [48]. PDZ domain is composed of six beta-strands and two alpha-helices, responsible for protein-protein interaction and the phosphorylation sites, especially serines, and it regulates PTPH1 activity [49]. The phosphatase domain is localized at the C-terminus of the protein (Fig. 3). Non-catalytic elements localized at the N- and C-terminus side of the catalytic domain inhibit the phosphatase activity in basal condition. Thus, these segments are characterized by autoinhibitory or pseudosubstrate motifs, that bind to the catalytic site and block the enzymatic function [49].

PDZ and FERM domains are responsible for important interaction between PTPH1 and other proteins, as 14-3-3β [50], VCP (Valosin Containing Protein) [51], TACE (TNFα converting enzyme) [52] and the cardiac sodium channel $Na_v1.5$ [53].

PTPH1 known substrates

14-3-3 family protein comprehends a group of highly conserved proteins that are involved in cell cycle regulation, apoptosis and in the control of different signaling pathways [54]. 14-3-3s are characterized by several isoforms differentially distributed in the tissues [55-57]. These proteins form homo and heterodimers that work as adaptors and scaffold proteins [58]. A yeast two-hybrid screening allowed identifying full length phosphorylated PTPH1 binding to 14-3-3β. Briefly, it has been demonstrated that PTPH1 is phosphorylated on Ser^{359} residues by C-TAK1 and PKC, enhancing the interaction between PTPH1 and 14-3-3β. Other Ser phosphorylation sites have been detected in PTPH1, suggesting that PTPH1 could interact with other 14-3-3 family members in response to distinct stimuli. Thus, depending on the association with a particular 14-3-3 isoform, PTPH1 might act as linkage between serine and tyrosine phosphorylation-dependent steps of the signal transduction [50].

Recent trapping mutant experiment allowed the identificantion of another PTPH1 substrate, VCP [51]. Valosin containing protein is a 97-KDa ATPase, belonging to the AAA (ATPase Associated with different cellular Activities) family. VCP, also known as p97, is a cell cycle regulator, critical for the fusion of endoplasmic reticulum (ER) membrane and for the rebuilding of Golgi cisternae [59-61]. Furthermore, VCP and its yeast orthologue CDC48 are localized mainly in the ER in G0 phase and are redistributed in the cell compartments in a cell cycle-dependent manner [59,62]. Tyrosine phosphorylation state has been suggested as key mechanism in the assembly of ER and is essential for VCP-PTPH1 interaction. *In vitro* studies identify JAK-2 as the kinase responsible for VCP phosphorylation [59], while PTPH1 is the PTPase crucial for VCP dephosphorylation, leading to a stop in cell cycle progression [51].

Yeast two-hybrid (Y2H) screening and *in vitro* binding assays identify a new enzyme interacting with PTPH1, TACE [52]. TACE is a member of the ADAM family protein, implicated in the ectodomain shedding of many cytokines, cytokine receptors and other proteins [63-65]. TACE is expressed in several cell types and tissues [66-68] and is involved in different signaling pathways as Notch [69] and MAPK [70,71]. Thus, unraveling the mechanism behind TACE regulation would be of importance in the understanding of different physiological functions, from development to inflammation [72]. Zheng and colleagues showed that PTPH1 binds to the cytoplasmic tail of TACE via its PDZ domain. The cytoplasmic domain of TACE is not dephosphorylated by PTPH1, but PTPH1 overexpression, results in a reduction on TACE

expression and activity, suggesting that PTPH1 negatively regulates TACE by acting on a yet unknown intermediate protein [52].

Cardiac voltage-gated sodium channel 1.5 (Na$_v$1.5) is another substrate for PTPH1, *in vitro* [53]. Na$_v$1.5 is a glycosilated protein and the pore-forming a-subunit protein that interact with several β-subunits to generate depolarizing current, important for the conduction of the cardiac impulse. Several studies report that Na$_v$1.5 is not expressed only in cardiac tissue, but is also expressed in the axons of cerebral cortex, cerebellum, thalamus and brain stem [73]. Several Na$_v$ channels are regulated by tyrosine phosphorylation [74]. In this regard, Ahern and colleagues showed that kinase Fyn binds to Na$_v$1.5, accelerating its recovery from inactivation state [75]. Y2H screening identifies PTPH1 as another protein interacting with Na$_v$1.5. In detail, PTPH1 binds to the cytoplasmic tail of Na$_v$1.5 via its PDZ domain and leads to the hyperpolarization of Na$_v$1.5 steady-state. Catalytically inactive PTPH1 is not able to reduce the potential values, thus suggesting Na$_v$1.5 as a substrate of PTPH1 activity [53].

PTPH1 known functional impact on CNS functions, GH signaling and innate immunity will be reported in the following paragraphs.

1.2.1. PTPH1 in the Central Nervous System (CNS)

PTPH1 expression has been analyzed by Northern blotting and *in situ* hybridization in adult and embryonic rat brain. PTPH1 mRNA is highly enriched in the adult thalamus, but it also present in the middle layers of neocortex, hippocampus and cerebellum [76]. Within the adult thalamus, the expression of PTPH1 is widespread, excluding only the ventral lateral geniculate and reticular thalamic nuclei. In detail, PTPH1 labeling is very intense in medial geniculate and lateral geniculate nuclei and in the ventral basal complex. Indeed PTPH1 mRNA is expressed in the ventral medial, ventral posterior, central median, mediodorsal, and lateral dorsal thalamic nucleic. No labeling is detactable in the reticular thalamic nuclei, zona incerta, subthalamus, and habenula. Both ventral and dorsal medial geniculate nuclei are labeled for PTPH1. In addition, the pretectum and superior colliculi do not display any PTPH1 signal. In the hippocampus, pyramidal cells in fields CA1-3 and granular cells of the dentate gyrus display very low level of hybridization.

PTPH1 expression pattern during development does not vary from the adult one. PTPH1 RNA is detectable in the thalamus already at embryonic stage E19 and is retained throughout postnatal development. In addition to the diencephalic labeling, PTPH1 mRNA is also present at high levels in the olfactory epithelium at E19. The expression in the olfactory epithelium is consistent with a previous study that used PCR to show PTPH1 expression in this tissue [77].

PTPH1 mRNA is present at very low levels also in the cortex and hippocampus at E19 and throughout the postnatal period.

Thalamus is part of a forebrain area, called diencephalon. PTPH1 is expressed in a segment-specific pattern in the diencephalon. As we have already mentioned, PTPH1 is not expressed in ventral lateral geniculate and reticular thalamic nuclei that are the only thalamic areas embryonically derived from the ventral thalamus and that do not project to the cortex. Indeed, the rest of the thalamus is derived from the embryonic dorsal thalamus and almost all have thalamo-cortical connections. In summary, PTPH1 seems to be expressed in all adult thalamic nuclei generated from the dorsal thalamus and is absent from the nuclei derived from the ventral thalamus. In the area between the dorsal and ventral thalamus, in the region called zona limitans, PTPH1 mRNA is not present.

Sahin and coll. suggest that PTPH1 expression pattern is very similar to pattern of expression of two other genes: Wnt-3 and Gbx-2. Similarly to PTPH1, Wnt-3 expression is also retained in the adult thalamus [78]. Both the Wnt family of glycoproteins and tyrosine phosphorylation can regulate cell-cell adhesion, acting on β-catenin [79], suggesting that PTPH1 may be a part of the effector pathway for Wnt-3 in the dorsal thalamus.

The restricted expression of PTPH1 to the thalamic nuclei, that send axons to the neocortex would be consistent with a structural or regulatory role specific to these axons. The FERM domain is responsible for the interaction of the protein with actin filaments [80] and PTPH1 could use this domain to regulate cytoskeleton-membrane interactions, thus maintaining the thalamocortical connections. In conclusion, since the thalamus is a relay station for sensory information to the neocortex, PTPH1 may participate in the phosphorylation/dephosphorylation cascades that regulate coordinated activity of thalamo-cortical neurons.

1.2.2. PTPH1 in growth hormone signaling pathway

Negative regulation of GH signaling can occur via induction of SOCS (Suppressor Of Cytokine Signaling), expression of regulatory proteins and phosphatases [81]. As already mentioned, several PTPs are known to interact with GHR and to affect its functionality *in vitro*, but their impact *in vivo* is still controversial. PTPH1 has been recently shown to bind GHR an *in vitro* system [19] and its *in vivo* relevance will be fully explained in the following chapter (page 72).

A substrate trapping mutant system has been used to test several PTPs for tyrosine phosphorylated GHR substrate specificity. A wide panel of PTPs carrying a mutation within the catalytic domain has been considered in the experiment and these results have been confirmed by a

targeted western blotting approach on PTPx-GHR binding, upon GH stimulation in cell culture. PTP1B, TC-PTP and PTPH1 have been found to act on GHR in the trapping mutant approach and PTPH1 and PTP1B have been shown to dephosphorylate GHR in a cellular system. A SPOT analysis allowed the identification of the tyrosine residue on GHR that was responsible for the binding with the respective PTP. In particular, it has been demonstrated that PTPH1 is only able to bind Tyr$_{534}$, while PTP1B and TC-PTP interact with multiple phosphorylation sites [19].

1.2.3. PTPH1 in innate immunity

PTPH1 is known to be expressed in the cytoplasm of Jurkat cells and also other T cell lines [47]. Its expression is significantly increased at the plasma membrane and this localization is due to the N-terminal FERM domain [47]. It has been demonstrated that PTPH1 has also a functional effect on T cell signaling. Its overexpression in Jurkat T cells reduces indirectly the TCR-induced serine phosphorylation of Mek, Erk and Jnk, leading to a decreased IL-2 gene expression, a T cell growth-promoting cytokine gene [82]. Furthermore the presence of the FERM domain of PTPH1 is necessary not only for PTPH1 localization on the plasma membrane of Jurkat T cells but also for its inhibitory effector properties [47]. These studies corroborate the hypothesis of a possible role for PTPH1 as negative regulator in TCR signaling. Indeed, biochemical approaches and substrate trapping experiments identify PTPH1 as the phosphatase able to physically interact with TCRζ and to dephosphorylate TCRζ ITAMs *in vitro* [83].

Comparatively, a recent *ex vivo* study shows that primary T cells lacking PTPH1 phosphatase domain (ΔPTP) do not display any alteration in cell development and homeostasis in basal condition. Furthermore, *ex vivo* stimulation of these PTPH1-ΔPTP T cells do not induce a modulation of IL-2, IL-4 and IFNγ production and proliferation [84]. Bauler and colleagues also demonstrate no modification in TCRζ dephosphorylation in PTPH1-ΔPTP T cells, thus excluding a possible role for PTPH1 in TCR signaling.

This discrepancy between *in vitro* and *ex vivo* studies has been explained by a possible redundant effect of other PTPs such as PTP-BL and especially PTPMEG, a PTP that belongs to the same family protein of PTPH1. The double PTPH1-PTPMEG ΔPTP and triple PTPH1-PTPMEG-PTP-BL T cells fail to show a T cell phenotype, comprising T cell development and TCR-induced cytokine secretion and proliferation [85]. These results indicate that neither PTPMEG nor PTP-BL compensate for the lack of PTPH1 action in primary T cells and underline the controversial role of these phosphatases within the immune system.

Further *in vivo* studies are needed in order to unravel the controversial PTPH1 impact in the complex immune system regulation.

1.3. Overview on Innate immunity

The mammalian immune system is comprised of a nonspecific, innate immune response and a specific, adaptive immune response. Together, these mechanisms protect individuals from pathogens and coordinate the complexities of healing. The innate immune response is phylogenetically ancient and is limited in its specificity and diversity. In contrast, the adaptive immune response represents an evolved mechanism of host defense capable of recognizing a wide range of pathogens. While innate immune cells react in essentially the same way to repeated infections, adaptive immune cells are capable of developing "memory" to antigens such that successive exposures to the same antigens evoke more rapid and efficient responses [86-88]. Indeed innate immune system is based on non-clonally distributed receptors that recognize pathogen-associated molecular patterns (PAMPs) that are specific for microbes and are not present in self-tissues.

The innate immune system is comprised of constitutive and inducible components. Constitutively, anatomic barriers (such as the skin) physically prevent microorganisms from accessing vulnerable parts of the organism. Chemical barriers, such as the acidic environment within the stomach, create microenvironments inhospitable to pathogens. In contrast, inflammation is an inducible mechanism of defense which is triggered by any disruption of tissue homeostasis.

Any local disruption of tissues and blood vessels, whether by pathogens or trauma, activates the innate immune system to initiate an inflammatory response. The first responders are usually tissue macrophages, which become phagocytic and begin to secrete proinflammatory cytokines (e.g., interleukin (IL)-1, tumor necrosis factor (TNF)-α, IL-6) and chemokines. These soluble mediators promote vasodilation, plasma protein exudation (edema), and the synthesis of adhesion molecules on adjacent endothelia. Such reactions focus leukocyte (e.g. neutrophil and monocyte) recruitment to the site of infection or injury. Monocytes and lymphocytes migrate into damaged or infected tissues after neutrophils due to the differential kinetics of vascular adhesion molecule and chemokine synthesis during an inflammatory response. As newly emigrating monocytes differentiate into mature macrophages, their effector potential changes. Like neutrophils, macrophages are phagocytic and produce ROS, NO, and proteolytic enzymes (e.g., matrix metalloproteinases). They also produce proinflammatory cytokines (e.g. IL-1β, IL-6, TNFα and IL-12) that complement the microbicidal activities of neutrophils and activate the effector cells of adaptive immunity [89-91]. As with neutrophils, the byproducts of acute macrophage activation cause damage to adjacent healthy tissues. Thus, non-specific bystander injury is a hallmark of innate immune cell activation during acute inflammation. Despite their potential to increase

bystander damage, macrophages are essential for the resolution of inflammation or infection. Cells of the adaptive immune system (e.g. T- and B-lymphocytes) are often necessary for complete eradication of a pathogen, but macrophage expression of major histocompatibility complex (MHC) and costimulatory molecules are required to activate these cells. Macrophages also secrete cytokines, such as IL-12 [92-94], that influence the efficacy of the adaptive response. Within the lesion, macrophages are responsible for tissue debridement (i.e., the breakdown and removal of extracellular matrix (ECM) and damaged tissue), that is essential for wound repair and tissue remodeling. Macrophages also promote wound healing by producing numerous soluble mediators, including growth factors which promote angiogenesis, stimulate fibroblast proliferation, and regulate connective tissue synthesis [95].

Although innate immunity and inflammatory processes have widely studied, most of the molecular mechanisms and regulators of these complex events are still unknown. In recent years, immunomodulatory molecules, as carrageenan and lipopolysaccharide (LPS), have been used in rodents to investigate innate immune responses [96,97] and to understand the role of target key players on immune system upon inflammatory challenge, thus in the complex *in vivo* machinery.

1.3.1. Lipopolysaccharide (LPS)

In the late 19th century, Richard Pfeiffer used heat-inactivated lysates of *Vibrio cholerae* to induce a range of pathophysiological reactions in guinea pigs. He named the toxic substance endotoxin [98]. The term 'lipopolysaccharide', which is descriptive of the structure of endotoxin, is now used as a synonym for endotoxin.

LPS is characteristic of Gram negative bacteria and present inside and outside the outer lipid layer of the bacterial cell wall. Innermost in the cell wall of Gram negative bacteria is a double lipid layer, and between the inner and outer layers there is a peptidoglycan layer, which is a network containing carbohydrate and peptide chains [99,100]. Indeed LPS consists of a lipid and a polysaccharide part. The polysaccharide portion includes a highly variable sugar chain and an intermediate variable core. The sugar chain may consist of up to 50 repeating oligosaccharide units, and it is unique for each bacterial strain and highly antigenic, determining the bacterial serotype. The lipid part is highly conserved among the bacterial strains and it is responsible for the endotoxic activity of LPS [101]. Mammals are in permanent contact with Gram negative bacteria and LPS. Low doses may be beneficial for enhancing resistance to infections, but larger doses lead indirectly to dramatic pathophysiological reactions, which are caused by excessive amounts of inflammatory endogenous mediators, such as cytokines and chemokines.

Subsequent exposure to LPS causes a phenomenon called LPS tolerance or LPS desensitization. Macrophages show a reduced response to second LPS exposure in a time- and dose-dependent manner determined by the reduced production of inflammatory cytokines.

It has been suggested that LPS interacts nonspecifically with a responsive host cell by hydrophobic insertion into the cell membrane, because of its amphipathic character. Nowadays, several cell surface receptors and other proteins specifically binding LPS have been described, including the LPS-binding protein (LBP), the glycerolphosphatidylinositol (GPI)-anchored protein CD14 and the macrophage scavenger receptor [102-105].

LPS mechanism to induce any cellular response in the host has been widely studied. LPS monomers bind specifically to receptor TLR4 on cell surface, leading to a host cell response. This inflammatory response has been mostly elucidated during the past 10 years and will be reviewed in the subsequent paragraphs.

1.3.2. Toll-like receptor 4 (TLR4)

Innate immune system has a great degree of specificity that is highly developed in its ability to discriminate between self and pathogens. This discrimination mainly depends on a family of well-conserved receptors, known as Toll-like receptors (TLR)[86,106]. The TLRs are type I integral membrane glycoproteins and are members of the interleukin-1 receptors (IL-1Rs) superfamily. The main difference between these two receptor-types resides in the extracellular region. TLRs are characterized by the presence of a leucine-rich repeat (LRR) motifs, while IL-1Rs contain immunoglobulin-like (Ig) domains [34]. Despite this difference in the extracellular portion, TLRs and IL-1Rs have both a conserved region of 200 amino acids in their cytoplasmic tails that is known as Toll/IL-1R (TIR) domain. The TIR domain is characterized by 3 highly homologous regions called boxes 1, 2 and 3 that have an important role in signaling cascade [34,107,108]. The LRR and the TIR domains of TLRs form a horseshoe structure and the concave surface of LRR domains is involved in the recognition of the pathogens. The subcellular localization of the different TLRs is related to the ligand specificity. In the present study, we focused our attention on LPS signaling and therefore on its specific receptor, TLR4.

TLR4 has been mapped to chromosome 4 in mouse [109] and to chromosome 9q32-33 in human [110]. Recently, TLR4 mouse and human genes have been cloned and sequenced [111]. The human gene is 19 kb in length and consists of three exons. Promoter analysis has shown that location approximately 75 bp upstream from the transcriptional start site is sufficient to direct the

gene expression. This promoter region is highly conserved between human and mouse. The major difference is due to longer intronic sequences that make mouse gene 91.7 kb-long [111].

The extracellular domain of the TLR4 protein contains 22 copies of LRRs [110]. Recent reports points out that LRRs do not present the LPS-binding property of TLR4, because mapping studies with its close binding partner CD14 revealed that most LRRs can be deleted without affecting LPS binding [112,113]. The extracellular part of TLR4 contains 9 N-linked glycosylation sites. Glycosylation is important for the transportation of the protein to the cell surface and the maintenance of the functional integrity of the LPS receptor complex [114]. TLR4 was discovered to be the principal mediator of the LPS response by characterizing the LPS-hyporesponsive mouse strains. The first studies on LPS pointed out that the mouse strains C3H/HeJ and C57BL/10ScCr show a deficient response to bacterial endotoxin [115,116]. These mice could tolerate enormous amounts of LPS without any lethal effects, but were highly susceptible to Gram negative bacterial infection. Genetic studies revealed a single *Lps* locus in chromosome 4, which was responsible for this LPS hyporesponsiveness. Only recently, this locus was mapped as the TLR4 gene [109,117,118]. The TLR4 knock-out mouse generated by Hoshino and his co-workers had the same phenotype as naturally occurring TLR4-mutant mice [119]. The animals developed otherwise normally, but showed no response to LPS or synthetic lipid A to a certain dose level. The hyporesponsiveness has been later suggested to be due to disruption of the TLR4-mediated signaling pathway resulting from the inability of mutant TLR4 to interact with the second messenger MyD88 [120].

TLR4 gene expression

TLR4 expression has been found in heart, lung, fetal skin, fetal brain, placenta, fetal ileum, and many other tissues [121-124]. The regulation of TLR4 expression is complex, involving tissue and cell-specific differences. Proper regulation, however, is crucial for the innate immune system. The amount of TLR4 receptors in the cell is small (only up to 1000), and over-expression of TLR4 not only enhances the sensitivity to LPS, but may also contribute to heart failure [125] and genetic susceptibility to ozone-induced lung hyperpermeability via inducible nitric oxide synthase [126,127]. Comparively, downregulation of TLR4 gene expression is involved in LPS tolerance [128].

Only a few mechanisms for regulating TLR4 gene expression have been characterized. First, there is an alternatively spliced form of mouse TLR4, in which an additional exon between the second and third exons of the reported gene encodes for 36 additional amino acids and a stop codon. This alternatively spliced form is expressed as a partially secretory 20 kDa soluble protein. It

significantly inhibits LPS-mediated TNF-α production and NF-κB activation in mouse macrophages and thus, it may function to inhibit an excessive LPS response [129]. Second, the TLR4 promoter region has a myeloid cell-specific transcription factor PU.1 and interferon consensus sequence-binding protein (ICSBP) binding sites. TLR4 promoter activity in myeloid cells is dependent on these sites. However, PU.1 and ICSBP in a non-myeloid cell line do not induce promoter activity, suggesting a need for additional transcription factors or some inhibitory regulation in other cells [130]. Third, alteration of mRNA stability serves another transcriptional and post-transcriptional regulatory mechanism. Fan *et al*. showed, in rodent *in vivo* and *in vitro* models, that the reduction of lung TLR4 mRNA after intratracheal LPS was due to a lowering of mRNA stability, and that the prevention of mRNA reduction after an antecedent shock was due to prevention of mRNA destabilization [131].

LPS signaling pathways via TLR4

LPS signaling through TLR4 is shown schematically in Fig. 4. According to current knowledge, LPS is first recognized near the cell surface by circulating LBP, which breaks down LPS aggregates and moves LPS monomers to the membrane protein CD14. LBP has a high-affinity binding site for LPS, and it functions as a catalytic lipid transfer protein [132-134]. The extracellular domain of CD14 is very similar to the extracellular domain of TLR4, but as it lacks the cytoplasmic domain, thus, it cannot induce cellular signaling.

TLR4 has been shown to be the signaling part of the receptor complex, which involves a myeloid differentiation (MD)-2. MD-2 is physically associated with TLR4 and essential for TLR4 to translocate on the cell surface and also for an efficient response to LPS [89,107,135,136]. The LPS-CD14-MD-2 complex signals via the TLR4 receptor and the downstream effector is an adapter protein MyD88. MyD88 interacts with the transmembrane receptor through the C-terminal TIR domain [137,138] and recruits Ser/Thr kinase IRAK (IL-1R associated kinase) to the receptor complex. IRAK associates and activates the adapter molecule TNF receptor associated factor (TRAF6) [139]. TRAF6 promotes the activation of the NF-κB inhibitor kinases (IKKs) and of the TAK1 (TGFβ-activated kinase 1)-induced MAP3K. MAP3K then enhances the sequential events of the canonical NF-κB pathway. Degradation of the NF-κB inhibitor I-κB releases NF-κB to subsequently translocate to the nucleus and induce target gene expression [108,120,140-144]. TAK1 is also responsible for the activation of Jun N-terminal kinases (JNK) such as p38, leading to expression of AP-1 transcription factor and the regulation of inflammatory cytokine expression [144]. Recently, a MyD88 adapter-like Mal/TIRAP has been reported to participate in the LPS-TLR4 pathway.

Fig. 4: TLR-signalling: MyD88-dependent and independent pathways, modified from Akira et al. [34]. The Toll/interleukin-1 (IL-1)-receptor (TIR)-domain-containing adaptor molecule MyD88 (myeloid differentiation primary-response protein 88) mediates the Toll-like receptor (TLR)-signalling pathway that activates IRAKs (IL-1-receptor-associated kinases) and TRAF6 (tumour-necrosis-factorreceptor- associated factor 6), and leads to the activation of the IKK complex (inhibitor of nuclear factor-κB (IκB)-kinase complex), which consists of IKK-α, IKK-β and IKK-γ (also known as IKK1, IKK2 and nuclear factor-κB (NF-κB) essential modulator, NEMO, respectively). This pathway is used by TLR1, TLR2, TLR4, TLR5, TLR6, TLR7 and TLR9 and releases NF-κB from its inhibitor so that it translocates to the nucleus and induces expression of inflammatory cytokines. TIRAP (TIRdomain-containing adaptor protein), a second TIR-domain-containing adaptor protein, is involved in the MyD88-dependent signalling pathway through TLR2 and TLR4. By contrast, TLR3- and TLR4-mediated activation of interferon (IFN)-regulatory factor 3 (IRF3) and the induction of IFN-β are observed in a MyD88-independent manner. A third TIR-domain-containing adaptor, TRIF (TIRdomain- containing adaptor protein inducing IFN-β), is essential for the MyD88-independent pathway. The non-typical IKKs IKK-ε and TBK1 (TRAF-family-member-associated NF-κB activator (TANK)-binding kinase 1) mediate activation of IRF3 downstream of TRIF. A fourth TIR-domaincontaining adaptor, TRAM (TRIF-related adaptor molecule), is specific to the TLR4-mediated, MyD88-independent/TRIF-dependent pathway.
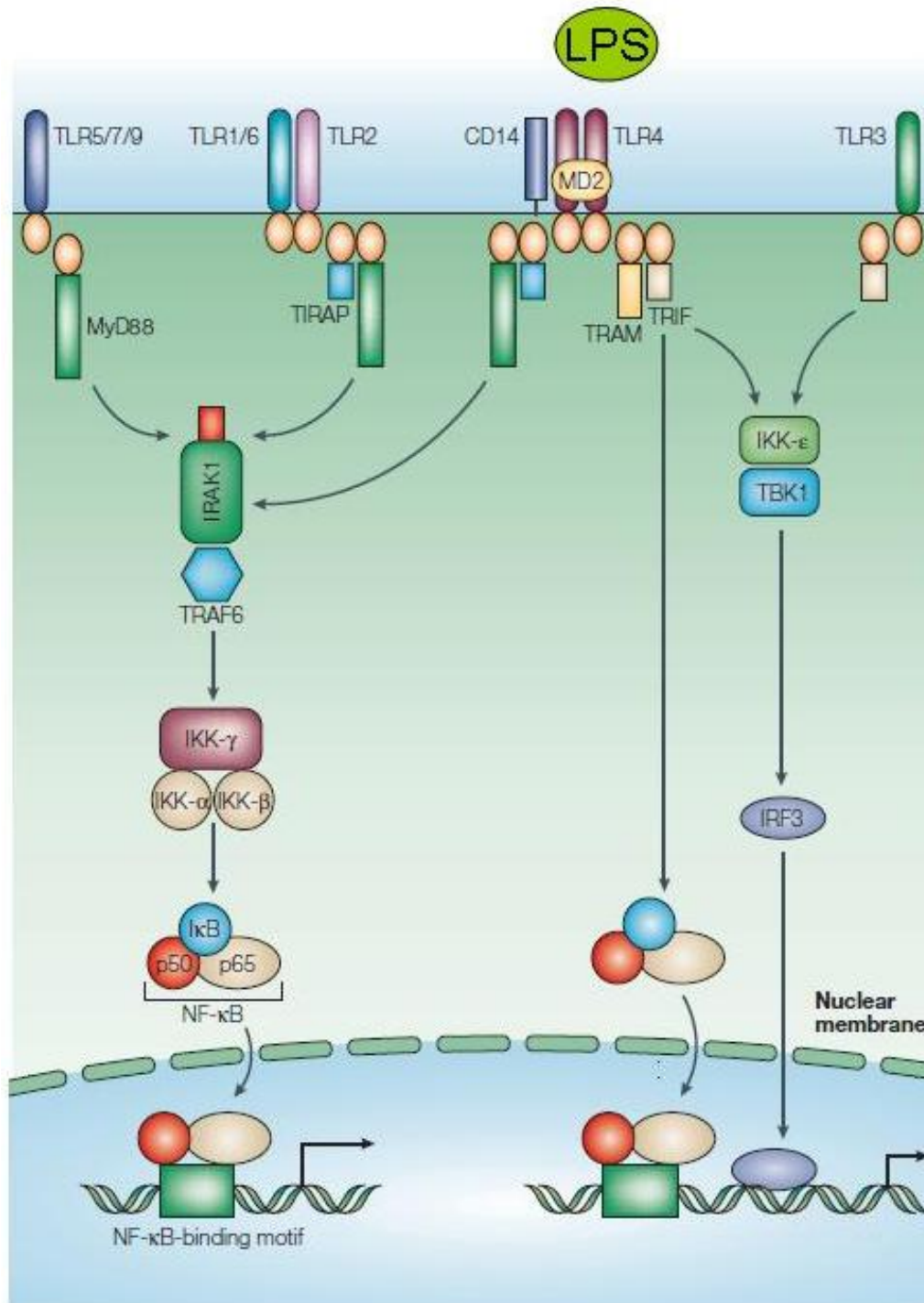
Mal/TIRAP is an adapter protein, which forms heterodimers with MyD88, activates NF-kB in association with IRAK-2, and also associates with TLR4 [145,146].

LPS can also induce a MyD88-independent TLR4-signaling pathway, which leads to the late activation of NF-κB pathway, by activating the IFN regulatory factor 3 (IRF3) [108,147,148]. The adapter protein TRIF (TIR domain containing adaptor protein) and TRAM (TRIF-related adaptor molecule) are essential in MyD88-independent signaling pathway. In detail, TRIF and TRAM activate the non-typical IKKs, IKKε and TBK-1 (TRAF-family member associated NF-κB activator TANK-binding kinase 1) leading to IRF3 activation and translocation to the nucleus.

LPS also activates other signaling molecules involved in inflammatory phenomena, such as phosphatidylinositol 3-kinase (PI3K), Akt (a downstream mediator from PI3K), and many others able to activate NF-κB [136]. The relationship, interplay and regulation (positive and negative) among these various signalling cascades are not fully understood and need further investigation [91,149].

1.4. Overview on GH signaling pathway

In the recent years, significant progresses have been made in unraveling the signaling pathways activated by growth hormone receptor (GHR). GH is secreted by the anterior pituitary gland into the circulation and stimulates body growth [150]. In addition to promoting growth, GH has an important role in metabolic [151] and CNS functions [152], in regulation of immune system[153] and aging [154,155].

Briefly, GH binds to the extracellular domain of GH receptor with a high affinity binding. This first step leads to the dimerization of GHR and to a subsequent contact of GH with the second GHR molecule, stabilizing the GHR dimer [156]. Following this binding, GH promotes phosphorylation of tyrosine residues on GHR and on signaling proteins. As already mentioned, the kinase responsible for these events is Janus Kinase 2 (JAK2). JAK2 rapidly associates to GHR, undergoes autophosphorylation and then phosphorylates GHR [13]. GH-activated JAK-2 phosphorylates STAT-1, STAT-3, STAT-5a and STAT-5b [157,158], leading to their dimerization, traslocation in the nucleus and transcription of targeted genes (Fig. 5) [18,159].

Recent studies have revealed that GH-JAK2 complex is regulated at different levels [81]. Suppressor of cytokine signaling (SOCS) family proteins are important inhibitors of GHR signaling pathways [160] (Fig. 5). SOCS1, 2, 3 and CIS are thought to inhibit GH signaling by competing with GHR for the binding to JAK2 [81,161]. SOCS-1 seems to inhibit JAK2 kinase activity by binding to JAK2 directly [162]. SOCS-1 inhibition of JAK2 activity involves interactions between SOCS-1 and the kinase of JAK2 (Ref. 58). It is thought that a region N-terminal to the SH2 domain of SOCS-1 acts as an inhibitory pseudosubstrate of JAK2 activation loop [163]. SOCS1 inhibition of JAK2 is effective even in absence of GHR, suggesting a first binding of SOCS1-JAK2 and subsequent GHR dephosphorylation [164]. CIS and SOCS-3 seem to behave differently from SOCS1 and do not bind directly to JAK2, inhibiting its intrinsic activity. Indeed, SOCS-3 only inhibits JAK2 kinase activity after binding to the GH receptor [164].

In addition to SOCS proteins, GH-induced signaling can be blocked by dephosphorylation of GHR by phosphatases. Dephosphorylation of specific tyrosine residues would stop the signaling cascade and could induce GHR internalization and degradation [165]. The role of phosphatase in the negative regulation of GH signaling pathway has been estensively explained in the previous chapter on class I tyrosine phosphatase (page 14), but other key players in GH regulation interplay have still to be identified.

Fig. 5: Regulation of GHR-JAK2 signaling modified from Herrington and Carter-Su [157]. Some of the signaling pathways initiated by GH activation of JAK2 are shown. JAK2 phosphorylates SHC, leading to activation of MAPK (blue arrows). JAK2 also phosphorylates STAT transcription factors. MAPK and STATs are important for GH regulation of gene transcription, comprising SOCS genes (purple arrows). JAK2 phosphorylates IRS proteins, which are thought to lead to activation of PI3′-kinase (PI3K: red arrows). GH activation of PI 3′-kinase via IRS proteins might be important for GH stimulation of glucose transport. SOCS proteins inhibits GHR signaling by binding JAK2 and decreasing its activity. Tyrosine phosphatases might also contribute to inhibiting GH receptor signaling by dephosphorylating tyrosines in the GH receptor and/or JAK2. **Abbreviations:** GH, growth hormone; GHR, growth hormone receptor; JAK2, Janus kinase 2; IRS, insulin receptor substrates; JAK2, Janus kinase 2; MAPK, mitogen-activated protein kinase; P, phosphate; PI 3′K, phosphatidylinositol 3-kinase; STAT, signal transducers and activators of transcription; SOCS, suppressor of cytokine signaling.
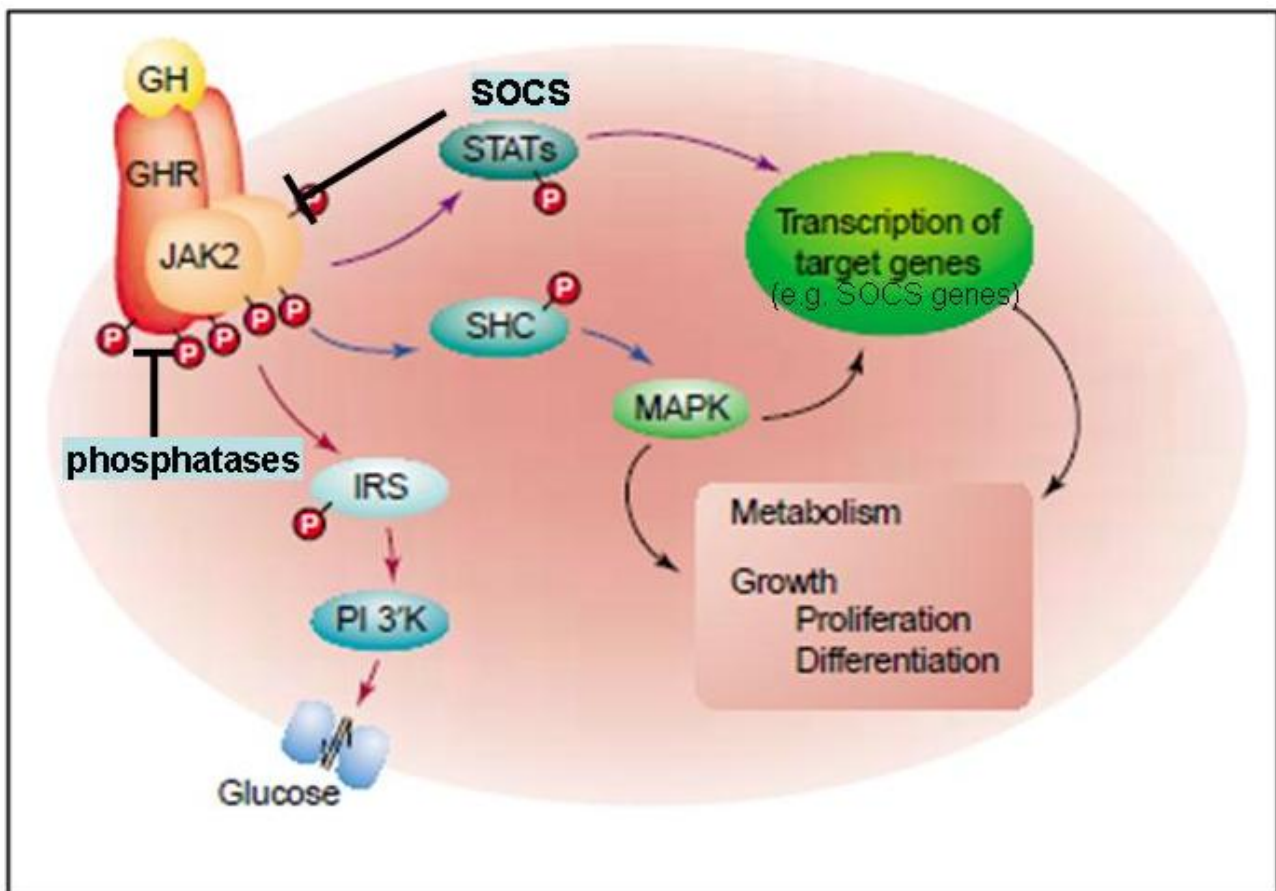
Aim of the study

The present PhD thesis aims to fully characterize PTPH1 gene and protein functions using PTPH1-KO mouse as a tool, in three major relevant areas: GH-signalling, CNS and inflammatory functions. Furthermore the present manuscript aims to understand whether these PTPH1-KO mice could be used as mouse model for metabolic and/or inflammatory-mediated diseases and to identify new potential PTPH1 targets and new signaling pathways, where PTPH1 role has still to be defined.

The major topics investigated during the PhD program and elucidated in the present thesis have been:

- Localization of PTPH1 expression through a deep analysis of LacZ staining in PTPH1-KO mice and *in vivo* relevance of PTPH1 in basic CNS functions through an extensive behavioral phenotyping of PTPH1-KO mice.

- In vivo relevance of PTPH1 on GHR signaling pathway through growth curve analysis and IGF1 quantification in PTPH1-KO mice.

- In vivo impact of PTPH1 in inflammatory response upon challengeof PTPH1-KO mice with two potent immunomodulatory molecules, carrageenan and LPS. Cytokine release, inflammatory pain and gene expression were investigated in challenged PTPH1-WT and KO mice.

Chapter 2: Materials and Methods

2.1. PTPH1 KO mice design

PTPH1-KO mice were generated using the Velocigene technology [166]. A mouse BAC containing the PTPH1 gene was modified: an in-frame LacZ reporter sequence and a neomycin-selectable marker replaced exons 15 to 22 encoding for the PDZ and the catalytic domain of PTPH1 (Fig. 6). BAC electroporation into embryonic stem cells was performed. F1 heterozygous mice were bred to generate F2 PTPH1-KO mice. The 5_- and 3_-flanking mouse sequences of the lacZ insert were . . . CTC TCA CGT GTC TTC TAG AGT GAC and AGA CAT CAA ACC CAC CCT TCT CC . . . .

Line breeding and animal care were performed in Charles River Italy and France.

Fig. 6: Construction of PTPH1-KO mice: schematic representation of the predicted mouse PTPH1 gene intron-exon organization and deleted exons 15–22, corresponding to the catalytic and PDZ domain. The LacZ coding sequence was inserted in-frame with upstream PTPH1 cDNA.
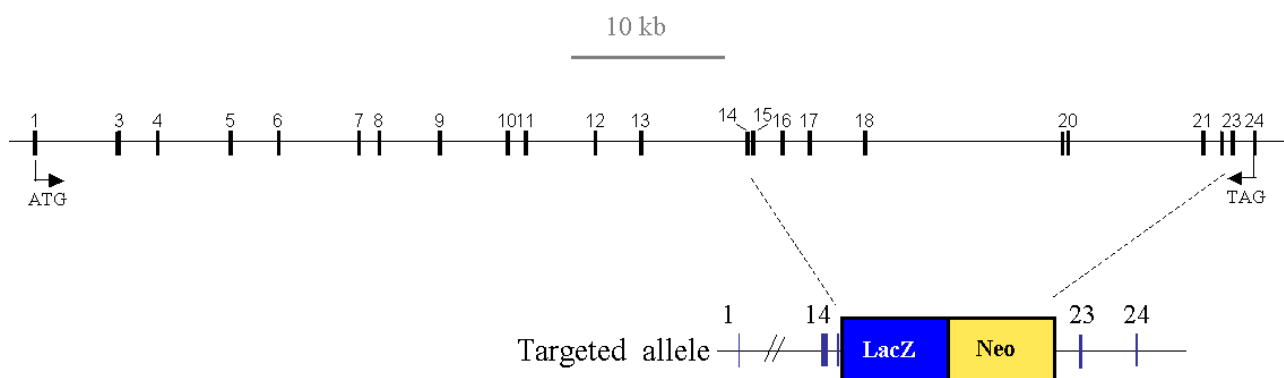
PTPH1-KO and wild type littermates (F2 generation, 87.5% C57Bl/6 – 12.5% 129S6SvEv) were individually housed in top filter cages and maintained in a 12:12 hours light: dark cycle (lights on at 7 am) at 21±1°C, relative humidity (55±10%), with food and water available *ad libitum*. Protection of animals used in the experiment was in accordance with Directive 86/609/EEC, enforced by the Italian D.L. No. 116 of January 27, 1992. Physical facilities and equipment for accommodation and care of animals were in accordance with the provisions of EEC Council Directive 86/609.

2.2. PCR-based Genotyping

Tail snips from mice were collected and genotyped. Tail snips were digested overnight with proteinase K (Sigma) and passed through a vacuum column (Promega, Wizard_ SV 96 genomic DNA purification system A2370) for DNA trapping. Genomic DNA was washed in Wizard SV Wash solution (Promega; containing 95% ethanol) and eluted in 200 µl of water at 65 °C. After protease inactivation at 95 °C, 2 µl of DNA were used for the PCR. Two PCRs were conducted in parallel (TAQ GOLD kit, 0.2 U/µl final; Applied Biosystems N8080256). A multiple PCR with three primers was used that distinguished WT, KO, and HET mice.

The forward primer was designed in the flanking region of the cassette insertion site, the "reverse1" primer was designed in the deleted region, and the "reverse2" primer was inside the cassette (primer sequences: forward, 5_-CTG CTC TCC AGA TGG AGT TG-3; reverse1, 5_GCC ATC TCC ATC GTC ACT CT-3_ (for WT/HET); and reverse2, 5_-CCT AGC TTC CTC ACT GTT TCT-3_ (for KO/HET)). The pair of primers "forward/ reverse1" gave an amplification product 254 bp (indicating WT or HET genotypes). The pair of primers "forward/reverse2" gave an amplification product 320 bp (indicating KO or HET genotype). In parallel to the multiple PCR, another PCR for LacZ insert was performed for confirmation to distinguish HET and KO mice from WT mice (primers sequences: forward, 5_-TCA TTC TCA GTA TTG TTT TGC C-3_; and reverse, 5_-CCA CTA TCA GTT GGT CAC TG-3_).

2.3. LacZ staining procedure and immunohistochemistry

PTPH1-KO and WT mice were sacrificed by intraperitoneal (i.p.) overdose of thiopental (5%), perfused with paraformaldehyde 4%. Organs and tissues of interest were collected (different muscles, bones, kidneys, liver, lungs etc.) then washed in PBS and incubated overnight at 37°C in a solution containing the substrate for beta-galactosidase (beta-gal, encoded by the LacZ cassette) coupled to a NBT salt. The organs and the tissues iwhen sectioned display a green/blue staining where PTPH1 gene is normally expressed. After rinsing into PBS, organs were postfixed in PFA 4% for 1 hour, then incubated in 50% glycerol overnight at 4°C and finally maintained in 70% glycerol at room temperature. LacZ staining was observed through a low magnification microscope and described by an operator blind to the genotypes.

LacZ staining was also performed on PTPH1-WT, KO and HET sections of adult animals. Mice (n=3, 12 months old) were sacrificed by i.p. injection of an overdose of thiopental (5%), perfused with PBS and PFA 4%. Tissues were removed and postfixed overnight at 4°C in PFA 4%,

then placed overnight at 4°C in 15% and finally in 30% sucrose buffer. The brains were then included in O.C.T. (Tissue-Tek) and 20 μm sections were cut on slides with a cryostat. The slides were incubated in LacZ staining solution (see above) overnight at 37°C, washed thrice in PBS (5min each) and either counterstained with H&E (Merck KGaA) or co-expressed with antibody immunostaining. Briefly, CNS sections were incubated for 3 hours at room temperature in blocking solution (Vectastain Kit), washed in TBS (Tris-buffered saline), incubated overnight at 4°C with a solution containing the primary antibody: mouse anti-mouse Neuronal Nuclei (Chemicon MAB377, 1/1000), rabbit anti-mouse Cholecystokinin A receptor (CCKAR; Abcam ab28627, 1/5000), rabbit anti-mouse Tyrosine hydroxilase (TH; Chemicon AB152, 1/1000), mouse anti-mouse glutamic acid decarboxylase (GAD-67; Chemicon MAB5406, 1/5000). The staining was revealed by ABC kit secondary antibody (mouse/rabbit Vectastain Kit), and DAB (Sigma). After dehydration, sections were transferred onto coverslips. LacZ staining and co-expression with the correspondent antibody immunoreactivity was observed by microscopy and described by an operator blind to the genotypes.

2.4. Materials and Methods 1: PTPH1 in CNS functions

2.4.1. Semiquantitative RT-PCR for beta galactosidase gene

Semiquantitative RT-PCR for PTPH1 and beta-gal gene expression was performed on different brain areas of PTPH1-KO and WT mice in order to confirm the presence of beta-galactosidase (LacZ) expression in the KO tissues replacing PTPH1 PDZ and catalytic domain. Brains from KO and WT mice (n=5, 6 months old) were freshly removed and rinsed in HBSS. Hippocampus, cerebellum, cortex, striatum, midbrain and olfactory bulbs were dissected. Total RNA was extracted using Trizol Reagent (Invitrogen) and cleaned-up by RNAeasy columns from Qiagen. 5μg of total RNA were used to perform the RT-PCR reaction (SuperScript II RT kit, Invitrogen). The primer sequences for LacZ amplification were the following: LacZ – forward 5'-GAT GTA CGT GCC CTG GAA CT/reverse 5'-GGT CCC ACA CTT CAG CAT TT. In order to load equally the reaction mixes, a 300 bp fragment of Histone 2A was amplified as a house keeping gene with the following primers: H2Az forward - 5' CGT ATT CAT CGA CAC CTG AAA; H2Az reverse - 5' CTG TTG TCC TTT CTT CCC GAT.

2.4.2. Behavioral phenotyping test battery

Neurological functions of PTPH1-WT and KO mice (males and females, 11 weeks-old, n=10 per gender per genotype) were assessed through a behavioral test battery.

The sequence of the test battery was chosen from the least invasive to the most ones. The schedule of the testing sessions included one week of recovery from one test to the next, as reported in Table 1.

Table 1: Schedule of the behavioral test battery.

Age (wks)	8	9	10	11	12	13	14	15
10M+10F	arrival	quarantine	adaptation	**Open Field**	**EPM**	**Rotarod**	**Y-maze**	**Hot plate**

Open field

After one hour of adaptation in the testing room, each mouse was placed in an open field chamber (50cm^2 wide with white floor and walls) (ViewPoint Life Sci. Inc.) to test locomotor activity and anxiety-like behaviors. Locomotion was recorded for one hour by a video camera and analyzed automatically by VideoTRACK$^®$ software (ViewPoint Life Sci. Inc.). Locomotor activity was evaluated by calculating the total path length traveled, whereas the relative time spent in the center was taken as indicative of anxiety-like behavior [167]. The tests were performed in two sessions with equivalent group representation.

Elevated plus maze

After one hour of adaptation in the testing room, anxiety-like behavior was tested for each mouse by EPM within one session. The apparatus consists of four arms (29.5 cm long and 5 cm wide each). Two arms are open whereas the 2 others are limited by 2 black walls (20 cm high). The number of entries of each mouse in the open and closed arms was recorded by a video camera during a period of 5 minutes and analyzed by the SMART Video-Tracking Software (ViewPoint Life Sci. Inc.). The total number of entries into the arms is an index of locomotion, whereas the percentage of time spent and percentage of entries in the closed arms is an index of anxiety-like behaviors [168] .

Accelerated rotarod

Motor ability, coordination and learning were evaluated by using an Accelerated Rotarod apparatus for mice (Cat. # 7650 by Jones and Roberts, distr. by Basile Instr., Italy). The apparatus

was placed within the animal colony room and was cleaned after each trial. Mice were tested for their abilities to maintain a balance on a rotating bar, which accelerated from 4 to 40 rpm/min in a 5 min trial. Latency to fall off was measured within one session and all mice underwent four trials (one every 30 min) [169-171]. The differences at the rotarod performances in WT and KO were assessed by a single set of trials [170,171]. This set-up allows a major focus on the early phases of motor learning, involving a strong activation of prefrontal cortex and of the associative areas of basal ganglia and cerebellum [172,173].

Y-maze alternation

After one hour of adaptation in the testing room, mice were tested on a Y maze apparatus (40 cm long /8 cm wide arms with transparent walls) to investigate spatial working memory [174]. The number and the sequence of the arm entries for each mouse were recorded during 5 minutes. The locomotion index was calculated as the overall number of arm entries, whereas the working memory index was calculated as following: number of exact alternations (entries into three different arms consecutively)/ possible alternations (i.e. the number of arms entered minus 2) X 100.

Hot plate

Thermal sensitivity was assessed by a hot plate apparatus for mice (Cat. # 7280 by Biol. Research Apparatus, distr. by Basile Instr., Italy) and lasted a maximum of 45 seconds, time at which damages could occur [175]. The apparatus was placed in the animal colony room and all the mice were tested within one session. Animals were placed on a surface heated at 52.5°C and the latency (seconds) to shake or lick the paw was recorded by the operator.

2.4.3. Superarray analysis

Hippocampus and cortex of PTPH1-KO and WT male (3 months-old) (n=3 per genotype) and female (n=4 per genotype) mice were collected and RNA was extracted and transcribed into cDNA. Two superarray plates were used: Mouse Signal Transduction Pathway Finder™ RT² *Profiler*™ PCR Array (#PAMM-014) and Mouse Neurotrophin and Receptors RT² Profiler™ PCR Array (#PAMM-031).

The Mouse Signal Transduction Pathway Finder™ plate profiles the expression of 84 key genes representative of 18 different signal transduction pathways listed in Table 1.

The Mouse Neurotrophin and Receptors RT² Profiler™ plate profiles the expression of 84 genes related to neuronal processes (Table 2). Neurotrophic signaling molecules are represented on

this array including neurotrophins and neuropeptides along with their receptors. Genes involved in the normal functions of the neuronal system including neuronal cell growth and differentiation and neuronal regeneration and survival are included. The cytokines and their receptors involved in neuronal signaling are contained on this array along with genes involved in the transmission of nerve impulses, genes involved in neuronal apoptosis in response to neurotrophic factors and transcription factors and regulators indicative of the activation pathways downstream of the neuronal system.

2.4.4. Statistical analysis

Statistical comparisons were performed by unpaired two-tailed T-test ($p<0.05$) and two-way ANOVA ($p<0.05$) followed by post-hoc test as necessary. In the accelerated rotarod, two-way ANOVA with repeated measures followed by T-test was used. Results are expressed as mean±SEM.

Table 2: Mouse Signal Transduction Pathway Finder™ RT² *Profiler*™ PCR Array (#PAMM-014).

Pathways	Genes
Mitogenic Pathway	Egr1 (egr-1), Fos (c-fos), Jun (c-jun), Nab2.
Wnt Pathway	Birc5, Ccnd1 (cyclin D1), Cdh1, Fgf4, Jun (c-jun), Lef1, Myc (c-myc), Pparg, Tcf7, Vegfa, Wisp1.
Hedgehog Pathway	Bmp2, Bmp4, En1 (engrailed), Foxa2 (forkhead box A2 / HNF3B), Hhip, Ptch1 (patched 1), Wnt1, Wnt2.
TGF-β Pathway	Cdkn1a (p21^{Waf1}, p21^{Cip1}), Cdkn1b (p27), Cdkn2a (p16^{Ink4}), Cdkn2b (p15 ^{Ink2b}).
PI3 Kinase / AKT Pathway	Bcl2 (Bcl-2), Ccnd1, Fn1 (fibronectin), Jun (c-jun), Mmp7 (matrilysin), Myc (c-myc).
Jak / Src Pathway	Bcl2 (Bcl-2), Bcl2l1 (Bcl-XL).
NFκB Pathway	Birc1a, Birc2 (c-IAP2), Birc3 (c-IAP1), Tert.
p53 Pathway	Bax, Cdkn1a (p21Waf1, p21Cip1), Ei24 (Pig3), Fas (Tnfrsf6), Gadd45a (gadd45), Igfbp3, Mdm2.
Stress Pathway	Atf2, Fos (c-fos), Hsf1 (tcf5), Hspb1 (Hsp25), Myc (c-myc), Trp53 (p53).
NFκB Pathway	Ccl20, Cxcl1, Icam1, Ikbkb, Il1a, Il2, Lta (TNFb), Nfkbia, Nos2 (iNOS), Tank, Tnf (TNFa), Vcam1
NFAT Pathway	Cd5, Fasl (Tnfsf6), Il2
CREB Pathway	Cyp19a1, Egr1 (egr-1), Fos (c-fos).
Jak-Stat Pathway	Cxcl9 (MIG), Il4ra, Irf1, Mmp10 (stromelysin-2), Nos2 (iNOS).
Estrogen Pathway	Bcl2 (Bcl-2), Brca1, Greb1, Igfbp4, Nrip1
Androgen Pathway	Cdk2, Cdkn1a (p21^{Waf1}, p21^{Cip1}), Tmepai.
Calcium and Protein Kinase C Pathway	Csf2 (GM-CSF), Fos (c-fos), Il2, Il2ra (IL-2 R?), Jun (c-jun), Myc (c-myc), Odc1, Tfrc.
Retinoic Acid Pathway	En1 (engrailed), Hoxa1, Rbp1 (CRBPI
LDL Pathway	Ccl2, Csf2 (GM-CSF), Sele, Selp (P-selectin), Vcam1
Insulin Pathway	Cebpb (C/EBP-?), Fasn (fatty acid synthase), Gys1 (GS, glycogen synthase), Hk2 (hexokinase II), Lep (Ob).
Phospholipase C Pathway	Bcl2 (Bcl-2), Egr1, Fos (c-fos), Icam1, Jun (c-jun), Nos2 (iNOS), Ptgs2 (cox-2), Vcam1.

Table 3: and Mouse Neurotrophin and Receptors RT² Profiler™ PCR Array (#PAMM-031).

Function	Detailed function	Genes
Neurotrophins and Receptors		Adcyap1r1, Artn, Bdnf, Cntfr, Crh, Crhbp, Crhr1, Crhr2, Fas (Tnfrsf6), Frs2, Frs3, Gdnf, Gfra1, Gfra2, Gfra3, Gmfb, Gmfg, Hcrtr1, Hcrtr2, Mt3, Ngfb, Ngfr, Ngfrap1, Nr1i2, Nrg1, Nrg4, Ntf3, Ntf5, Ntrk1, Ntrk2, Pspn, Ptger2, Tfg, Cd40 (Tnfrsf5), Tro, Ucn, Zfp110, Zfp91 (Cntf).
Neuropeptides and Receptors	Neuropeptide Hormone Activity	Npff.
	Bombesin Receptors	Grpr, Nmbr.
	Cholecystokinin Receptors	Cckar
	Galanin Receptors	Galr1, Galr2
	Neuropeptide Y Receptors	Nmbr, Npy1r, Npy2r, Ppyr1.
	Neurotensin Receptors	Ntsr1.
	Other Neuropeptides and Receptors	Npffr2 (Gpr74), Hcrt, Mc2r, Npy, Nrg1
Neurogenesis:	Central Nervous System Development	Cxcr4, Fgfr1, Ngfr, Ntf3.
	Peripheral Nervous System Development	Artn, Gdnf, Gfra3, Ngfb, Nrg1, Ntf3.
	Axon Guidance	Artn, Gfra3, Ngfr.
	Gliogenesis	Fgf2, Nrg1, Ntf3.
	Dendrite Morphogenesis	Bdnf, Mt3
	Other Neurogenesis Genes	Bax, Fos, Galr2, Gfra1, Gfra2, Ntf5, Ntrk1, Ntrk2.
Synaptic Transmission		Cbln1.
Cell Growth and Differentiation	Growth Factors and Receptors	Artn, Bdnf, Fgf2, Fgf9, Fgfr1, Gdnf, Gmfb, Gmfg, Il10, Il1b, Il6, Lif, Mt3, Ngfb, Nrg4, Ntf3, Ntf5, Pspn, Tgfa, Tgfb1, Tgfb1i1, Tro, Trp53.
	Cell Cycle	Fgf2, Fgf9, Il1b, Ntrk1, Tgfa, Tgfb1, Trp53.
	Cell Proliferation	Bax, Cxcr4, Fgf2, Fgf9, Grpr, Il10, Il1b, Myc, Stat4, Tgfa, Tgfb1, Trp53.
	Cell Differentiation	Fgf2, Fgf9, Nf1, Nrg1, Stat3, Trp53, Zfp91 (Cntf).
	Cytokines and Receptors	Cx3cr1, Cxcr4, Il10, Il10ra, Il1b, Il1r1, Il6, Il6ra, Il6st, Lif, Lifr, Nrg1, Stat4.
Apoptosis:	Anti-apoptosis	Bcl2, Bdnf, Il10.
	Caspase Activation	Bax, Myc, Trp53.
	Induction of Apoptosis	Bax, Fas (Tnfrsf6), Myc, Ngfr, Ngfrap1, Trp53.
	Other Apoptosis Genes	Hspb1, Il6, Cd40 (Tnfrsf5).
Immune response	Acute-phase response	Il6, Stat3.
	Inflammatory response	Il10, Il1b, Tgfb1.
	Lymphocyte activation	Il10, Cd40 (Tnfrsf5).
	Other immune reponse genes:	Fas (Tnfrsf6), Lif.
Transcription factors and regulators	Positive regulation of transcription	Fus, Ntf3, Tgfb1i1.
	Transcription coactivator activity	Maged1, Tgfb1i1.
	Other transcription factors and regulators	Atf2, Fos, Mef2c, Myc, Nr1i2, Stat1, Stat2, Stat3, Stat4, Trp53, Zfp110

2.5. Materials and Methods 2: PTPH1 in GHR signaling

2.5.1. Animals

PTPH1 heterozygous (HET) aged 3-4 months were used for mating. Prior to mating, mice were housed in separate cages. For mating, one male and one female for each genotype were housed together and maintained as previously described. Weaning of pups occurred at 21st day of age and they were housed 2-3 per cage. At 21 days of age a tail snip was taken for genotyping. Pups were weighed every 2 days, and were sacrificed at 80 days of age by inhalation of CO_2 and analyzed by DEXA.

PTPH1-KO female and male littermates (n=4 animals per group), 3-4 months old were used for IGF-1 quantification in the serum and in the liver. Briefly, PTPH1-WT and KO mice were sacrificed by inhalaton of CO_2 and blood and liver were collected.

2.5.2. DEXA analysis

Lunar PIXImus II Densitometer (GE Medical Systems was used to measure bone and tissue composition by dual-energy x-ray absorptiometry (DEXA) densitometry on 80 day mice. After sacrifice, animals were positioned on the DEXA plate. X-ray were applied and total body images were recorded in less than 5 minutes.

2.5.3. Serum IGF-1 Quantification

Blood from wild type and PTPH1 KO female and male littermates (n=4 animals per group) were sampled individually and clotted for 2 h at room temperature. The serum was removed after a 20-min centrifugation at 1000 g, and IGF-1 concentration was measured with a mouse IGF-1 Quantikine enzyme-linked immunosorbent assay kit (R & D Systems, MG-100).

2.5.4. mRNA quantification by qPCR

Total RNA was extracted from the liver of WT and KO mice using TRIzol reagent (Invitrogen 15596-026) using the manufacturer's protocol. Taqman analysis was performed on igf1 gene (#Mm00439560_m1, Applied Biosystems) using SYBR GREEN PCR master mix (4309155 from Applied Biosystems).

2.6. Materials and Methods 3: PTPH1 role in inflammatory process in vivo

2.6.1. Animals

To investigate the role of PTPH1 in the inflammatory process in vivo, two different approaches were used. Inflammation was induced by LPS and carrageenan (see method below) on PTPH1 KO and WT mice.

PTPH1-KO mice were generated and housed as previously described. The experiments were performed on female animals. Animals were allowed to acclimate for 1 week before the beginning of the experiments. All behavioral tests were performed during the light phase and animals were allowed 1-hour habituation to the test room, if different from the holding room, before testing. Testing sequence was randomized between KO and WT animals, and all apparatus were thoroughly cleaned between two consecutive test sections.

2.6.2. Cytokine beads assay (CBA)

In both LPS and carrageenan experiments, a panel of cytokine was analyzed in blood. At sacrifice, whole blood was collected from the heart of the animals and plasma was obtained by centrifugation. 25 µl of plasma were used to quantify the levels of the circulating inflammatory cytokines TNFα, MCP-1, IL-6, IL-10, IFN-γ, IL-12p70 using a mouse inflammation cytometric beads array kit (BD Bioscience), according to the manufacturer's instructions. Data were acquired with a FACSCalibur flow cytometer and analyzed with BD CBA Software (BD Bioscience).

2.6.3. LPS-induced inflammation

PTPH1-WT and KO female mice (*young:* n=3-6, 8 weeks old; *aged:* n=3-6, 34-36 weeks old) received an i.p. injection of 200 µl of 1mg/kg lipopolysaccaride (LPS) (Escherichia coli 0127:B8, batch 032K4099, L3880, Sigma) and randomized groups of mice were sacrificed by an ip overdose of thiopental at 30, 60 and 180 minutes after LPS injection. The test was performed in three sessions with equivalent group representation. 200 µl of WFI were administer to control mice.

2.6.3.1. RTPCR on PBMC

At the defined timepoints (see above), whole blood was collected, red blood cells were lysed using BD PharM Lyse (BD Biosciences/BD Pharmingen) and RNA was extracted from the white cells by TriZol reagent (Invitrogen). Taqman analysis was performed on LPS- and vehicle-treated white cells of both genotypes. The PCR was carried out on cytokine genes: ccl2 (#Mm00441242_m1, Applied Biosystems), IL1b (#Mm01336189_m1, Applied Biosystems), IL12a (#Mm00434169_m1, Applied Biosystems), IL6 (#Mm00446190_m1, Applied Biosystems), TNF (#Mm00443258_m1, Applied Biosystems). The expression of PTPH1-related genes was also investigated: adam17 (#Mm00456428_m1, Applied Biosystems), ghr (#Mm00439093_m1, Applied Biosystems), IGF1 (#Mm00439560_m1, Applied Biosystems), IGF1R (#Mm01318459_m1, Applied Biosystems). 200ng of total RNA were used to perform the RT-PCR reaction (SuperScript II RT kit, Invitrogen). The qPCR experiment was carried out using the Taqman Universal PCR master mix (Applied Biosystems) and the gene assays mentioned above. The comparative Ct method [176] was used for data analysis, where:

$$\Delta\Delta Ct = \Delta Ct_{sample} - \Delta Ct_{reference}$$

and ΔCt_{sample} is the Ct value for any sample normalized to the endogenous housekeeping gene (beta-2-microglobin, Applied Biosystems) and $\Delta Ct_{reference}$ is the Ct value for matched PTPH1-WT vehicle treated value, also normalized to the endogenous housekeeping gene.

2.6.4. Carrageenan-induced inflammation

Female PTPH1-KO and WT mice (n=7, 12 weeks old; n=7, 12 months old) were tested for inflammation-induced edema and hyperalgesia/allodynia.

On the test day n=7-8 animals per genotype were injected subcutaneously in the right hind paw plantar surface with 30μL of a solution of 2% carrageenan λ (Sigma, Germany) freshly prepared in saline. 30μL of saline was injected as control in the controlateral paw. Animals were tested at automated Von Frey and Hargreaves apparatus, to evaluate respectively tactile allodynia and thermal hyperalgesia, at 1, 3, 5 and 24 hours after carrageenan/saline injection, followed by paw thickness measurement, using a precision caliper (Mitutoyo, Japan). Mice underwent also to a Catwalk analysis at the same time points. Mice were sacrificed by an intraperitoneal (ip) overdose of thiopental, and paws were removed for histological evaluation.

2.6.4.1. Hargreaves' plantar test

Thermal hyper/hypoalgesia was assessed by Hargreaves' plantar apparatus (Plantar test, Ugo Basile, Italy)[177].The test was performed at 1, 3, 5 and 24 hours post 2% carrageenan injection. Animals were accustomed to the apparatus for 1 hour during 2 days preceding the test. On the test day, mice were individually placed in a clear acrylic box on a glass platform and a removable infrared generator (radiant heat 137mW/cm^2/s) was placed underneath the hind paw. The apparatus automatically detects the withdrawal of the paw. Latency of each paw withdrawal was recorded and mean values of left and right paw used as reaction index for the individual animal. A cut-off of 25 seconds was used to avoid tissue damage in case of absence of response.

2.6.4.2. Automated Von Frey test

Tactile hyper/hypoalgesia was assessed by a Dynamic Plantar Aesthesiometer (Ugo Basile, Italy). The test was performed immediately after the Hargreaves's test. PTPH1-WT and KO mice were accustomed to the apparatus for 1 hour during 2 days preceding the test day. On the test day, animals were individually placed in a clear acrylic box with a grid floor. A blunted probe was placed under the plantar surface of one hind paw and automatically exerted a constantly increasing force to the plantar surface (from 0 up to 5 grams over 20 s). Force applied (g) at the retraction reflex was automatically recorded. Each hind paw was tested 3 times and mean values used as individual parameter for group statistic.

2.6.4.3. CatWalk

Detailed analysis of gait was performed on walking WT and KO mice using the CatWalk™ (Noldus Information Technology) method [178,179]. Briefly, light from a fluorescent tube is distributed through a glass plate. Light rays are completely reflected internally. As soon as the paw of the animal was in contact with the glass surface, light was reflected downwards. It resulted in a sharp image of a bright paw print. The whole run was recorded via a camera placed under the glass plate.

In the present study, the following parameters related to single paws were analyzed:

- *Intensity* (expressed in arbitrary units in the range 0-255): this parameter describes the mean pressure exerted by one individual paw during the floor contact, during the whole crossing of the walkway. The intensity parameter is highly correlated with the Von Frey thresholds [180].

- *Duty cycle* (expressed in %): the duty cycle represents stand duration as a percentage of step cycle duration. It is calculated according to the formula: stand duration/(stand + swing phases

duration)×100, where the stand phase is indicated as the time of contact (in seconds) of one paw with the glass plate in a single step cycle and the swing phase is indicated as seconds of non-contact with the plate during a step cycle. The duty cycle parameter is highly correlated with the Von Frey thresholds[181].

- *Maximum contact area* (expressed in mm2): the maximal contact area describes the paw area at the moment of maximal paw-floor contact, during stand phase.

- *Print area* (expressed in mm2): this parameter describes the surface area of the complete paw print during the stand phase.

2.6.4.4. Hematoxylin and Eosin histology

At sacrifice paws were collected and placed in 4% formalin. Paws are then incubated for 10-15 days in Shandon TBD2 decalcifier (Thermo-Scientific) and subsequently cut in 7 μm thick slices by a microtome. After mounting, the slides are let overnight at 37°C, dehydrated and stained with hematoxylin and eosin in a multiple steps procedure. Histological evaluation was observed by microscopy and described by an operator blind to the genotypes.

2.6.5. Statistical analysis

Statistical comparisons were performed by Two-way Anova followed by T-test (RT-PCR) and Bonferroni's (CBA) post-hoc analysis ($p<0.05$) at each time points. Results are expressed as mean±SEM. Significant difference were highlighted when $p<0.05$.

Chapter 3 - PTPH1 in CNS functions

3.1 Results on PTPH1 involvement in CNS funtions

3.1.1. PTPH1-KO mice generation

The human and predicted mouse PTPH1 orthologs are well conserved (840 of 913 amino acid identities, or 92% at the protein level). The mouse PTPH1 coding sequences are spread out over 24 exons (Fig. 6). Using the Velocigene® strategy [166], exons numbered 14–23 that encode the PTPH1 catalytic domain were replaced by a LacZ (β-galactosidase)-encoding cassette. Genetic disruption was confirmed using a standardized "loss of native allele" procedure [166]. Transcript mapping on RNA from various organs from wild type and knock-out animals confirmed loss of expression of the PTPH1 catalytic domain but showed that the modified transcript was expressed. Animals carrying one or two copies of the mutant gene were healthy, reproduced normally and showed no obvious phenotype.

3.1.2. LacZ staining in whole mount

PTPH1-KO embryos at embryological stage (ES 14 day and 16 day) display a positive LacZ staining in the hypothalamic area and in the dorsal root ganglia of the spinal cord, excluding the spinal cord itself (Fig. 7). No staining is detectable in the WT embryos.

In PTPH1-KO adult animals, LacZ staining in the brain was observed in the cerebellum, hippocampus and in the thalamic nuclei. In addition a strong staining was observed in the cerebral cortex, tenia tecta and septum (Fig. 8a, 8b).

Fig. 7: LacZ staining on PTPH1-WT and KO embryos. PTPH1-WT embryos do not show any staining either at embryological stage 14 (Es14) or at Es16. PTPH1-KO embryos display a positive LacZ staining in the hypothalamic area and but also in the dorsal root ganglia of the spinal cord, excluding the spinal cord itself.
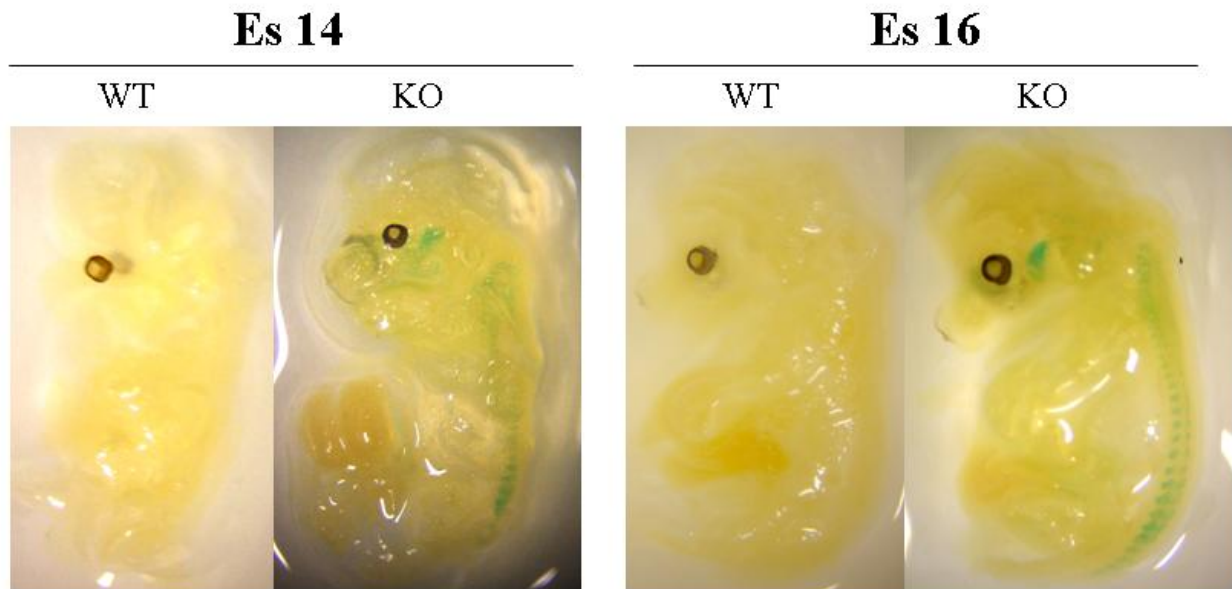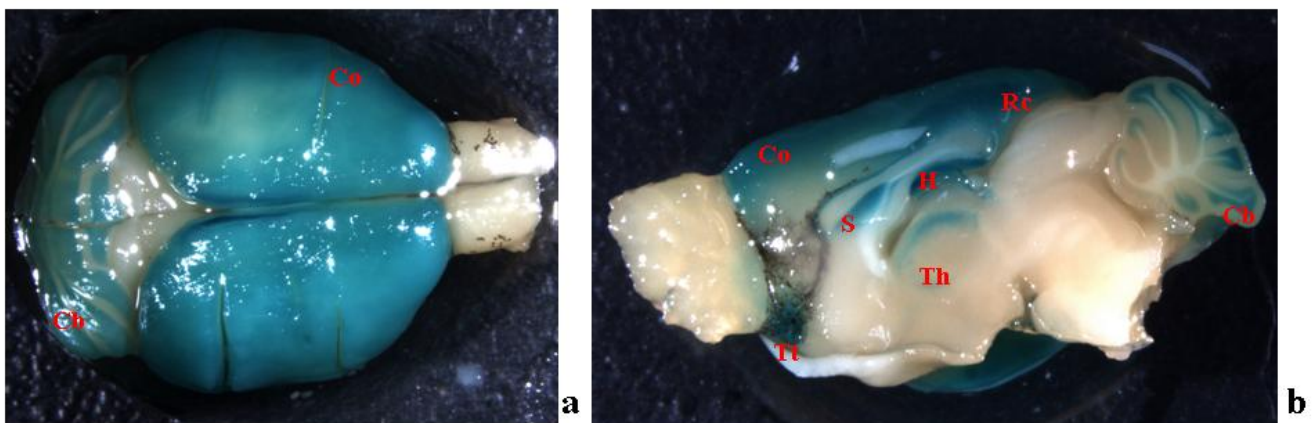

Fig. 8: PTPH1-KO adult mouse brain. a) whole brain, dorsal view, staining in cerebellum (Cb) and cortex (Co); **b)** LacZ staining on brain, sagittal view: detection in the tenia tecta (Tt), cortex (Co), thalamus (Th), hippocampus (H), retrosplenial cortex (Rc), septum (S) and in the granule cell layer of cerebellum.

3.1.3. LacZ staining in sections and RT-PCR results

No gross cytoarchitectural brain differences were observed by simple visual observation at the microscope in the cortex, hippocampus and thalamus in PTPH1-KO mice compared to WT littermates. LacZ staining was performed on frozen brain sections to confirm and to describe the expression of PTPH1 at the brain structural level (Table 4).

Table 4: Qualitative estimation of LacZ staining intensity in the different brain areas. -: absent; +/-: faint; +: present; ++: intense; +++: very intense staining. Cornu Ammonis (CA), Dentate Gyrus (DG), mediodorsal lateral (MDL), anteroventral (AV), ventromedial (VM) ventral posteromedial (VPM), ventrolateral (VL), ventral posterolateral (VPL), laterodorsal (LD), posterior (Po) and reticular (Rt), ventral posteromedial parvicel (VPPC) thalamic nuclei, lateral geniculate nucleus (DLG), parafascicular thalamic nuclei (PF), nuclei (nu).

Brain Area	Intensity of LacZ staining	Brain Area	Intensity of LacZ staining
Cerebral cortex	+	Dorsal Tenia Tecta	++
Retrosplenial cortex	++	Septohippocampal nu	+
CA1 oriens layer	+++	VPL	+
CA1 radiatum layer	+++	MDL	++
CA1 pyramidal cell layer	+	AV	++
CA2 oriens layer	-	VPM	++
CA2 radiatum layer	-	VL	+
CA2 pyramidal layer	+	VM	++
CA3 oriens layer	+	Po	++
CA3 radiatum layer	+/-	LD	+
CA3 pyramidal layer	+	Rt	+
DG granular cell layer	-	DLG	++
DG molecular layer	+++	VPPC	++
DG hilus	-	PF	-
Fascicola cinereum	++	cerebellum	+
Indisium griseum	+		

In cortical regions, LacZ was expressed in the external pyramidal (III) and internal granular layer (IVA) of the cerebral cortex (Fig. 9a, 9b), in the retrosplenial cortex (Fig. 10a-10c; Fig. 11a, 11b) and indusium griseum (Fig. 10a, 10b).

Fig. 9: PTPH1-KO cortical regions a) PTPH1-KO cerebral cortex (10X, scale bar: 220µm). **b)** positive cytoplasmatic and perinuclear LacZ staining (blue dots) in the external pyramidal (III) and internal granular layer (IVA) (63X, scale bar: 10µm).
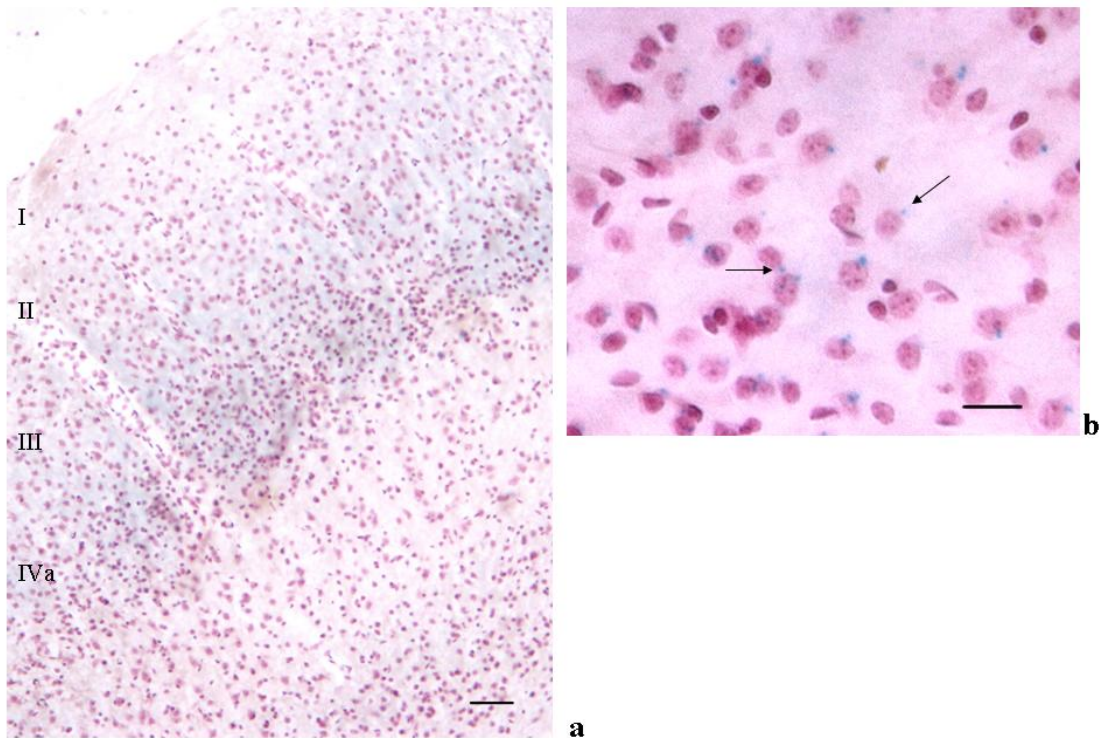

Fig. 10: PTPH1-KO retrosplenial cortex. **a)** LacZ detection in retrosplenial cortex (Rc) and indusium griseum (ig) staining (4X, scale bar: 80µm). **b)** detail of the Rc and ig (40X, scale bar: 20µm); **c)** positive cytoplasmatic staining of the neurons of Rc (63X scale bar: 10µm); the interneural LacZ signals are due to the presence of trans-sectioned axons and dendrites.
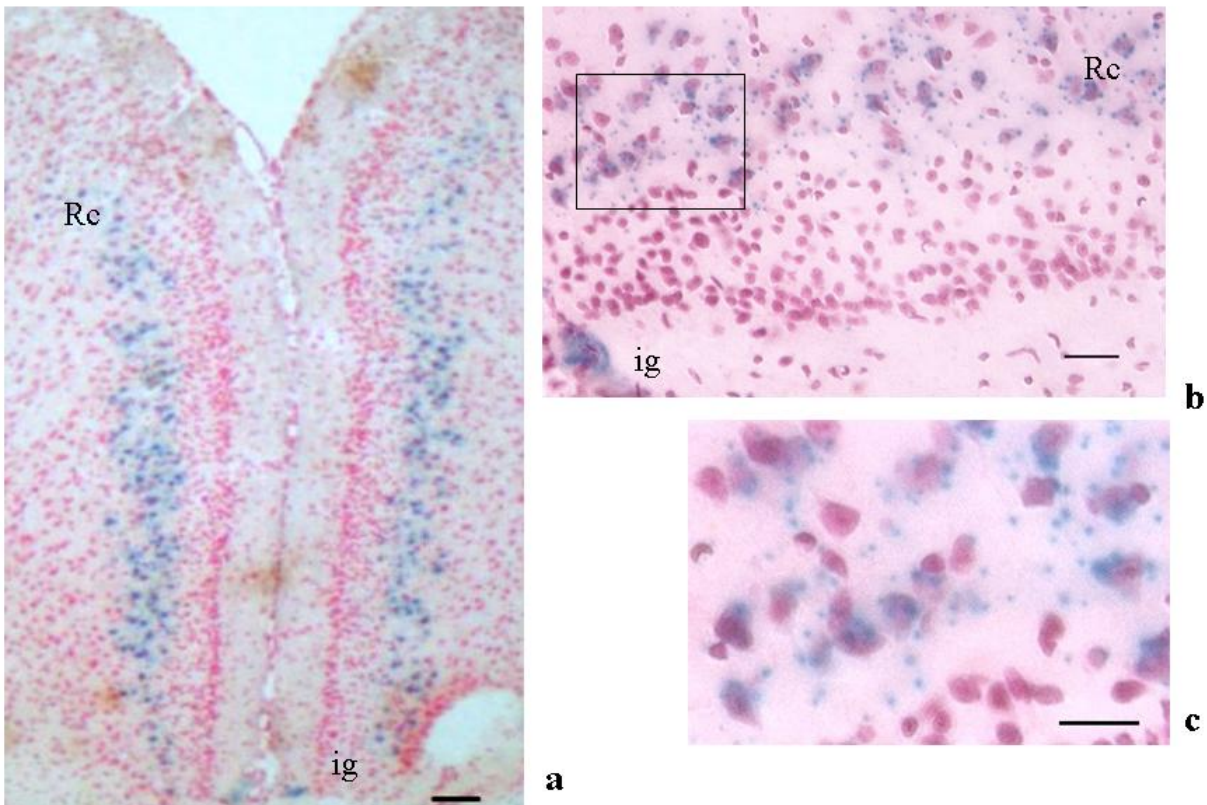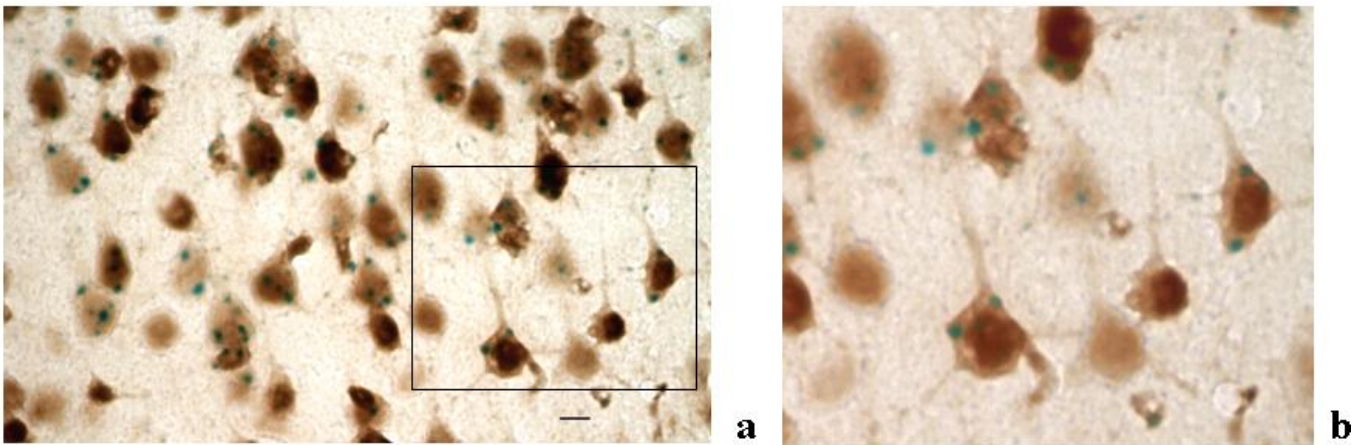
Fig. 11: PTPH1-KO cerebral cortex. **a)** colocalization of NeuN-ir and LacZ staining signal in the Rc (100X, scale bar: 4.5μm).; **b)** detail of the cytoplasmatic signal of LacZ in neurons.

In the cerebellum, in spite of a strong staining in the whole mount (Fig. 8), only a faint LacZ signal was observed in sections (Fig. 12a, 12b) in particular in the granule cells, close to the nuclei. The RT-PCR on cortical and cerebellar extracts confirmed the presence of LacZ expression in these brain areas (Fig. 13).

Fig. 12: PTPH1-KO cerebellar cortex. a) faint LacZ staining in the granule cell layer (20X, scale bar: 16.5μm); **b)** perinuclear staining in the granule cell layer of the cerebellum (63X; scale bar: 5μm).
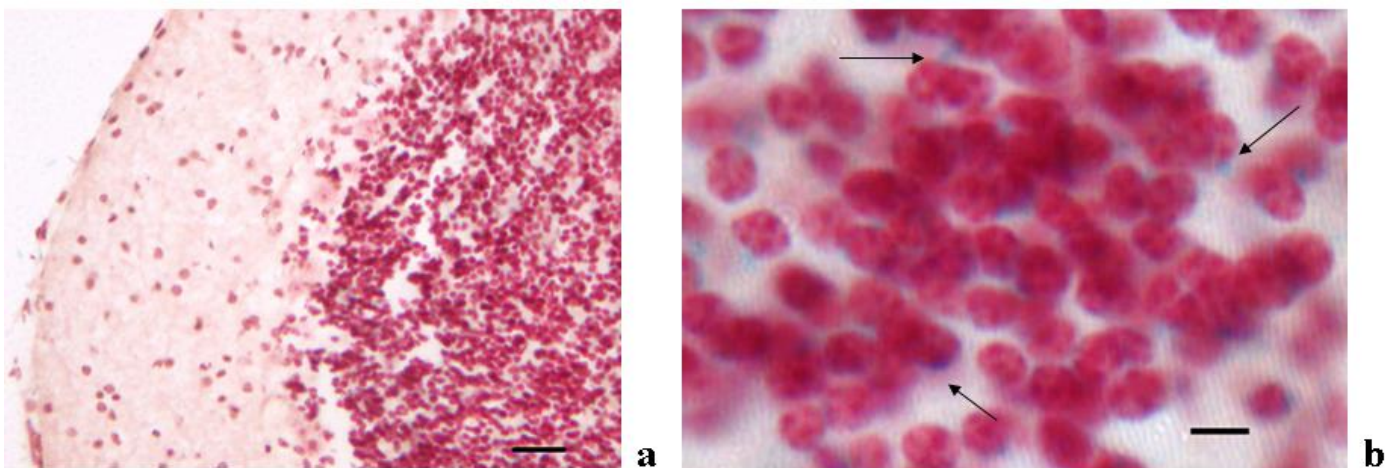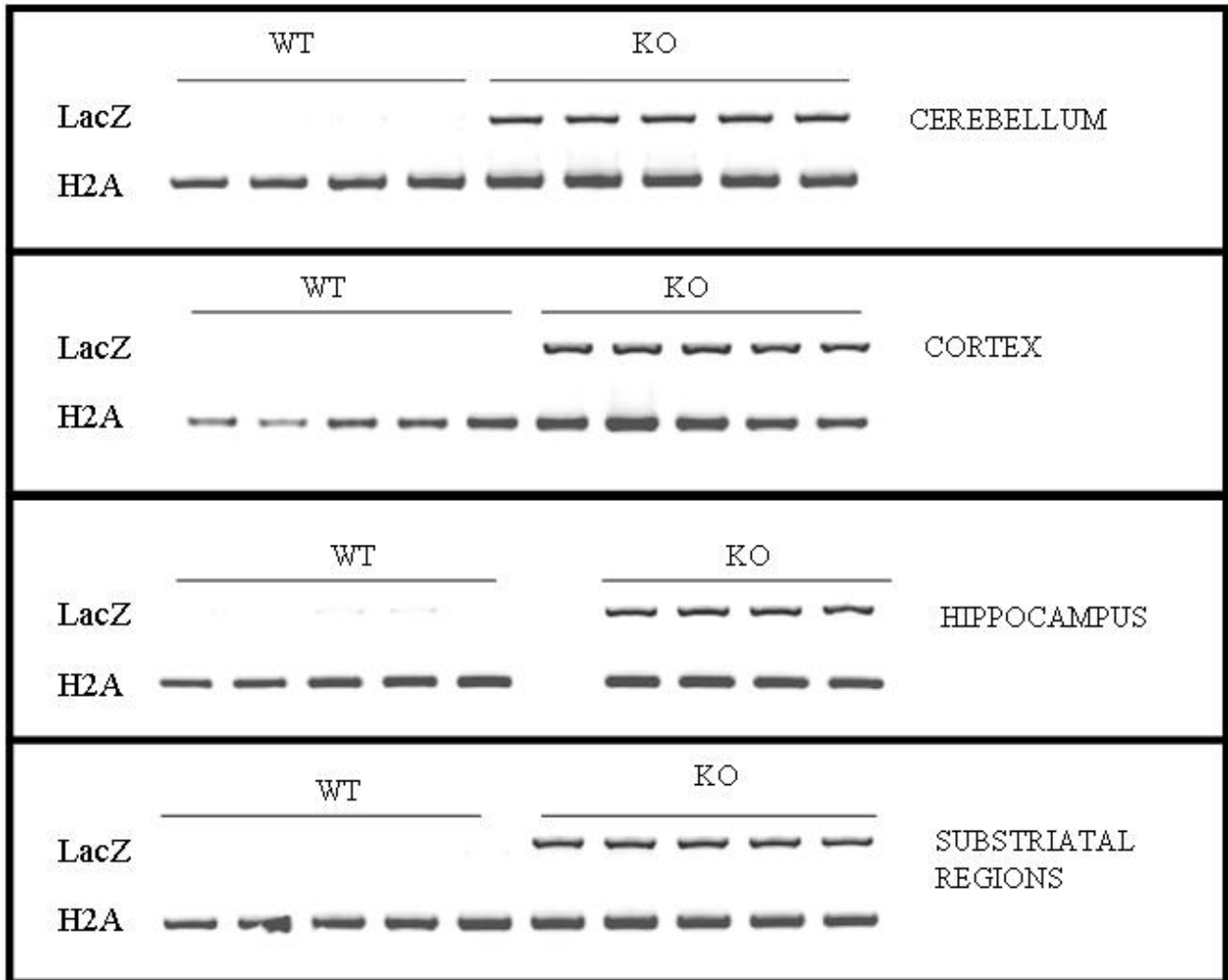
Fig. 13: RT-PCR for beta-galactosidase expression in brain extracts. Beta-gal mRNA is expressed in PTPH1-KO cerebellum, cortex, hippocampus and substriatal regions (midbrain, thalamic nuclei, pontine region); no beta-gal expression detected in WT brain extracts (first lane of each block); histone H2A gene was used as positive control (second lane).

In subcortical regions, LacZ was detected in the anterior ventral, mediodorsal, ventrolateral, anteromedial and central lateral thalamic nuclear groups (Fig. 14a). In more caudal thalamic areas, LacZ was again detectable in the posterior thalamic nuclear group (Po), and to a lesser extent in posteromedial, in posterolateral and in reticular thalamic nuclei and also in the dorsal lateral geniculate nuclei (Fig. 14b-14e). In the tenia tecta, LacZ staining visible in the whole mount preparation was confirmed (Fig. 9, 16a, 16b). The RT-PCR on substriatal regions including the thalamus, the midbrain and the pontine areas confirmed the presence of LacZ expression in some of these brain areas (Fig. 14).

Fig. 14: PTPH1-KO thalamus [182]. **a)** LacZ expression detected in several thalamic nuclei (4X; scale bar: 165 μm): mediodorsal (MD), central lateral (CL), anteroventral (AV), anteromedial (AM), ventromedial (VM) ventral posteromedial (VPM) and ventrolateral (VL) thalamic nuclear groups. MHb: medial habendular nuclei. **b)** LacZ expression detected in the ventral posteromedial thalamic nuclei (VPM) and it is present also in ventrolateral (VL), ventromedial (VM), ventral posterolateral (VPL), laterodorsal (LD), posterior (Po) and reticular (Rt) thalamic nuclei (2.5X, scale bar: 130 μm). **c)** LacZ is expressed in the dorsal lateral geniculate nucleus (DLG) and in the lateroposteral thalamic nuclear group. In this caudal section LacZ staining is more intense in the posterior nucleus, but present also in VPM, VPL and VPPC (ventral posteromedial parvicel) thalamic nuclei (2.5X, scale bar: 130μm). **d)** Detail of beta-gal expression in neural cell body of VPL and VPM at 40X (scale bar: 20μm) and **e)** at 63X (scale bar: 10μm).
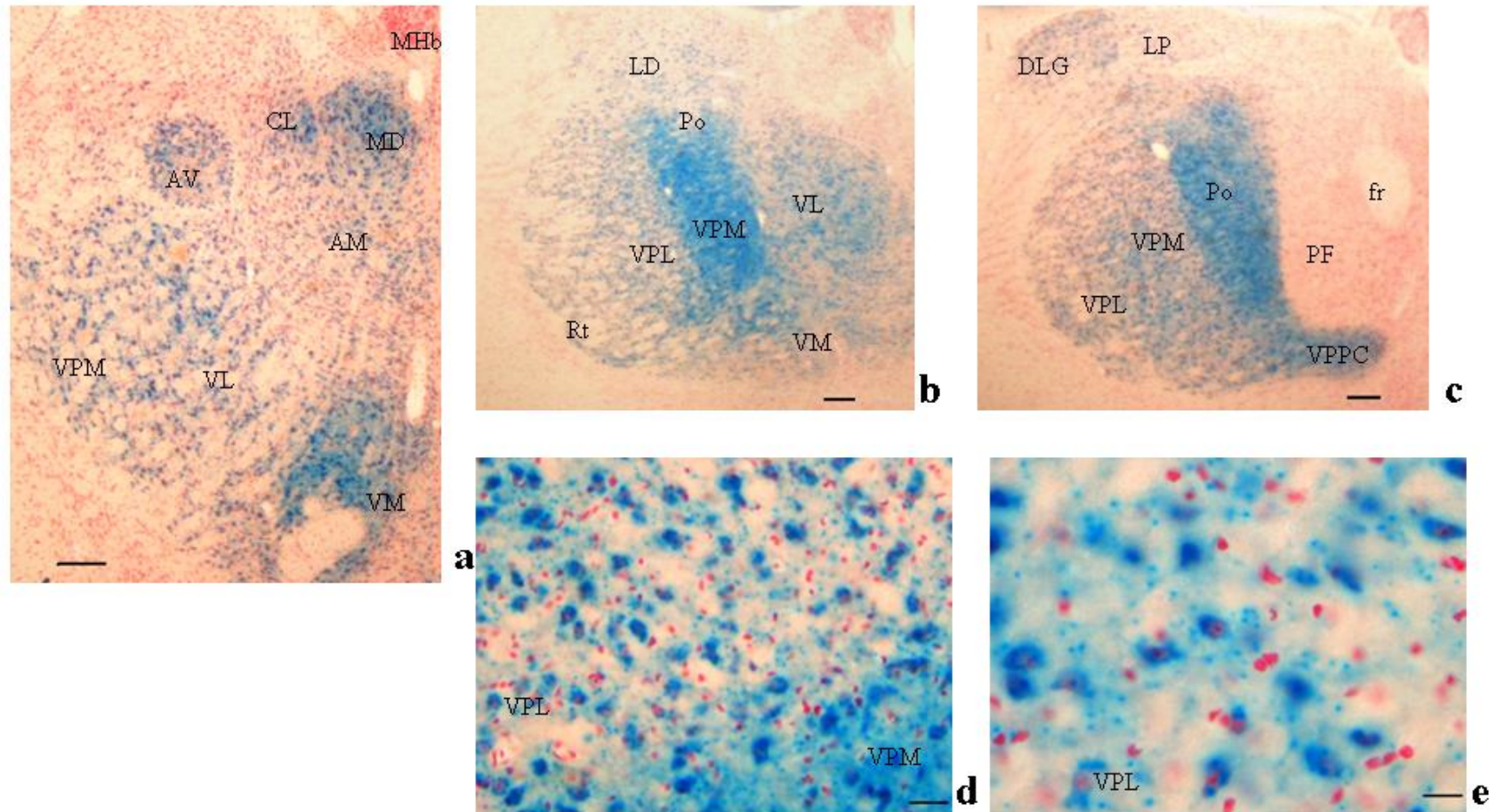
Fig. 15: PTPH1-KO hippocampus [182]. **a)** Hippocampus at 4X; **b)** CA1 area of hippocampus shows very intense LacZ staining in both oriens and radiatum layers and to a less extent in the pyramidal cell layer (20X; scale bar: 90μm). **c)** CA2 area of hippocampus displays LacZ-positive staining in the pyramidal cell layer. **d)** CA3 area shows an intense beta-gal expression in the oriens and pyramidal cell layer, and in a less extent in the radiatum (20X). **e)** The dentate gyrus (DG) displays a strong LacZ staining in the molecular layer and not in the hilus (20X) (scale bar: 20μm). pyr: pyramidal cell layer; oriens: oriens layer; rad: radiatum layer; mol: molecular layer: gr: granule cell layer; lac/mol: lacunosum-molecular layer.
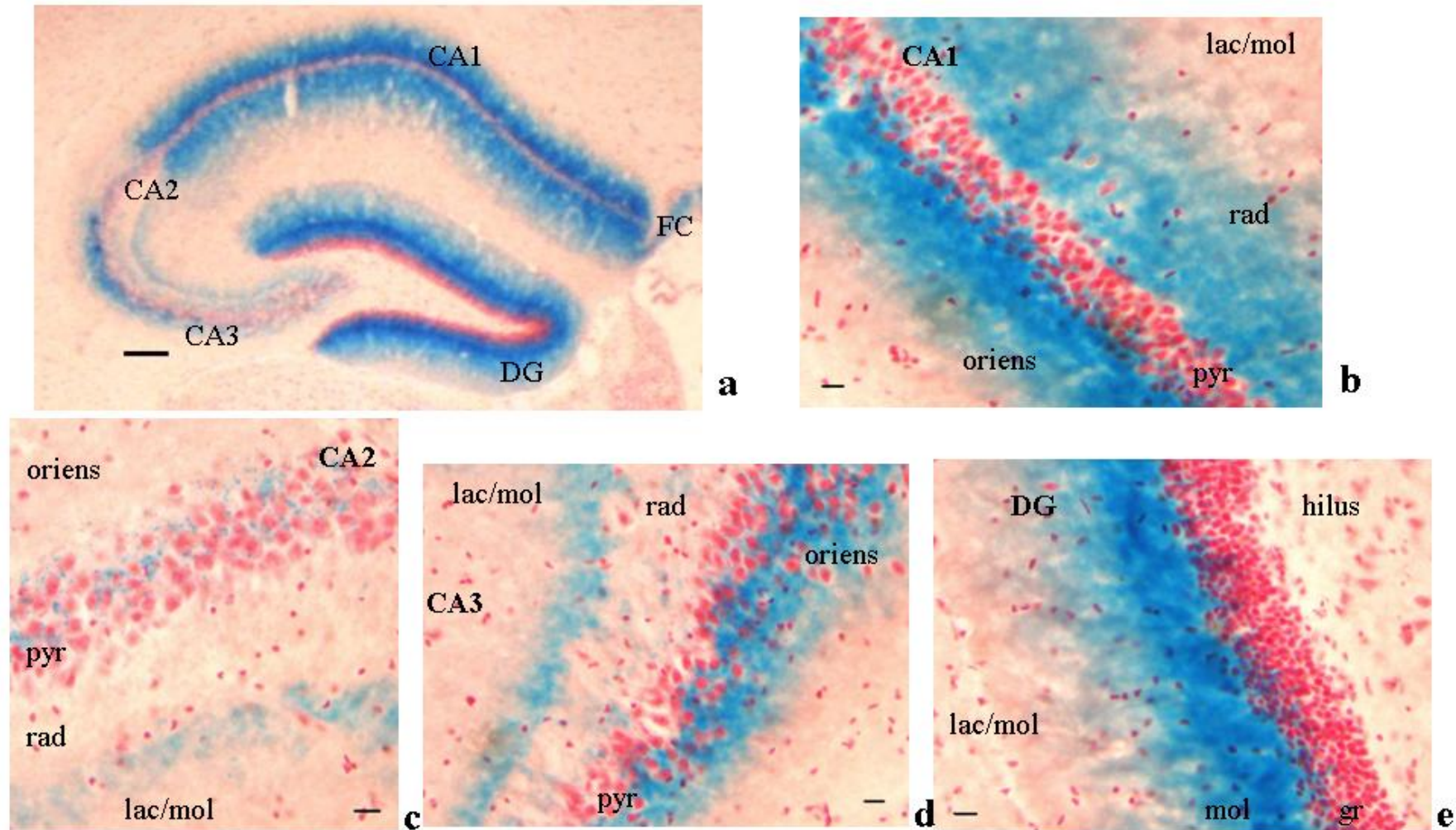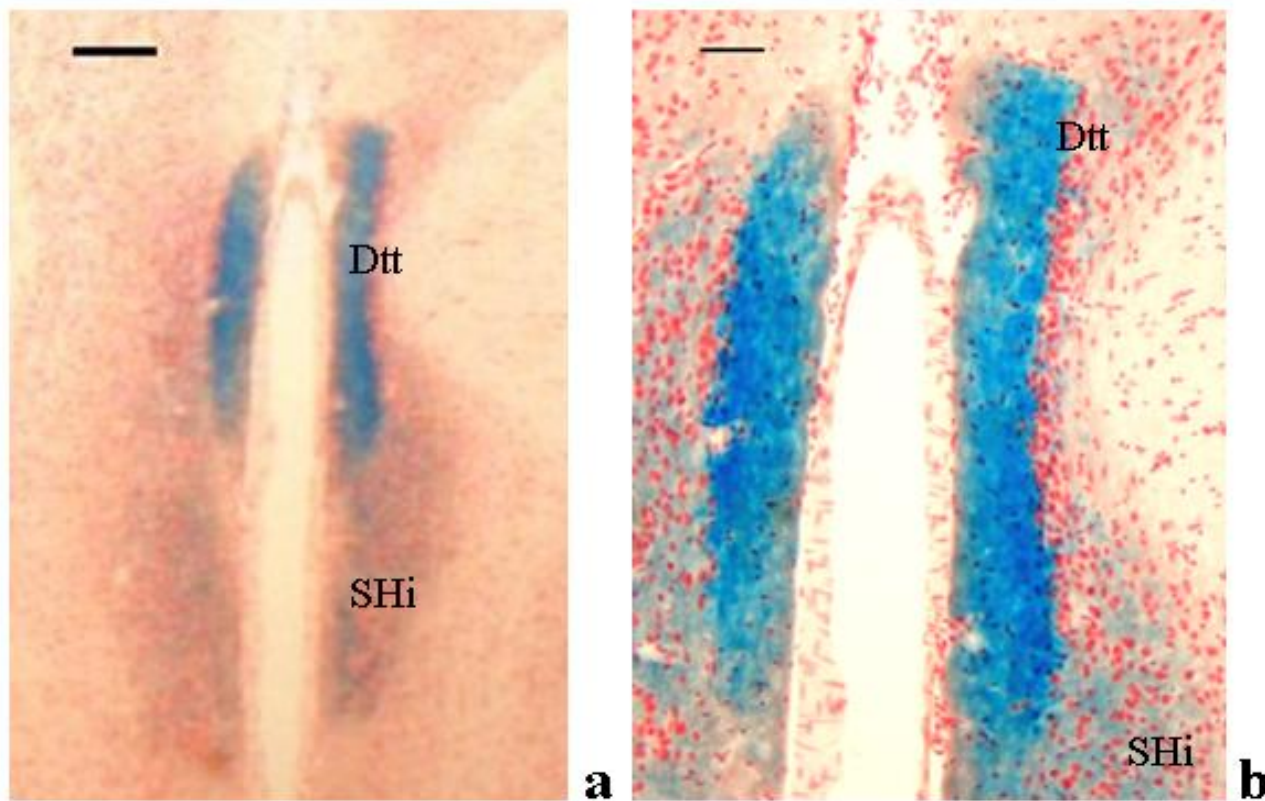
Fig. 16: PTPH1-KO adult mouse brain. a) beta-gal expression detected in the dorsal tenia tecta (Dtt) and in the septohippocampal nuclei (SHi) (4X; scale bar: 165μm). **b)** Detail of cytoplasmatic LacZ staining in the Dtt and SHi (10X; scale bar: 70μm).

In the hippocampus, LacZ expression was observed in the cytoplasm of a few pyramidal cells and through the fibers of the oriens and radiatum layer in a rostral caudal spread (Fig. 15a). In rostral sections, LacZ was expressed in the septohippocampal nuclei (Fig. 16a, 16b). In more caudal sections LacZ was present in the CA1 and CA3, and in a lesser extent in the CA2 (Fig. 15b-15d). In the CA3, LacZ was strongly expressed in the oriens and pyramidal cell layer (Fig. 15d), but its intensity was reduced in the radiatum and oriens compared to CA1 (Fig.15b). No staining was detected in the lacunosum-molecular layer in CA1, CA2 and CA3 (Fig. 15b-15d). The dentate gyrus showed a strong positive LacZ signal in the molecular layer, but not in the hilus (Fig. 15e).

3.1.4. Behavioral phenotyping of PTPH1-KO mice

As previously demonstrated, PTPH1-KO mice were healthy, reproduced normally and did not show any phenotypic traits distinguishing them from their WT littermates by simple visual observations [84,183].

In EPM, open field test and hot plate tests (anxiety-related behavior and thermal pain sensitivity), PTPH1-KO male and female mice did not show any significant difference in comparison with their WT littermates *(data not shown)*.

In the accelerated rotarod and Y-maze test, significant differences were observed between PTPH1-KOs and WTs based on gender and genotype factors. In the accelerating rotarod test PTPH1-WT mice did not show any gender differences (P_{2WAY}=0.5824 (WT gender vs WT activity); P_{AUC}=0.3218 (PTPH1-WT male vs female)) (Fig. 17a). PTPH1-KO male mice displayed an overall significant better performance compared to their matched female littermates (P_{2WAY}=0.007 (KO gender vs KO activity) (Fig. 17b). Post-hoc T-test analyses showed that the difference was significant at the second trial of the test (P_0=0.109; P_{30}=0.015; P_{60}=0.067; P_{90}=0.835), and the area under the curve for PTPH1-KO male mice was significantly higher (by 50%) compared to the matched values of the female littermates (P=0.0194) (Fig. 17c).

Fig. 17: Rotarod test on PTPH1-WT and KO mice males and females. **a)** WT males and WT females do not display any significant different performance at the rod (P_{2WAY}=0.5824) **b)** KO males and KO females display a significant different performance (P_{2WAY}=0.007) (post-hoc T-test: P_0=0.109; P_{30}=0.015; P_{60}=0.067; P_{90}=0.835). **c)** 50% difference in the area under the curve represented in figure 10a (unpaired T-test, P=0.0194). **d)** Female KO mice display a worse performance at the rod compared to WT females (P_0=0.171; P_{30}=0.002; P_{60}=0.028; P_{90}=0.025) **e)** No significant difference in the performance on the rod between male KO and WT mice. **a, b, d, e:** All the data were analyzed by Two-way Anova followed by T-test; *:p<0.05; **:p<0.01.
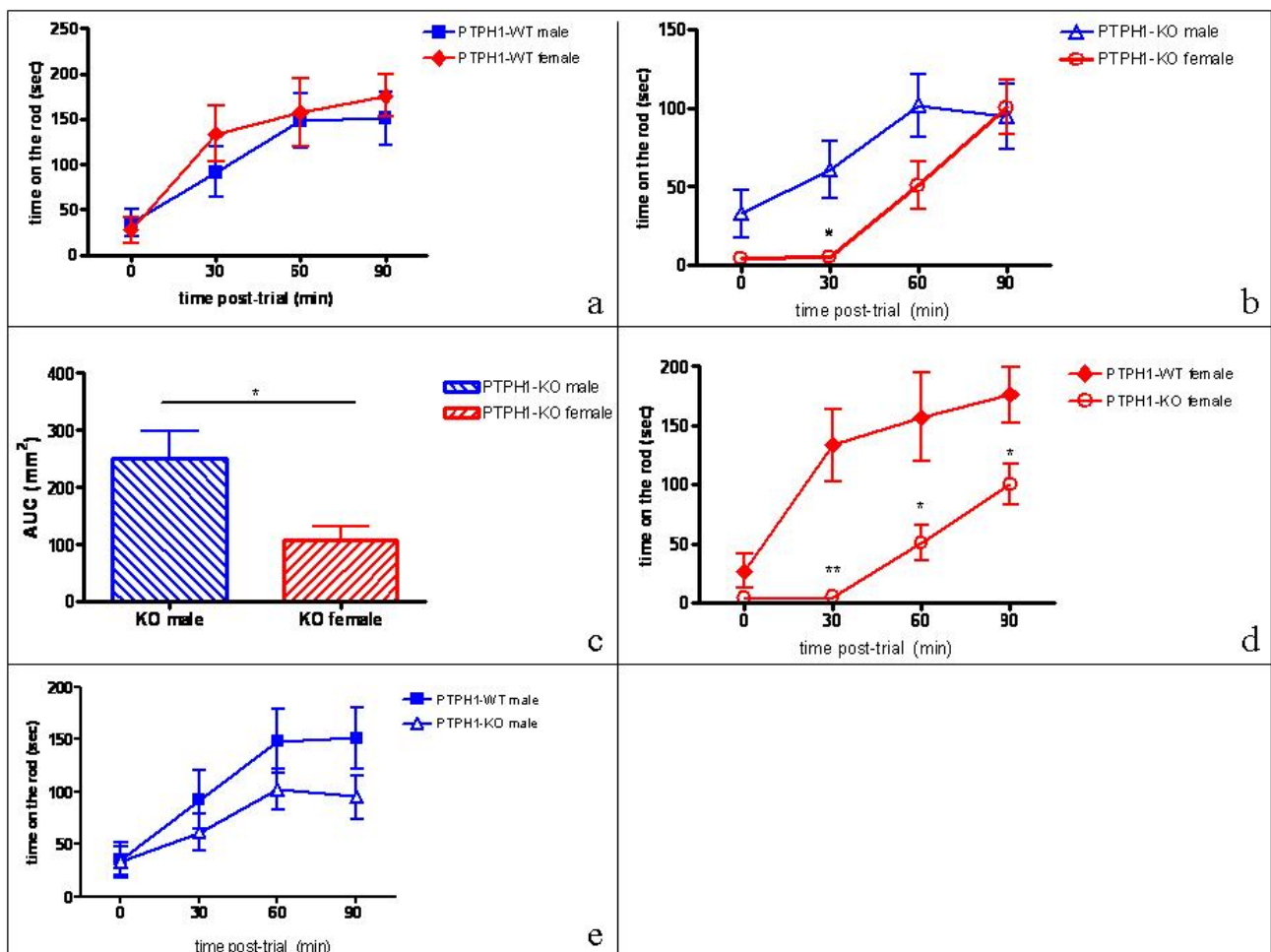
Considering this gender effect, the follow up analysis was carried out in males or females assessing genotype effects on activity. PTPH1-KO female mice performed significantly worse compared to their matched WT littermates, starting from the second trial and onwards (P_0=0.171; P_{30}=0.002; P_{60}=0.028; P_{90}=0.025) (Fig. 17d). No significant differences were observed in PTPH1-KO male mice compared to their matched WT littermates (P_0=0.92; P_{30}=0.363; P_{60}=0.222; P_{90}=0.135) (Fig. 17e).

In the Y-maze test, no differences were detected between PTPH1-KO and WT female mice either in working memory (P_{female}=0.972) or in locomotion indices (P_{female}=0.73; Fig. 18a, 18b). On the other hand, PTPH1 KO male mice displayed a significantly higher working memory index (percentage of exact alteration; P_{male}= 0.041) but similar locomotion activity (total arm entries) (P_{male}= 0.348) compared to their matched WT littermates (Fig. 18a, 18b).

Fig. 18: Y-maze behavioral test on PTPH1-WT and KO mice males and females. **a)** Male KO mice display higher working memory index compared to WT male littermates (P_{male}= 0.041); no differences recorded in the female mice. **b)** No significant differences recorded in the locomotion index, represented by the total arm entries between PTPH1-WT and KO males and females. T-test, *: p<0.05.
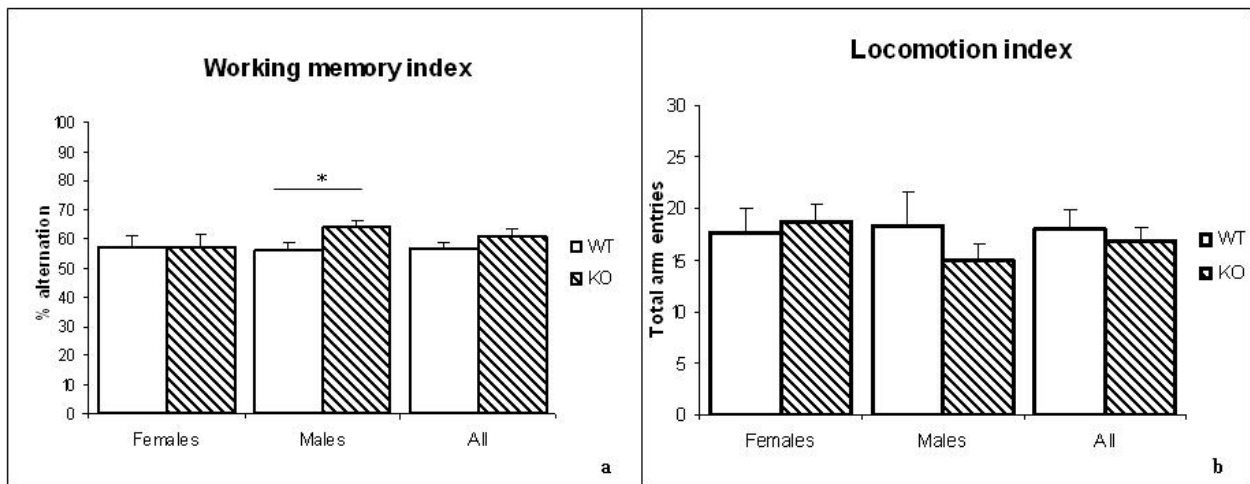
3.1.5. Superaray analysis

In vivo studies of KO animals are often biased by compensatory mechanisms, due to the redundancy of the enzymatic action. Superarray analysis has been performed in order to understand whether the action of other PTPs was modified in our PTPH1-KO mouse and also to identify new molecular targets. Superarray analysis has been performed on cortex and hippocampus of PTPH1-WT and KO mice (12 months-old).

The Pathway Finder™ array has been carried out on female mice and did not reveal any significant gene deregulation in the signaling pathways investigated (see Table 2) in both cortex and hippocampus (*data not shown*).

The Neurotrophin and Receptors plate has been performed on both female and male WT and KO cortex (Table 5) and hippocampus. The superarray plate on female cortices shows a significant 10-fold upregulation of *cckar* (cholecistokinin A receptor)gene (P<0.001) (Fig. 19) and a 2-fold upregulation of *mc2r* (melanocortin 2 receptor) and *galr1* (Galanin receptor 1)genes (P<0.05) in KO *versus* matched WT mice. *Ngfr* gene shows a trend of 2.5-fold upregulation in KO versus WT cortices, but this difference does not reach statistical significance (Table 5).

Table 5: SuperArray summary results in female cortex and fold regulationvalues above 1.5 have been reported. In red: upregulation and in gree: downregulation. In blue: significant p-values.

| Gene Symbol	Fold Regulation	p-value
Cckar	10,9884	0,000377
Fos	1,6945	0,341339
Galr1	1,9058	0,04335
Gdnf	1,7416	0,195511
Npffr2	1,8424	0,414438
Il10	1,9879	0,468466
Mc2r	1,9168	0,02131
Ngfr	2,4548	0,095257
Npy2r	1,6256	0,154414
Ntrk1	3,724	0,118724
Ppyr1	1,7911	0,501378
Stat4	2,9075	0,183158
MGDC	1,7381	0,485785
Hcrtr1	-1,5675	0,371327
Trp53	-1,8363	0,451328

The superarray analysis on male KO cortices reveals a significant downregulation of *hcrt* gene (2.3-fold; P=0.014) (Fig. 19) compared to matched WT animals. Furthermore *hcrtr2* and *ptger2* genes display a slightly but significant downregulation in KO vs WT male cortices. *Cckar* gene is slightly downregulated but this difference does not reach statistical significance (Table 6).

Table 6: SuperArray summary results in male cortex and fold regulationvalues above 1.5 have been reported. In red: upregulation and in gree: downregulation. In blue: significant p-values.

Gene Symbol	Fold Regulation	p-value
Il10	1,9718	0,214872
Nrg4	1,572	0,360769
RTC	1,5467	0,084437
Cckar	-2,1702	0,338973
Npffr2	-1,8432	0,183416
Hcrt	-2,344	0,014133
Hcrtr2	-1,5354	0,048352
Ntrk1	-1,7891	0,113361
Ptger2	-1,6702	0,028429

The Neurotrophin and Receptors plate has been carried out on hippocampus of WT and KO animals. No difference in gene modulation has been detected in the hippocampi of KO vsWT female mice (Table 7).

Fig. 19: Superarray analysis on neurotrophin receptor genes on PTPH1 KO *vs* WT male and female cortex. Some of the KO modulated genes are represented here in red. Abrreviations cckar: cholecistokinin A receptor; galr1: Galanin receptor 1; mc2r: melanocortin 2 receptor; stat4: Signal transducer and activator of transcription 4; Hcrt: Hypocretin ; Hcrtr2: Hypocretin (orexin) receptor 2; Ptger2: Prostaglandin E receptor 2 (subtype EP2).

Female cortex

Male cortex
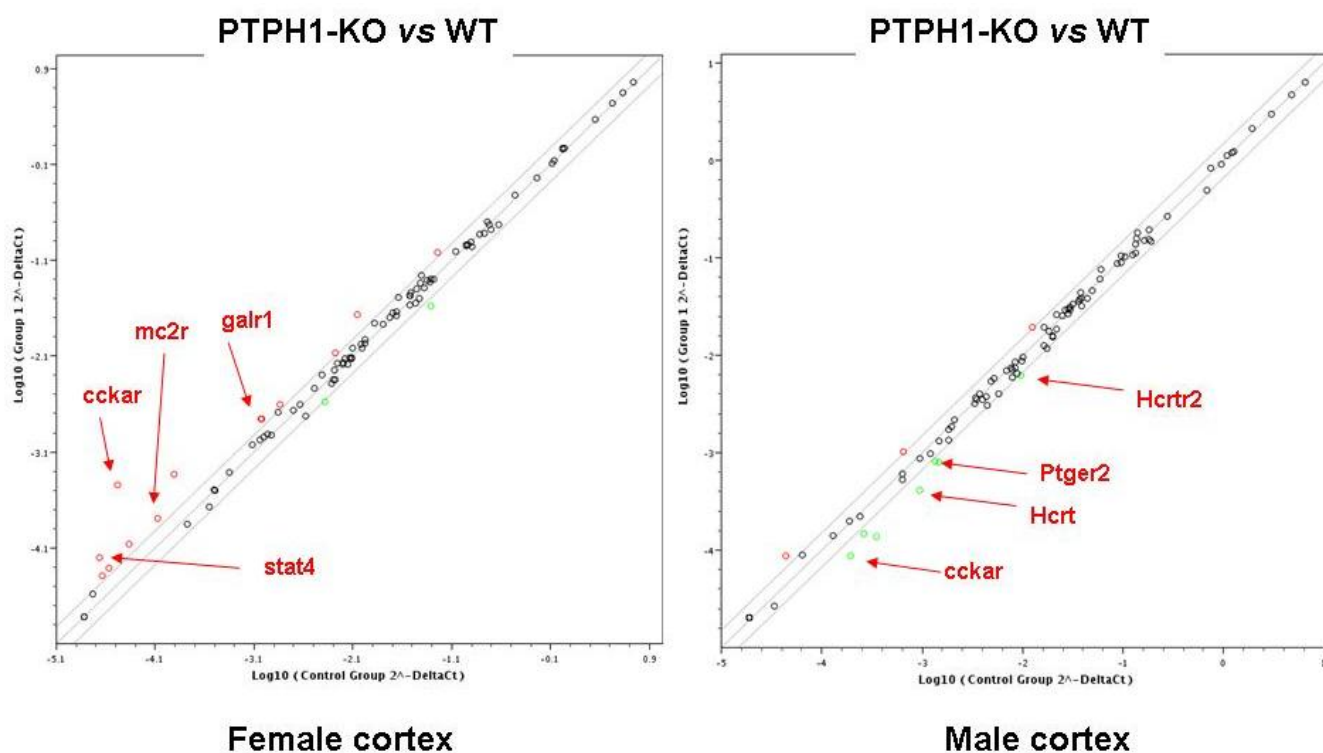
As for male mice, a trend of slight overexpression of Cbln1 (1.5-fold; P=0.06) is detectable in KO vs WT hippocampi. Furthermore, *hcrt* (Hypocretin)and *ptger2* (Prostaglandin E receptor 2) genes display a 2-fold underexpression in KO hippocampus compared to matched WTs, but only *ptger2* modulation is statistically significant (P_{hcrt}=0.0532; .P_{ptger2}=0.04774) (Table 7).

Table 7: SuperArray summary results in male and female hippocampus. Fold regulationvalues above 1.5 have been reported. In red: upregulation and in gree: downregulation. In blue: significant p-values

Male			Female		
Gene Symbol	**Fold Regulation**	**p-value**	**Gene Symbol**	**Fold Regulation**	**p-value**
Cbln1	1,5547	0,066558	Cbln1	1,9185	0,30425
Gfra3	2,1381	0,232091	Fos	1,994	0,273959
Npffr2	1,9548	0,514115	Gfra3	1,5435	0,249189
Il6	2,0798	0,475907	Npffr2	1,701	0,347043
Cckar	-1,5303	0,419526	Il10	1,5855	0,45425
Galr2	-1,6258	0,180174	Nrg1	1,5067	0,36732
Hcrt	-2,2339	0,053215	Gusb	-1,647	0,155702
Ppyr1	-1,8559	0,334184			
Ptger2	-1,8145	0,04774			

3.1.6. Histological Analysis

3.1.6.1. CCKAR immunoreactivity

LacZ staining and co-expression with the CCKAR immunoreactivity was carried out, in order to evaluate CCKAR protein level in PTPH1-WT and PTPH1-KO mice and also to understand whether PTPH1 and CCKAR colocalized in mouse brain.

In agreement with other reports [184], CCKAR was expressed in most of the brain areas as primary cortex, hippocampus and with a lower intensity in the thalamus (Fig. 20a), in PTPH1-WT and KO mice. CCKAR immunoreactivity seemed to be mainly localized in the cell body of the neurons, with different intensity (Fig. 20c).

In paragraph 3.1.3. (page 48), we extensively showed PTPH1 localization in the brain, including those areas where CCKAR was expressed. Indeed CCKAR immunoreactivity and LacZ staining colocalized in the brain areas investigated, as (Fig. 20d, Fig. 21b), in ventral posterolateral (VPL) and ventral psteromedial (VPM) thalamic nuclei (Fig. 22, 23) and in all the regions of hippocampus (Fig. 24). Comparatively a cellular colocalization of CCKAR and LacZ staining could not be assumed in cortical regions (Fig. 20) by simple visual observation. No major differences in cortical expression of CCKAR protein levels were detected by simple visual observation in PTPH1-KO mice compared to WT littermates (Fig 20, 21).

Fig. 20: CCKAR immunoreactivity and LacZ staining in primary cortex of PTPH1 WT (**a-c**) and KO mice (**b-d**) at 10X and 40X. No difference in CCKAR protein expression (brown) was deteclable by simple visual observation. LacZ staining (blue) was present in primary cortex but no cellular colocalization with CCKAR-postive IHC could be assumed.
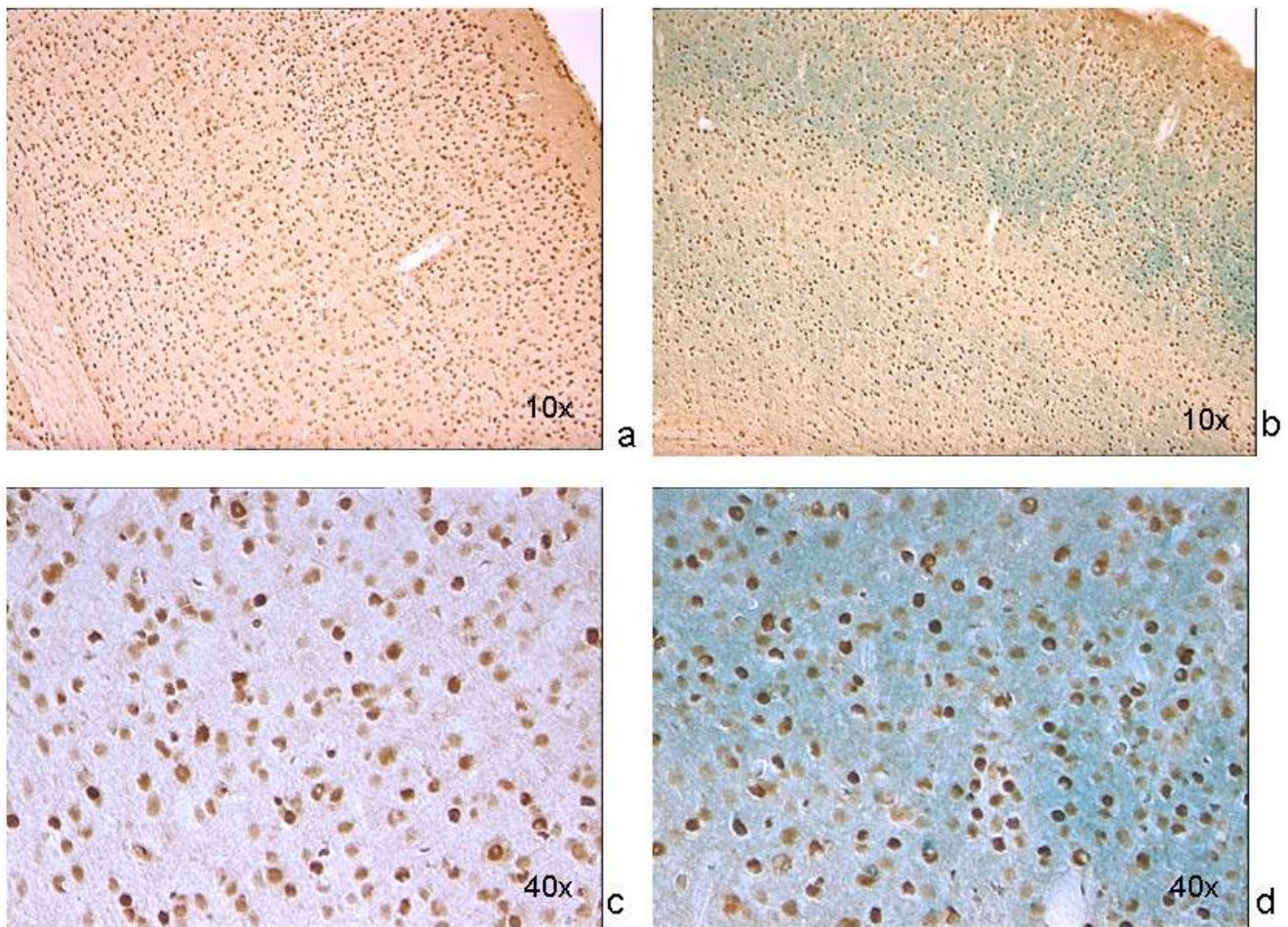

Fig. 21: CCKAR immunoreactivity in retrosplenial cortex of PTPH1 WT (left panel) and KO mice (right panel) at 10X. CCKAR immunoreactivity (brown) and LacZ staining (blue) were present in retrosplenial cortex and indisum griseum, but no colocalization could be proved. No difference in CCKAR protein expression deteclable by simple visual observation.
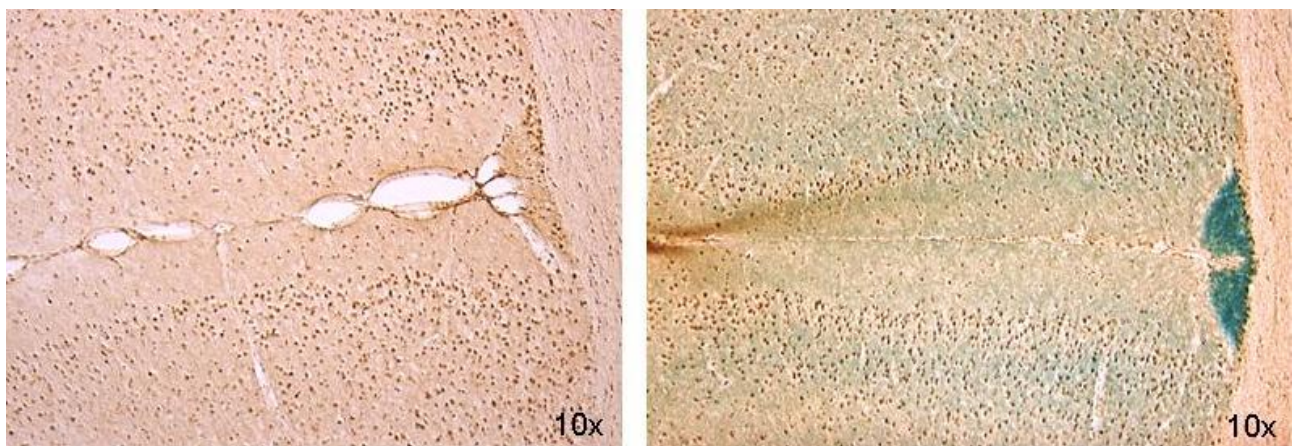
Fig. 22: CCKAR immunoreactivity in brain of PTPH1 WT (right panel) and KO mice (left panel) at 4X. CCKAR protein expression seems to colocalize in hippocampus and thalamus. In blue: LacZ staining; brown: CCKAR positive cells.
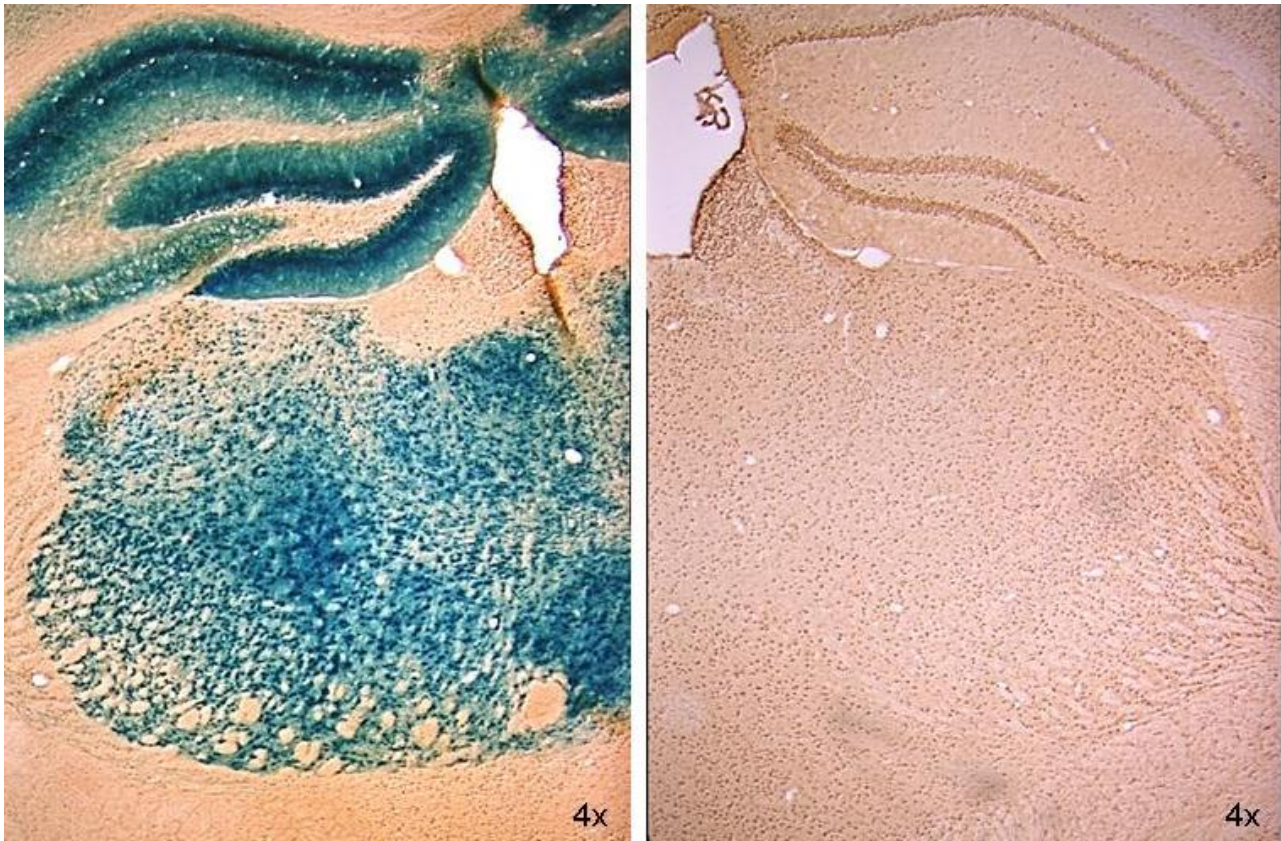

Fig. 23: CCKAR immunoreactivity in thalamus of PTPH1 KO mice at 40X. CCKAR was localized in neuron cell body of ventral posteromedial (VPM) and ventral posterolateral (VPL) thalamic nuclei, areas LacZ staining-positive.
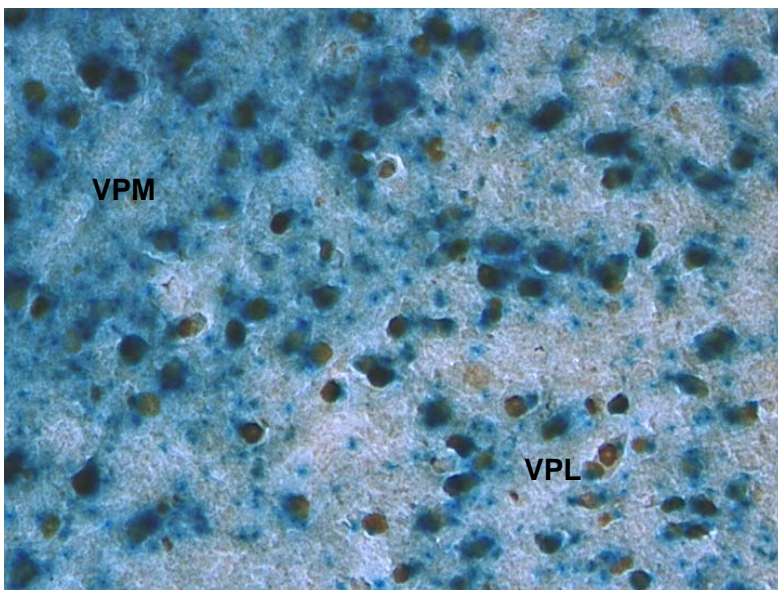
Fig. 24: CCKAR immunoreactivity in hippocampus of PTPH1 KO mice at 40X. CCKAR (brown) was localized in neuron cell body of pyramidal layer of **a)** cornu ammonis (CA) 1; **b)** CA2; **c)** CA3; and **d)** in the granula cell layer of dentate gyrus. LacZ staining is in blue. pyr: pyramidal cell layer; oriens: oriens layer; rad: radiatum layer; mol: molecular layer: gr: granule cell layer; lac/mol: lacunosum-molecular layer.
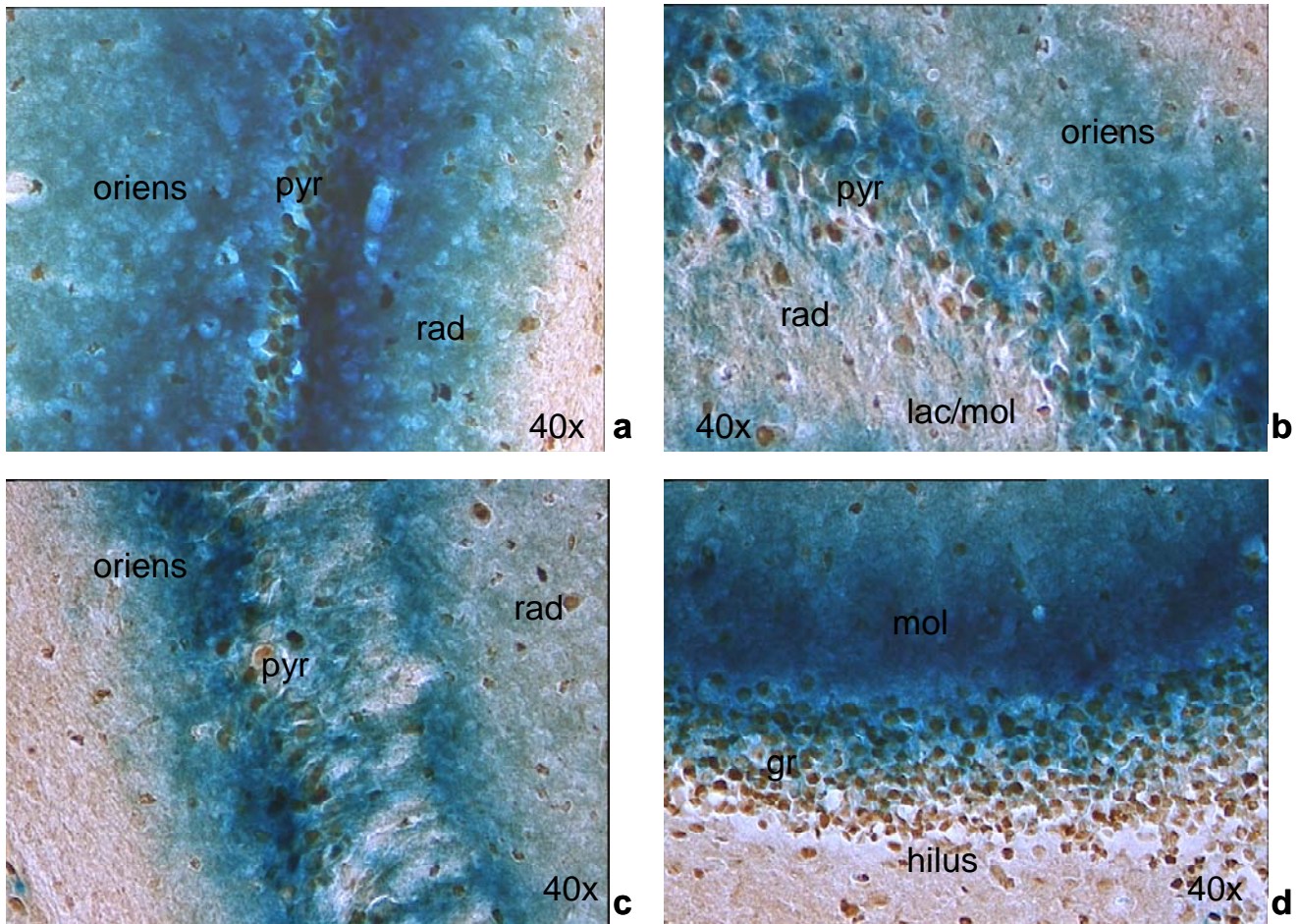
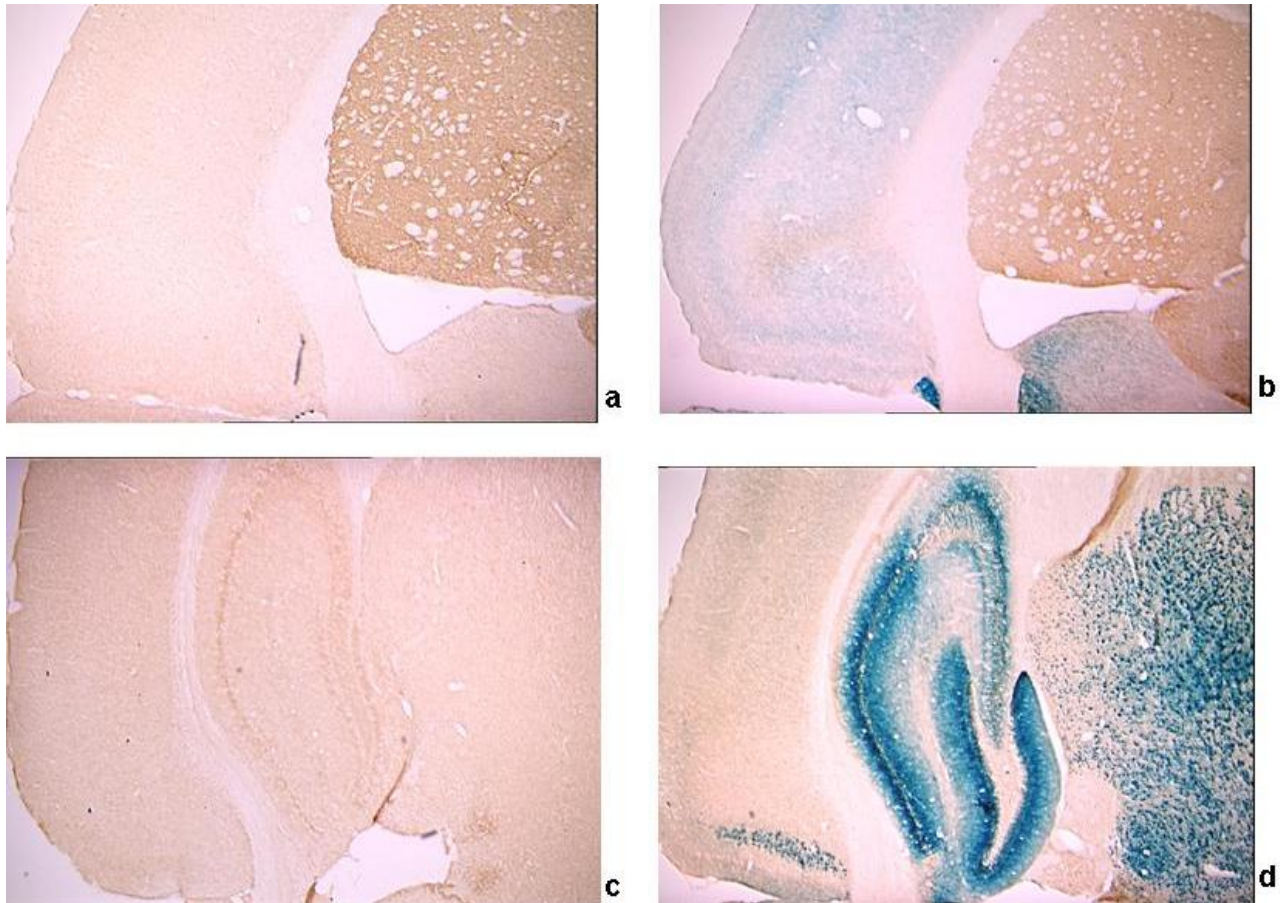### 3.1.6.2. Neurotransmitters immunoreactivity

PTPH1 impact on cognition arised several questions on its impact on neurotransmitter pathway. Thus, IHC study was performed on PTPH1-WT and KO mice, in order to understand whether PTPH1 silencing could impact neurotransmission. . LacZ staining and co-expression with GAD-67 and TH immunoreactivity was performed also in order to localize PTPH1 in glutamaergic and/or dopaminergic neurons.

Tyrosine hydroxylase immunoreactivity

Tyrosine hydroxylase (TH) is a marker for dopaminergic neurons. TH immunoreactivity was mainly expressed in the striatum and where no LacZ positive staining was detectable (Fig. 25). LacZ staining was detectable in all the brain areas previously described (page 48), as primary and retrosplenial cortex, hippocampus and thalamus. No colocalization of TH and LacZ was detectable

in the brain of PTPH1-KO mice (Fig. 25b, 25d). Furthermore, no difference in TH protein expression between PTPH1-WT and KO brain area was detectable by simple visual observation.

Fig. 25: TH immunoreactivity in brains of PTPH1-WT **(a-c)** and KO **(b-d)** mice at 4X. TH (brown) and Lacz (blue). TH was strongly expressed in striatal region of **a)** WT and **b)** KO mice but no difference in TH protein expression between genotypes was detectable by simple visual observation. No colocalization of TH and LacZ was detetctable.

Glutamic acid decarboxylase-67 immunoreactivity

GAD-67 is a marker for glutamargic neurons and its immunoreactivity was investigated in combination with LacZ expression in PTPH1-WT and KO mice. GAD-67 was expressed in primary and retrosplenial cortex, in the septum and in the cornu ammonis of hippocampus. GAD-67 immunoreactivity colocalized with LacZ staining in the cells of septum (Fig 26a, 26b) and ventro-lateral thalamic nuclei (Fig. 28d). Cell proximity of GAD-67-positive and LacZ staining-positive cells was detectable in other areas, as in cortical layers II, III and V (Fig 26c, 26d) and in cornu ammonis of hippocampus (Fig. 27b-27d), but no colocalization in the same cell was possible by simple visual observation.

Fig. 26: GAD-67 immunoreactivity of PTPH1-KO septum **(a-c)** and cortex **(b-d)** mice at 4X and 10X. Colocalization of GAD-67 (brown) and LacZ (blue) was detectable in the cells of **b)** Septum, but no cellular colocalization was detected in **d)** cortical region, where LacZ-positive and GAD-67-postive cells were present; in red are underlines two cells: the blue one is LacZ-positive and the bown one is GAD-67- positive.
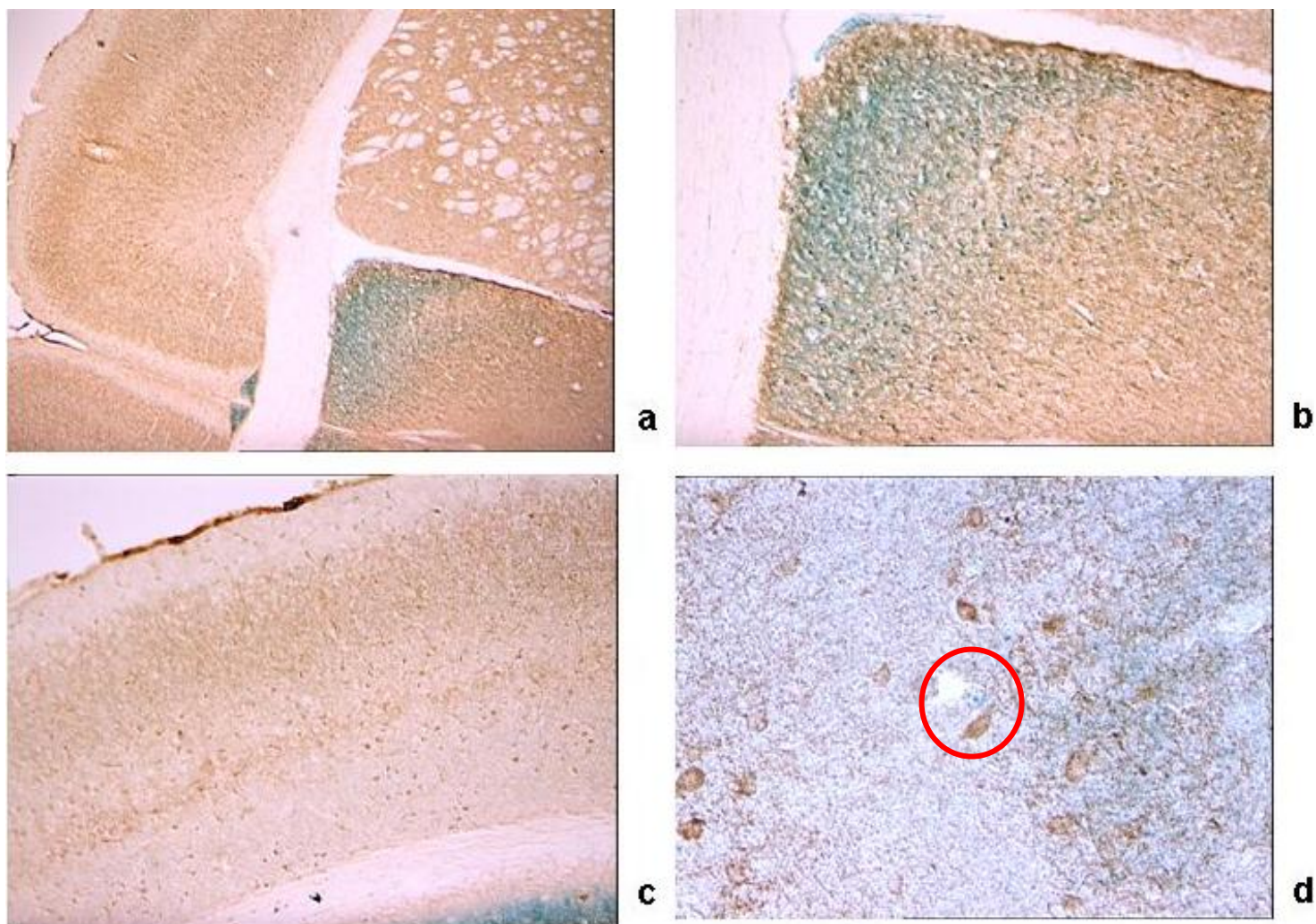
Fig. 27: GAD-67 immunoreactivity in hippocampus of PTPH1-KO. **a)** Hippocampus in toto at 4x; **b)** CA1 and CA3 region where was visible the colocalization of LacZ and GAD-67 at 40X; **c)** CA1 display GAD-67 positive staining in pyramidal cells at 40X; **d)** CA3 display a faint but present GAD-67 positive staining in pyramidal cells at 40X; e) no GAD-67 positive staining in granule cell layer of dentate gyrus at 40X.

Fig. 28: GAD-67 immunoreactivity in thalamic nuclei of PTPH1-KO. **a)** positive LacZ staining and GAD-67 staining at 4X; **b)** positive GAD-67 staining in reticula and vetro-lateral thalamic nuclei at 10X and **c)** in vetromedial nuclei; **d)** details of reticular and vetro-lateral nuclei at 40X.

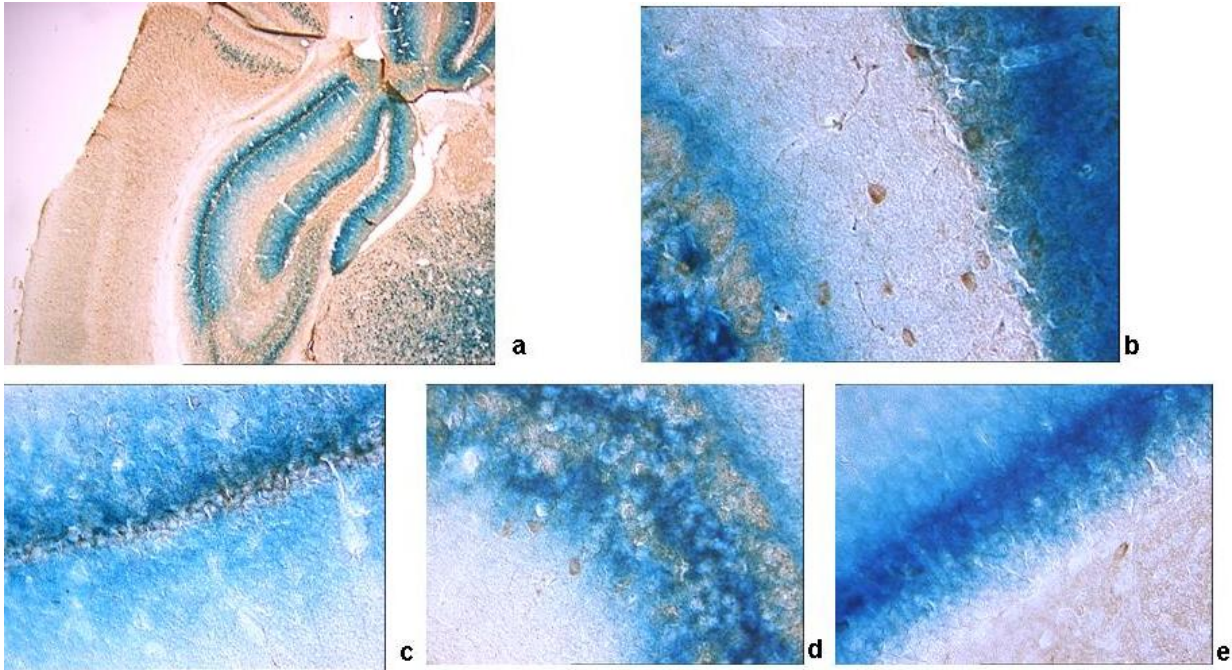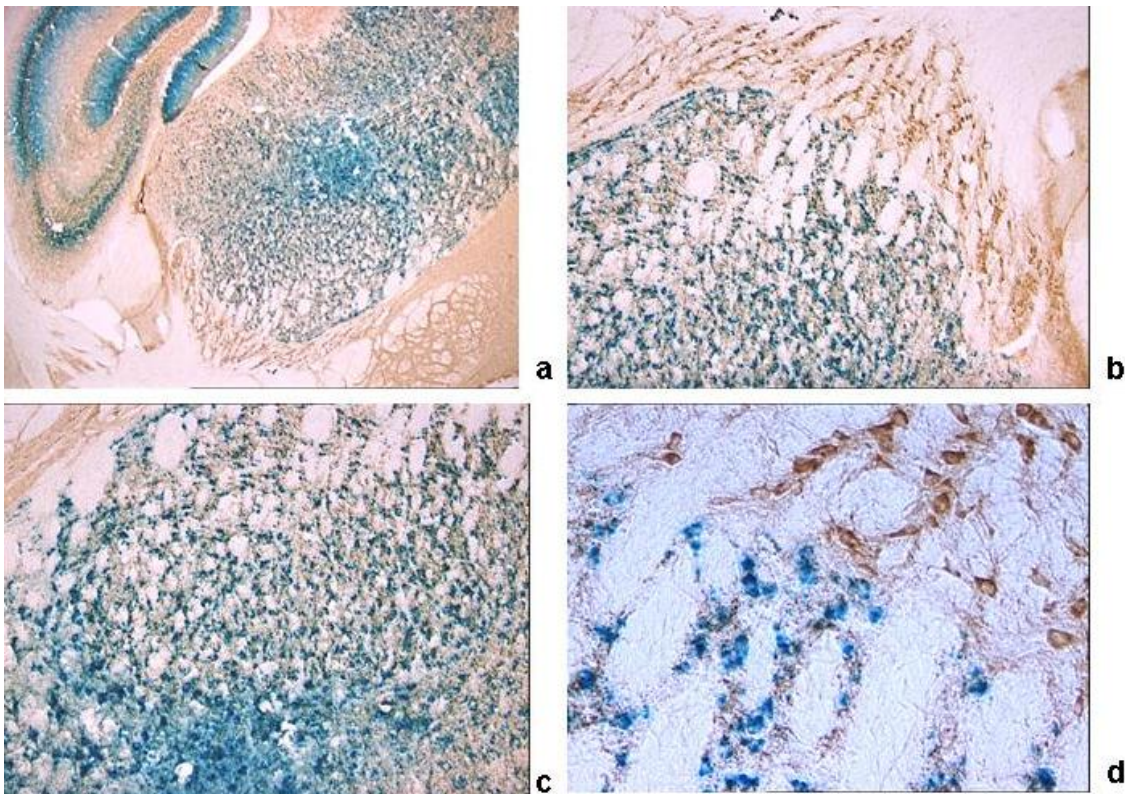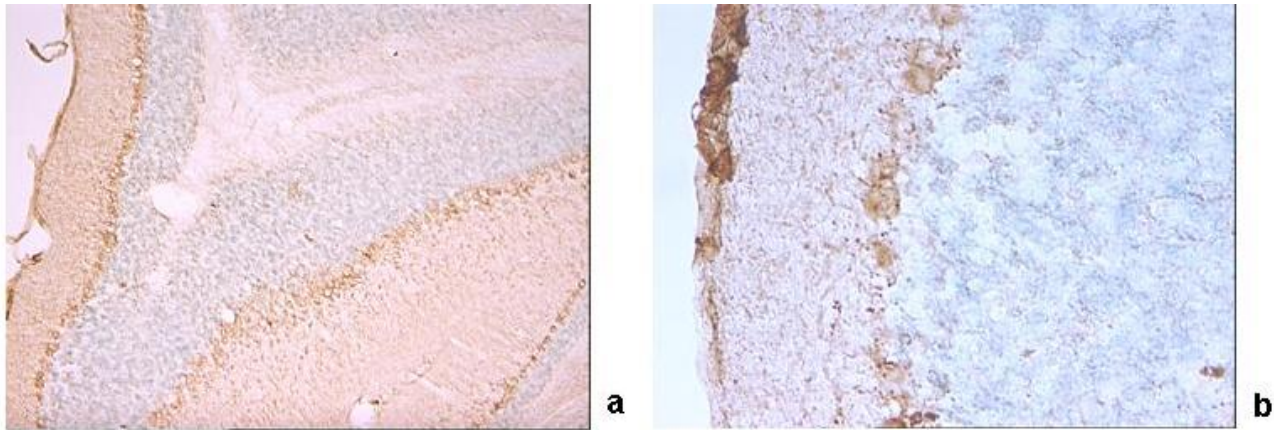No colocalization of GAD-67 and LacZ staining positive cells was detetcted in cerebellar cortex and in ventromedial and reticular thalamic nuclei (Fig. 29).

Fig. 29: GAD-67 immunoreactivity in cerebellum of PTPH1- KO mice at 10X and 40X. **a-b)** No colocalization of LacZ (blue) and GAD-67 staining (brown) in cerebellar cortex.

3.2. Discussion: PTPH1 in CNS functions

PTPs are key factors in multiple signaling pathways, leading to modulated functional activities in various cell types [3,185]. Among all PTP forms, PTPH1 has been shown *in vitro* to modulate cardiac sodium channel $Na_v1.5$ [53], that it is also known to be expressed in the axons of cerebral cortex, cerebellum, thalamus and brain stem [73]. Moreover, PTPH1 contains a domain with high sequence homology with the members of the band 4.1 superfamily protein, FERM. This domain mediates the linkage of actin filaments to the plasma membrane [186], and therefore may be involved in cytoskeleton-membrane interactions, crucial for axon functionality. To further understand the potential role of PTPH1 in neural functions *in vivo*, we first investigated its expression pattern in embryonic and adult PTPH1-KO mice CNS by LacZ staining, and second its role in CNS functions by behavioral phenotype characterization.

PTPH1 is differentially expressed throughout development

In rat embryonic stage Es19, PTPH1 expression through FISH analyses has already been shown in the dorsal thalamic nuclei, which give rise to the thalamo-cortical connections in adulthood [76]. Thus, it has been suggested to play a role in the maintenance of these connections in adults. We replicated these data in PTPH1-KO mice at Es14 and Es16 embryonic stages (Fig. 7). PTPH1 was expressed in the hypothalamic area and but also in the dorsal root ganglia of the spinal cord, excluding the spinal cord itself [187]. Moreover, at postnatal P1, PTPH1 expression was also present in peripheral organs such as muscles and intestines as in the adults [183]. On the other hand,

the CNS expression at P1 appeared weaker than in the adults suggesting a pattern of PTPH1 expression corresponding to specific developmental stages of the CNS as well as peripheral organs (data not shown). These changes in expression might play a role in various developmental functions that need to be further understood.

PTPH1 expression and functionality in adult mouse brain

In PTPH1-KO adults, LacZ was expressed in different CNS areas such as cerebral and retrosplenial cortices (Fig. 9, 10), hippocampus (Fig. 15), thalamus (preferentially ventral thalamus) (Fig. 14), cerebellum (Fig. 12) and in the region of the tenia tecta (Fig. 8, 16). This data confirmed previously observed expression patterns in the rat brain by Sahin et al. [76] and extended the observation to other brain regions. We demonstrated that PTPH1 was expressed within the cytoplasm and close to the cell membrane of neurons in most of the brain area investigated (Fig. 11). We, furthermore, showed that PTPH1 was differentially expressed in the GABAergic neurons of hippicampus CA1 and CA3 and in VPL and VPM thalamic nuclei (Fig. 28), but not in cerebral (Fig. 26) and cerebellar cortical regions (Fig. 29). In these areas, PTPH1 seems to be expressed in a different neuronal sub-population, that needs to be further investigated.

It is known that the FERM domain is indeed necessary for PTPH1 localization close to the plasma membrane in Jurkat T cells [47] and it could be responsible for the punctate expression pattern of PTPH1 in the cytosol of the neurons (Fig. 11b) [188]. This supports the concept that PTPH1 may be involved in cytoskeleton-membrane interaction within extended neuronal population in the CNS, potentially playing a role in various neuronal functions.

Indeed the neural expression of PTPH1 in CA1, CA3 and DG of the hippocampus (Fig. 15), in the retrosplenial cortex (Fig. 10, 11) and in a series of thalamic nuclei (Fig. 14) suggested an involvement of PTPH1 in the modulation of the memory circuit. Both hippocampus and retrosplenial cortex are key regions in the spatial working memory functions [189-195]. Moreover, several thalamic nuclei have also been shown to be important in the memory process [196,197]. For example, a strong loss of dorsomedial and ventral posterior thalamic neurons is associated with severe cognitive and memory disabilities in patients affected by traumatic brain injury [198]. Lesions in the lateral thalamus may lead to important working memory defects in rodents [199]. The anterior thalamic nuclei project via the retrosplenial cortices to the hippocampus [200,201], thus underlying the importance of both these circuits and of PTPH1 in the mnemonic process.

Another interesting PTPH1-positive area is the indusium griseum (Fig. 10) whose role in the adult brain is not clear. It is thought to be part of the limbic system, receiving afferents from the

entorhinal and pyriform cortex and projecting to the septohippocampal nuclei, olfactory tubercle (presumably the tenia tecta) and the medial frontal cortex [202,203]. The expression of PTPH1 in these specific regions suggests a potential role in the processing/integration of memory and sensory information to the SHi and likely the cortex.

Indeed PTPH1 expression is also detectable in the pyramidal neurons in layer III and IVA of the cerebral cortex of the mouse (Fig. 9), in agreement with Sahin's findings in the rat brain. The middle layers (III and IV) of the cerebral cortex are key sites for thalamic inputs [204,205] especially for VPM and VPL, primary thalamic nuclei for somato-sensory information integration [206]. Furthermore a strong cortico-cortical communication has been assessed between these two layers [207], thus suggesting a role for PTPH1 as key regulator in the transmission of the thalamo-cortical and cortico-cortical information.

The cerebellar cortex is also positive for PTPH1 expression, in particular in the cytoplasm of granule cells (Fig. 12). The cerebellum is known to be the main structure for motor learning functions. In particular, the cerebellar cortex seems to be involved in the early learning phases of motor activities [208,209] that include also a strong activation of other areas such as prefrontal cortex and basal ganglia [172,173]. PTPH1 expression in the granule cells seems to indicate a potential involvement in the processing of afferent information to the purkinje cells, since it is known that afferents fibers to the cerebellar cortex will project in part through the granule cell layer.

PTPH1 expression pattern observed in our analysis points out a potential involvement of this phosphatase in numerous CNS processing functions such as locomotion, sensorial integration, learning and memory. In this study, the behavioral phenotyping of the PTPH1-KO mice allowed us to test these hypotheses *in vivo*. Indeed, as already demonstrated by our group [183] and also by others [84], PTPH1-KO mice are healthy and do not display any phenotype, distinguishing them from their matched WT littermates, detectable by simple visual observation. Therefore PTPH1-WT and KO mice underwent a battery composed by five behavioral tests, from the least to the most invasive (Table 1), with the tolerable limitation of the handling bias.

Behavioral testing revealing locomotor dysfunctions, such as open-field, EPM and Y-maze did not highlight differences between the two genotypes (Figure 18b), suggesting that PTPH1 does not play a critical role in the integration of locomotor information.

Anxiety-like behaviors measured by open-field (as path in the center) and EPM (as time spent in the open arms), exploiting rodents natural aversion to open space, did not show any differences between the two genotypes (data not shown), leading to the conclusion that PTPH1 may not be involved in the integration of thalamo-limbic information, key paths for anxiety behavior

processing. Similar conclusions can be drawn from the lack of difference between the genotypes regarding integration of nociceptive information, based on hot plate test.

In the behavioral test, that partly depends on working memory performances (Y maze), PTPH1-KO male mice showed a slightly better short-term memory than their WT littermates (Figure 18a). Thus, PTPH1 may be involved in the integration of memory information. This was further strengthened by results obtained with a test assessing learning and coordination, the rotarod. Contrary to other behaviors where little differences have been observed, learning and coordination capacities in PTPH1-KO female mice are significantly impaired (Figures 17b, 17c). The low rotarod performance on the early trials, compensated by the last trial, is suggestive of a delay in learning acquisition (Figures 17b, 17d).

As reported in Pilecka et al., our PTPH1-KO mice express the non-catalytic part of PTPH1 in frame with the enzymatically active part of LacZ gene. LacZ is widely used as a reporter for promoter activity in KO mice and all those mice express a modified protein, whose full function is not known. So far it was never reported a function of LacZ alone in cognition and we consider quite unlikely that this is the case in our mice. Thus, it is very likely that the behavioral phenotype we detect in our mice is linked to the deletion of the catalytic domain of PTPH1.

The impairment in learning and coordination of PTPH1-KO female mice may be resulting from the involvement of PTPH1 in the GH signaling pathway [19]. Indeed our group has already shown that PTPH1-KO mice display higher GHR response *in vivo* and consequently a higher expression of its down-stream effector hormone, the IGF1 in liver and plasma [183]. GHR is highly expressed in most areas of the CNS, in particular in the choroid plexus, hippocampus, putamen, thalamus and hypothalamus. Similarly IGF1 and IGF1-receptors are localized predominantly in hippocampus, but also in amygdala, cerebellum and cortex [155]. Although IGF1 is considered a neuroprotective hormone, it can be produced in the CNS, it is primarily synthesized in the liver and can cross the blood–brain barrier [152,210-212]. The GH-IGF1 axis is also known to influence cognitive functions due to several neuroprotective effects on the hippocampus [213]. Furthermore it has been recently pointed out that old conditional liver-IGF1-KO mice display impaired spatial learning and memory [214]. The presence of PTPH1 in key CNS regions, as well as the consequent deregulation of the GH-IGF1 axis in KO mice, strengthens the concept that the PTPH1 network (CNS and downstream peripheral effectors) may be involved in cognitive functions.

The behavioral tests assessing working memory and specifically learning revealed not only a genotype effect but also a gender effect, as mentioned above. Sex hormones are known to modulate

the somatotropic system [215,216]. In humans, testosterone has an important effect on GH axis, in part by its aromatization to estradiol. Administration of estrogens, or aromatized androgen, modulates GH axis neuroregulation [216,217]. In particular, chronic E2 administration has been shown to reduce GH-induced IGF1 increased expression in liver and plasma via a negative feedback mechanism, while acute E2 administration leads to the expected GH-induced IGF1 release [218]. Furthermore, it has been reported that estrogens play not only regulatory functions on neuroendocrine systems but can also have stimulatory or inhibitory impacts on the inter-connectivity of the hippocampal structure depending on the gender [219-222], meaning that the same stimulus can have opposite effects in male *vs* female mice. Thus, the cognitive behavioral differences observed in our KO mice are underlying the potential impact of the PTPH1 network on neuroendocrine regulation as well as on cellular architecture within specific brain regions.

Another strong correlation between hormonal regulation and PTPH1 was pointed out by superarray analysis on female cortex. In this area, a 13-fold increase in CCKAR mRNA expression was detected (Fig. 19). IHC characterization demonstrated that CCKAR colocalized with PTPH1 in hippocampal regions (Fig. 22, 23), and in the primary cortex proximity of LacZ-positive and CCKAR-positive cells was detected (Fig. 20). Comparatively, no difference in CCKAR protein expression could be detected between genotypes by simple visual observation.

Cholecystokinin (CCK) is a brain-gut peptide that exerts a variety of physiological actions in the gastrointestinal tract and central nervous system [223-227]. CCK mediates its effects through interaction with specific receptors subdivided in two subtypes, CCKAR (present in the periphery and brain nuclei [184]) and CCKBR (predominant in the brain). CCK is implicated in variety of behavioral functions as satiety, anxiety, exploratory and locomotor activity and learning and memory [223,227,228]. OLETF rats, that lack in CCKAR, diplayed impaired learning and memory performance at the radial maze [228] and polymorphisms on human CCKAR gene are associated with differential learning performances [227]. A recent study suggests that cannabinoid-dependent deficits in learning and memory could be due to CB1 receptors, that are localized exclusively in CA1 and CA3 cholecysto-kinin-positive GABAergic interneurons [229]. GABAergic, thus inhibitory, interneurons lead to a reduction in transmitter release below the levels required to trigger long-term synaptic changes that underlie memory formation. Thus, PTPH1 colocalization with CCKAR in hippocampus (Fig. 24) and CCKAR mRNA increase in cortex (Fig. 19) (due to PTPH1 silencing) could have positively impacted learning perfomance at rotarod of PTPH1-KO female mice (Fig. 17). Further neurochemical characterizations are needed to corroborate this hypothesis

and to understand the role of PTPH1 in the learning process, that could be mediated either by CCKAR or by GH/IGF1 axis or by both mechanisms.

In conclusion, we have demonstrated that PTPH1 is expressed in neural populations, and in particular also in GABAergic sub-population, present in adult brain areas mainly involved in locomotor and cognitive functions. The behavioral assessments have allowed us to reveal PTPH1 functionality especially within cognitive domains. Better understanding the interplay between various phosphatases regulating CNS functions, which now includes PTPH1, will be key in the future to unravel some of the complexity of CNS signaling pathways necessary for information processing.

Chapter 4 - PTPH1 in GHR signaling

4.1. Results on PTPH1 in GHR signaling

4.1.1. LacZ staining on PTPH1-HET mice

We have already showed that because of the in-frame LacZ insertion, PTPH1 promoter activity could be followed by X-gal staining in adult heterozygous animals. Strong staining was observed in striated muscles (considering hind limb, abdominal wall, esophagus and intracostal muscle) (Fig. 30a-30d), the diaphragm (Fig. 30e), and colon lining (Fig. 30f). Weaker staining was observed in kidney, liver, and heart (Fig. 30g-30i).

Fig. 30: LacZ staining PTPH1-HET mice: whole mount. Positive LacZ staining in the scheletal muscle of **a)** Hind limb b) Abdominal wall, c) Esophagus, d) intracostal muscle e) Diaphragm. A weaker signal is detected in the f) epithelium of the colon, g) kidney, h) liver and i) heart.
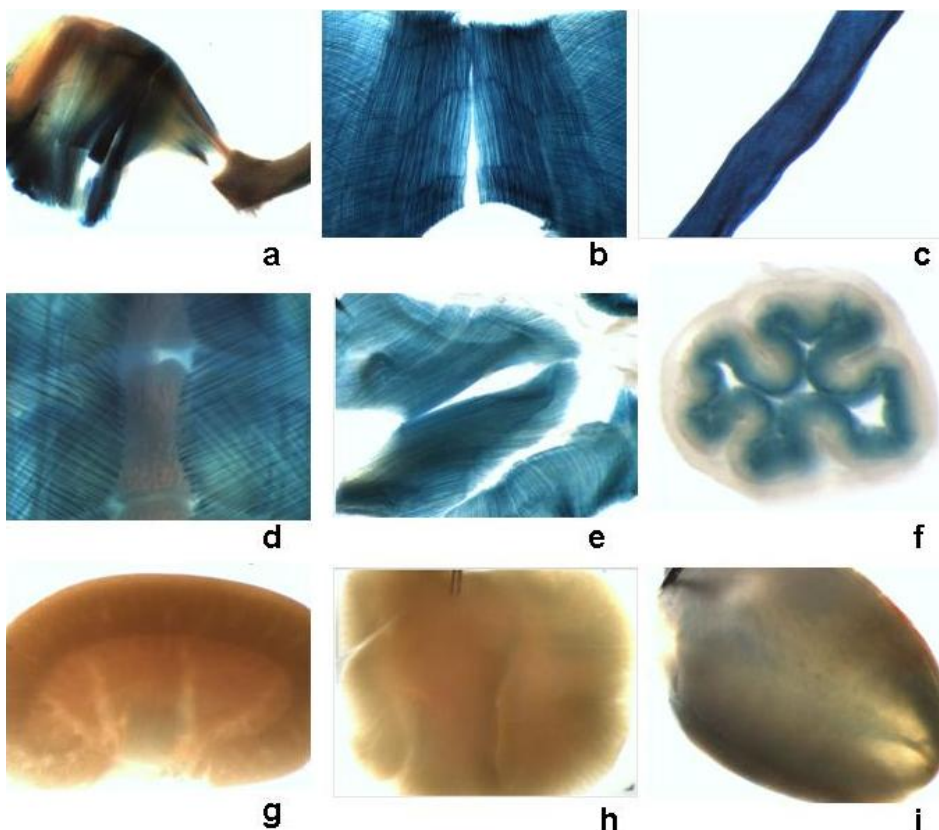
Histology on hind limbs indicated that muscular staining was non uniform (Fig. 31a), with a pattern that reflected the distribution of slow and fast oxidative fibers (Fig. 31b-31d). The LacZ

staining on the section of colon lining shows that LacZ is present in the cytoplasm of the epithelial cells (Fig. 32a, 32b).

Fig. 31: LacZ staining PTPH1-HET mice: sections of scheletal muscle of hind limb. LacZ staining and Neutral Red counterstaining; the muscular staining is non uniform with a pattern that reflected the distribution of slow and fast oxidative fibers at a) 2.5x, b) 10x, c) 20x, d) 40x.
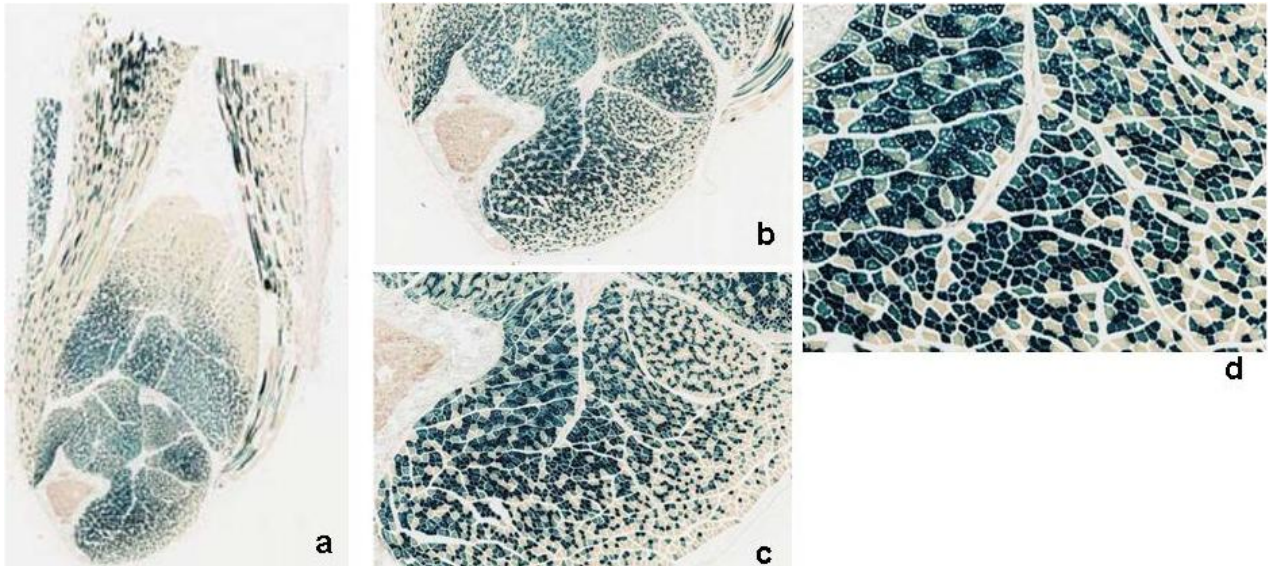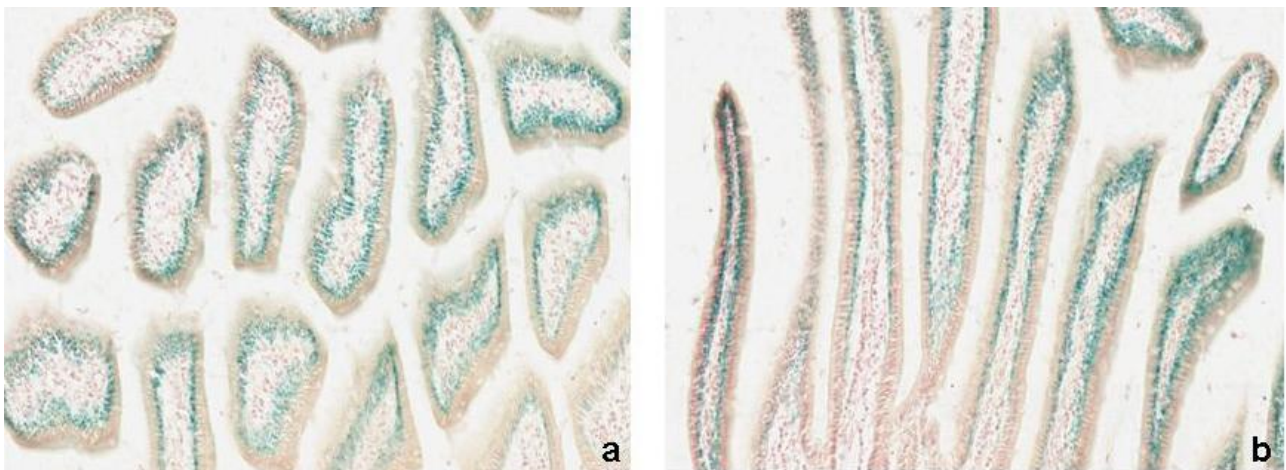

Fig. 32: LacZ staining PTPH1-HET mice: sections of colon epithelium. a) coronal and b) sagittal view of the LacZ staining in colon epithelium (40x).

4.1.2. Growth curve on PTPH1-KO mice

We noted that among adult (13 weeks old) animals, homozygous PTPH1-KO animals were larger in size than their WT littermates, with the difference being particularly significant for males (Fig. 33a). Male PTPH1-KO mice were 11% heavier than WT littermates (P_{male}=0.0001). We decided to mate new PTPH1-HET couples, to follow growth from birth onwards in new litters, which confirmed our observation (Fig. 33b). The difference in body weight between WT and homozygous KO animals (as measured by weight) started. The gap between PTPH1-WT and KO animals started to develop after weaning (on day 21), therefore it was not a result of parental behavior and/or litter competition. The difference became prominent at the onset of sexual maturation (around 28 days) and was higher in males than in females.

**Fig. 33: Phenotype of PTPH1-KO mice**. **a)** Weight variation of 13 wk old PTPH1-KO and WT littermate animals, females (left panel) and males (right panel; ten animals per datapoint, all born from heterozygous parents). **b)** Growth curve of KO and wild type animals (separate litters from **A,** born from homozygous parents; 6 female mutant, 5 female wild-type animals, 6 wild type and 4 mutant males).
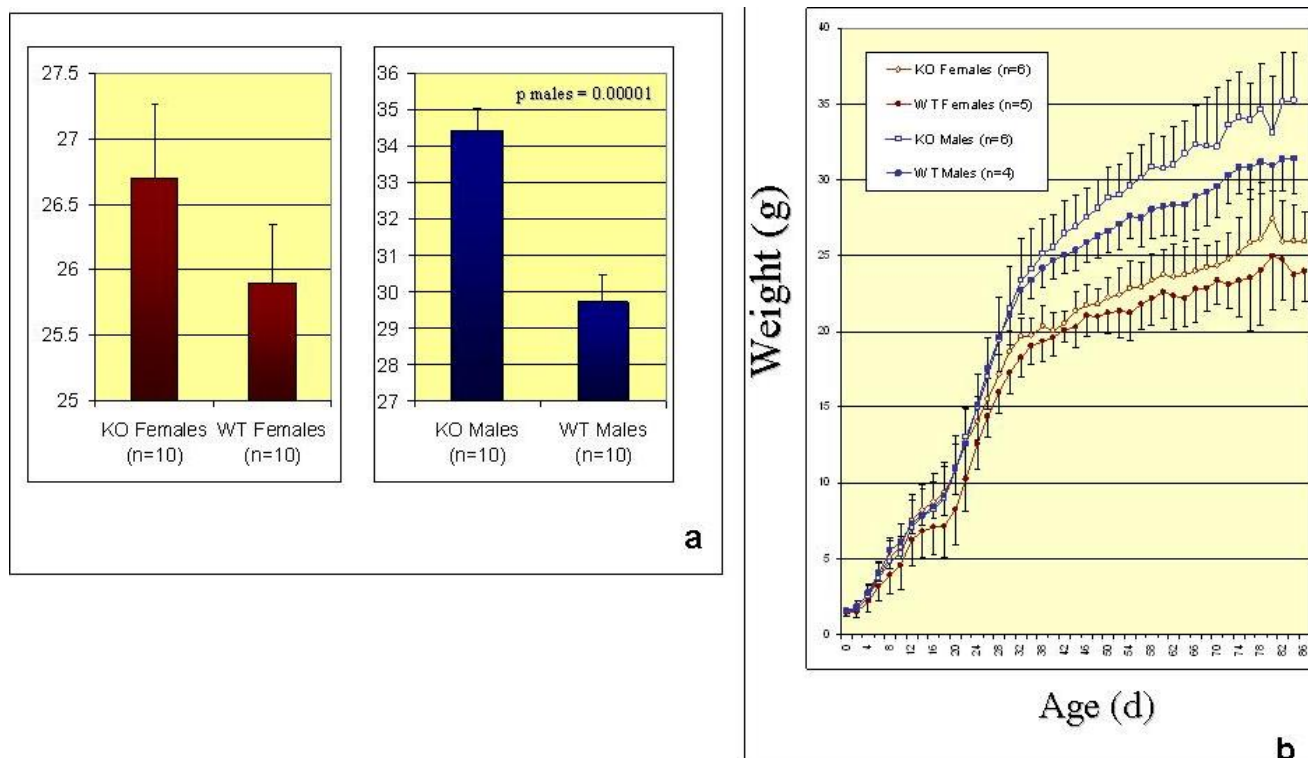
4.1.3. GH/IGF-1 axis in PTPH1-KO mice

The key endocrine mediator of GH is IGF-1 (40). To further understand the PTPH1-KO growth phenotype, we evaluated expression of IGF-1 mRNA in liver and plasma IGF-1 concentration from wild type and mutated animals. IGF1 mRNA was two times higher in male KO mice compared to matched WTs (P_{male} =0.02) (Fig. 34a), and one time in female KO *vs* WT littermates (P_{female} =0.0001). IGF-1 protein levels in plasma were significantly increased in mutant *versus* wild type animals (P_{male} =0.03; P_{female} =0.006), confirming the widest gap in male animals (Male$_{KOvsWT}$= 2x; Female$_{KOvsWT}$= 1.2x) (Fig. 34b).

Fig. 34: IGF-1 quantification in PTPH1-KO mice. **a)** Expression of IGF-1 mRNA in liver and **b)** IGF-1 protein in serum from WT and KO male and female littermates (four animals per group, sampled individually).
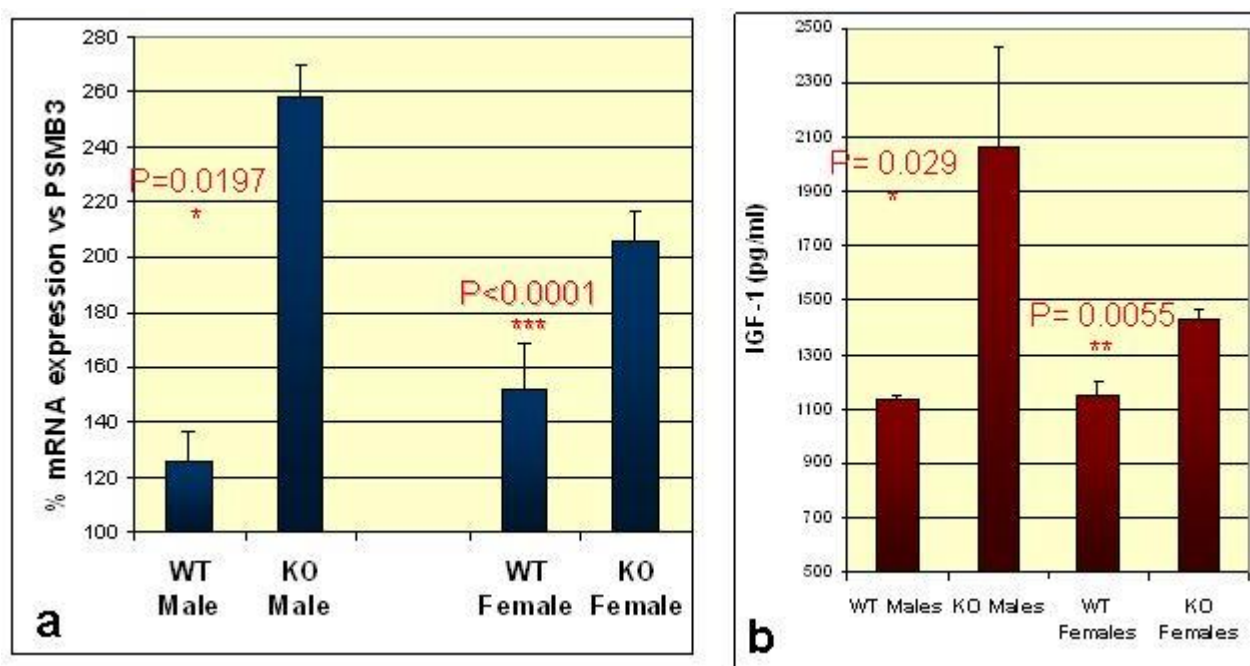
4.1.4. Analysis of body composition of PTPH1-KO mice

Finally, we evaluated body composition using DEXA. PTPH1-KO male animals showed significantly increased bone mineral content and a trend toward increased lean body mass and bone mineral density (Fig. 35a-35c) compared their matched WT mice. No differences were detected in females. Percentage of fat in PTPH1-KO *versus* WT mice did not show any modification (Fig. 35d).

Fig. 35: Body composition analysis of PTPH1-KO mice. **a)** Bone mineral density, **b)** mineral content, **c)** lean mass and **d)** body fat as determined by dual-energy x-ray absorptiometry (DEXA) (four animals per datapoint).
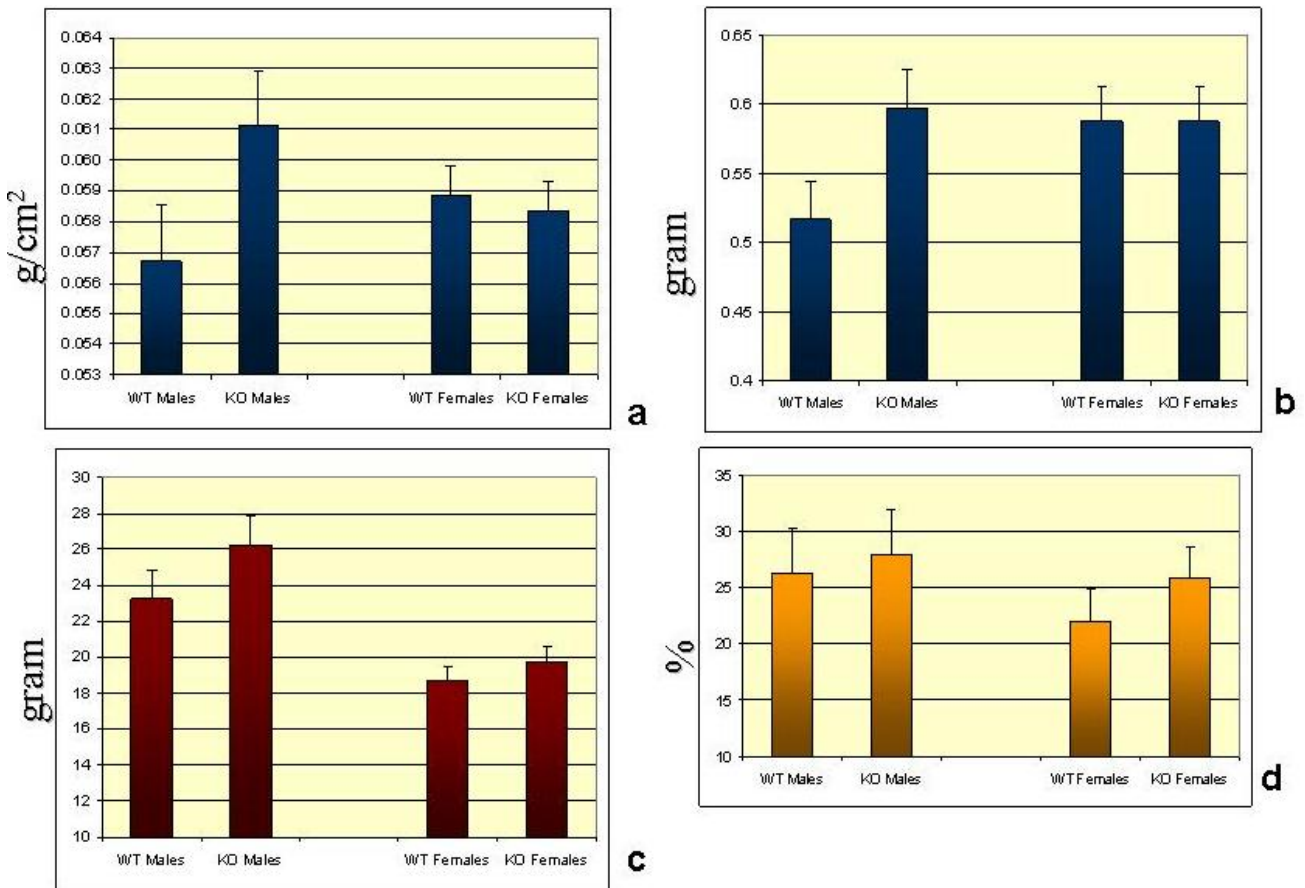
4.2. Discussion: PTPH1 in GHR signaling

To date, about 39 PTP knockout mouse phenotypes have been described (Reviewed in [230]), none of which show enhanced growth. While PTP1B has been strongly linked to some aspects of GHR signaling, PTP1B mutant mice are actually smaller than wild-type animals due to their lower fat content, linked to increased energy expenditure [26]. PTPH1 is the first PTP that seems to affect GHR signaling *in vivo*.

Several observations suggest that the increased size observed in PTPH1 knockout animals is related to enhanced GHR sensitivity. IGF-1, a key mediator of GH, was increased in the livers (as mRNA) and in serum of the knockout animals. The gender difference, with a more pronounced phenotype in males is significant for all readouts. In humans, females secrete higher amounts of GH [231] but respond with decreased IGF-1 secretion when given equal doses of GH, to the extent that half the GH dose to produce a given IGF-1 response is sufficient in male as compared to

female subjects [154,232]. In addition, GH treatment is known to enhance bone mineral density and lean body mass in humans as measured by Dual energy X-ray absorptiometry [233], as we found in PTPH1 knockout mice (Fig. 35).

The patchy muscle expression of PTPH1 (Fig. 31) suggests that it is specifically expressed in a single muscle fiber type- probably the slow oxydative (Type I) fibers, which have a smaller diameter than Type II fibers. Type I fibers are mitochondria-rich and are adapted to long-term muscle efforts. This finding is intruiging in the context of GHR signaling, as GH treatment is known to increase the proportion of type-1 fibres in skeletal muscle, whereas hypophysectomy (GH depletion) reduces the number of type 1 fibres by half [150]. Finally, GHR mRNA abundance is higher in type 1 slow-twitch oxidative muscles [234]. These observations suggest that PTPH1 plays a role in the GH-induced control of type 1 muscle fiber differentiation.

The relatively modest effect of PTPH1 mutation on growth may be related to this enzyme's unequal distribution pattern. Expression is relatively low in liver, a major source of IGF-1, yet the fact that hepatic IGF-1 expression directly depends on the GHR [235] and our finding that serum GH levels are not significantly altered in PTPH1 mice (data not shown) suggests a direct role for PTPH1 in GH-induced IGF-1 secretion. From a drug discovery perspective, while PTPH1 would seem a safe target, finding a phosphatase inhibitor that would affect growth may be a challenge. We tested bioavailable PTP inhibitors for PTP1B and PTPH1 (3-5 μM IC$_{50}$) in hypophysectomized young (26-28 d) female rats over 4 days, plus or without a half-maximal efficacy-dose of GH (0.025 IU rhGH), but saw no PTP-inhibitor-related effect on weight gain or tibial growth plate thickness. Possibly more potent PTPH1 inhibitors may show efficacy [236].

PTPH1 had earlier been associated with T-cell receptor signaling [47,82,83] and cancer [237-239]. Our new work shows that PTPH1 plays a role in growth, most likely by providing negative feedback to GHR signaling, although we have not investigated possible additional causes, such as effects on IGF-1 receptor signaling. PTPH1 may affect the dephosphorylation state of one or multiple phosphotyrosines on the GHR intracellular domain itself, JAK2, STAT-3 or STAT-5, or a combination thereof. *In vivo* evidence for a link between PTPH1 and GHR signaling stems from the increase of IGF-1 expression seen in absence of functional PTPH1 (Fig. 34), and enhanced bone density (Fig. 35). Our work also suggests that PTPH1 is at least partly responsible for the difference in size between male and female animals (as the effect of PTP loss is larger in males)

and might therefore have been more important in animals that display more prominent sexual dimorphism.

Furthermore, PTPH1 connection to CCKAR, that we have previously showed (page 57), should be considered. Indeed, CCK is a peptide hormone and neurotransmitter that was first postulated to regulate feeding behavior more than 35 years ago [226]. Administration of cholecystokinin reduces food intake and recent studies have suggested that the decrease in food consumption resulting is mediated by the CCKAR [225]. Comparatively, cholecystokinin-A and cholecystokinin-B/gastrin receptor knock-out mice maintained normal body weight well into adult life [223,224]. Thus, CCKAR could be part of the complex mechanism under the control of PTPH1, but it cannot be the only player. Further studies should be performed, to understand the mechanism of regulation of PTPH1 on CCKAR in the brain and in the pancreatic tissue, where CCKAR is also expressed [223]. Furthermore, we cannot exclude that PTPH1 works in concert with other PTPs to control GHR and CCKAR, as some of our *in vitro* and *ex vivo* studies suggest. Such cooperation could be revealed by generating animals that lack multiple PTPs.

Chapter 5 - PTPH1 role in the inflammatory process *in vivo*

5.1. Results on PTPH1-KO impact in two inflammatory models

Two different mouse models of inflammation were used to challenge PTPH1-WT and KO mice. Two sets of experiments per model have been performed, analyzing the inflammatory response respectively in young and aged PTPH1-WT and KO female mice.

5.1.1. LPS-induced inflammation

No complication was observed after ip injection of 1mg/kg LPS on PTPH1-WT and KO young and old female mice. All the animals stayed alive until the end of the experiment. At sacrifice blood was collected and serum and PBMC were isolated as previously described. RT-PCR on PBMC analysis has been carried out on the genes encoding for some cytokines and also for other cytokine genes of interest.

5.1.1.1. LPS-induced inflammation on young mice – RT-PCR analysis

RT-PCR has been carried out on cytokine genes: TNFα, ccl2 (MCP-1), IL12a, IL-1b, IL-6, IL-10 and IL-2.

TNF gene expression levels were slightly increased in white cells of LPS-treated mice compared to vehicle-treated animals 30 minutes post treatment (mpt) in both genotypes (Fig. 36). At 60 mpt TNFα mRNA levels of PTPH1-WT LPS treated mice were significantly higher (26 fold) compared to vehicle-treated WTs ($P_{WT\ 60mpt} < 0.05$; Fig. 36b). At 60 mpt PTPH1-KO white cells displayed a trend of increased TNFα mRNA levels (3.5 fold) in LPS-treated vs vehicle-treated mice ($P_{KO\ 60mpt} = 0.42$). Two-way Anova analysis pointed out a genotype related decrease of TNFα gene expression (16.5 fold) in the LPS-treated mice group, KO *vs* WT ($P_{KOvsWT} < 0.05$; Fig. 36b). At 180 mpt, both PTPH1-WT and KO LPS-treated mice showed a highly significant increase of TNFα expression in white cells compared to vehicle-treated animals (4.9 and 7.3 fold respectively) (PTPH1-KO LPS *vs* vehicle; $P_{KO\ 180mpt} < 0.001$; PTPH1-WT LPS *vs* vehicle; $P_{WT\ 180mpt} < 0.01$; Fig. 36c). No genotype-related differences in TNFα mRNA level were recorded at this late time point.

Fig. 36: RT-PCR on white cells of LPS-treated WT and KO young mice: TNFα gene. In graph are reported minus ΔΔCt values of WT LPS-treated, KO vehicle-treated and KO LPS-treated versus WT vehicle-treated. **a)** PTPH1- WT and KO mice displayed a trend in LPS-induced increased expression of TNFα in white cells at 30 after treatment, that **b)** became significant at 60 mpt in WT mice; at this time point also a genotype-related difference in TNFα expression was recorded between WT and KO mice; **c)** at 180 minutes TNFα levels were significantly increased by LPS in both WT and KO mice. 2way Anova followed by T-test; *:$p<0.05$; **:$p<0.01$; ***:$p<0.001$.
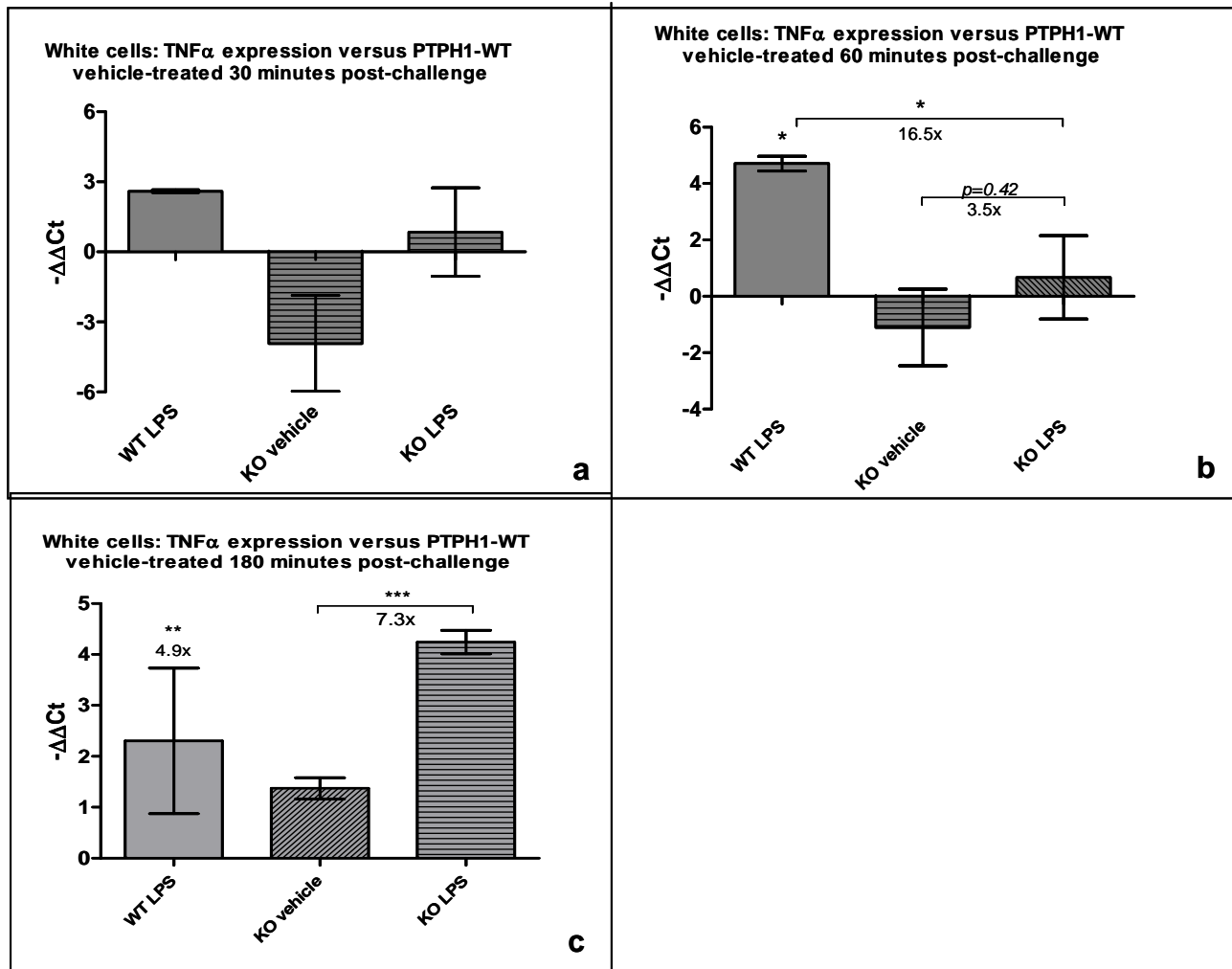
Ccl2/MCP1 gene expression in white cells showed a significant increase (187 fold) in WT LPS-treated compared to vehicle treated mice at 60 mpt (Fig. 37a), whereas no alteration was observed in KO mice or within or between genotypes, at 30 (data not shown) and 60 minutes post treatment (Fig. 37b).

IL1β, IL6, IL-10, IL-2 and IL12a expression levels were not significantly altered in total white cells extracted from LPS-treated vs vehicle-treated in both PTPH1-WT and KO mice at any time point investigated (data not shown).

Fig. 37: RT-PCR on white cells of LPS-treated WT and KO young mice: ccl2 gene. In graph are reported minus ΔΔCt values of WT LPS-treated, KO vehicle-treated and KO LPS-treated versus WT vehicle-treated **a)** 187 fold increase in ccl2 gene expression in WT white cells due to LPS treatment, and no difference in KO mice; **b)** No difference in ccl2 expression in white cells of WT and KO mice 180 minutes post LPS treatment. 2way Anova followed by T-test; *:$p<0.05$; **:$p<0.01$; ***:$p<0.001$.
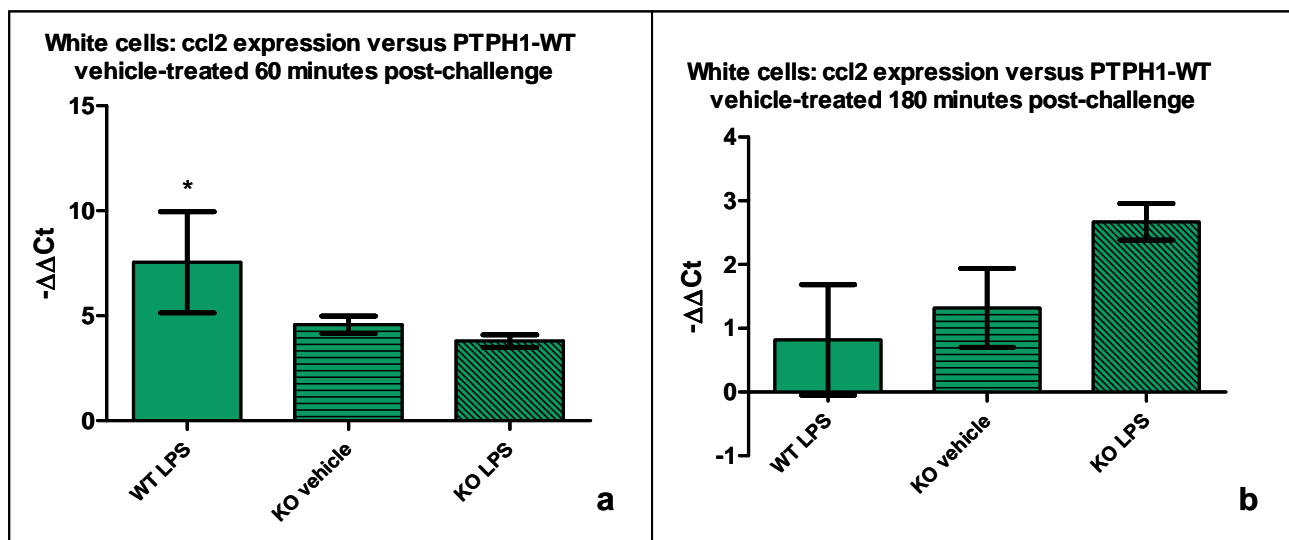
5.1.1.2. LPS-induced inflammation on young mice - Cytokine Beads Assay

Six cytokines (TNFα, MCP-1, IL-6, IL-10, IFN-γ, IL-12p70) were analyzed in the plasma of LPS and vehicle treated WT and KO mice. IFN-γ and IL-12p70 release did not display a significant modulation in our mouse model at the time points investigated. Values recorded below detection limit were excluded from the final analysis.

- *30 minutes post treatment*

TNFα overall release in the plasma was increased in LPS-treated mice compared to vehicle-treated ones 30 minutes post LPS injection (P_{2way}=0.0199), but Bonferroni's post hoc test revealed no significant differences in the PTPH1-WT and KO groups associated with either treatment or genotype (Fig. 38).

MCP-1 levels were slightly modulated in WT LPS-treated plasma compared to the vehicle-treated group at 30 mpt, while no difference in the KO mice group was detectable at this time point. A genotype-related 50% decrease in MCP-1 release in plasma was recorded in LPS-treated KO vs WT mice (P_{KOvsWT}<0.05).

IL10 levels in plasma were significantly increased due to LPS treatment in WT mice at 30 minutes (165%, P_{WT}<0.05), whereas no difference in the KO mice group was found. However a genotype-related decrease in IL10 release in plasma was detectable in LPS-treated KO vs WT mice (150%, P_{KOvsWT}<0.05).

IL6 release was significantly higher in the plasma of WT LPS-treated compared to vehicle-treated mice 30 minutes post LPS injection (P_{WT}<0.05), while no modulation in IL6 levels was seen in KO mice, LPS vs vehicle. No genotype-related differences in IL6 release were detected in LPS-treated WT vs KO animals.

Fig. 38: CBA analysis on plasma from young PTPH1-WT and KO mice 30 minutes after 1mg/kg LPS injection. Genotype-related difference in MCP-1 and IL10 between WT and KO LPS-treated animals. WT animals displayed a LPS-induced increase in IL10 and IL6; dot line indicates the detection limit of CBA kit, as reported by the supplier. 2way Anova followed by Bonferroni post test; *:p<0.05; **:p<0.01; ***:p<0.001.

Cytokine release in plasma 30 min after LPS injection
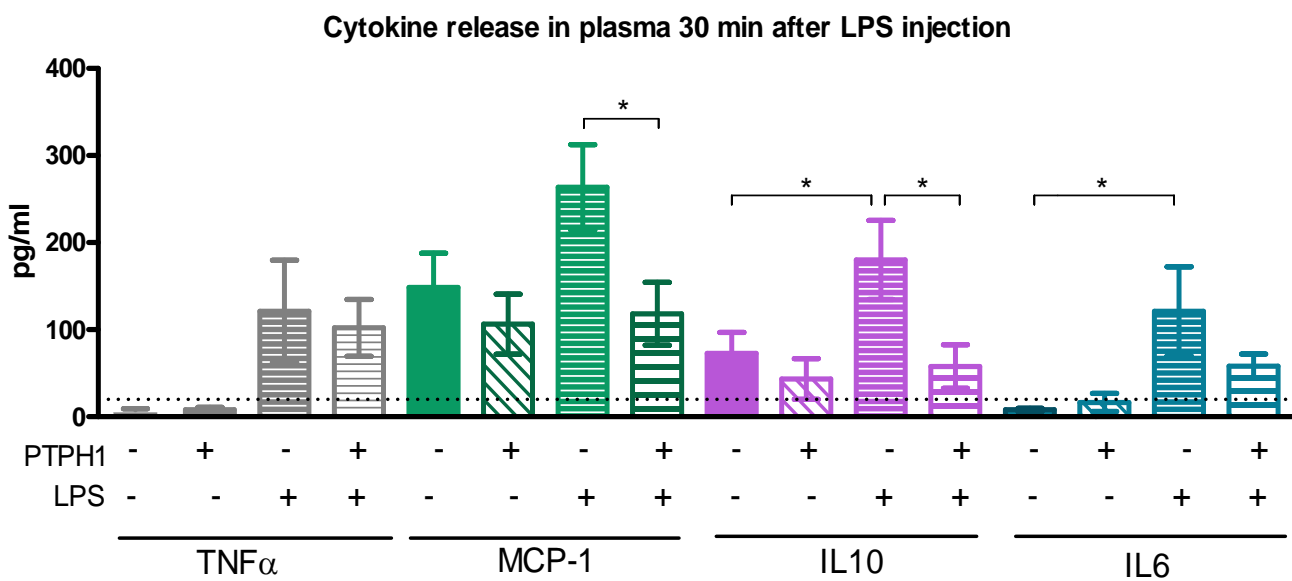
- *60 minutes post treatment*

At 60 minutes post LPS/vehicle injection TNFα, MCP-1, IL-6 and IL-10 release was highly significantly increased in the plasma of LPS-treated animals compared to vehicle-treated mice in both WT and KO groups (Fig. 39). Moreover a genotype-related 50% decrease (P_{KOvsWT}<0.01) in TNFα, MCP-1 and IL-10 plasma level was seen in LPS-treated KO vs WT young mice (Fig. 39). No genotype-related differences were detected in IL-6 plasma release between PTPH1-WT and KO animals (Fig. 39).

Fig. 39: CBA analysis on plasma from young PTPH1-WT and KO mice 60 minutes after 1mg/kg LPS injection. Genotype-related difference detected in TNFα, MCP-1 and IL10 between WT and KO LPS-treated animals. Both WT and KO mice displayed a LPS-induced increase in TNFα, MCP-1 and IL10; IL6 level was significantly increased by LPS in both WT and KO mice. 2way Anova followed by Bonferroni post test; *:p<0.05; **:p<0.01; ***:p<0.001
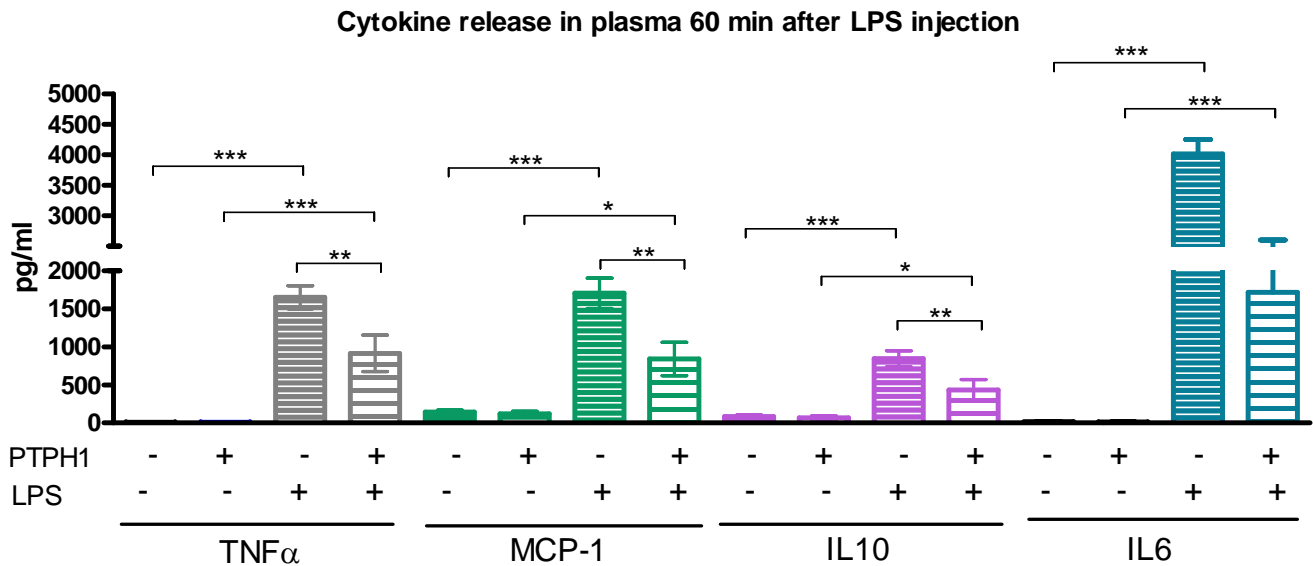
- *180 minutes post treatment*

At 180 minutes post LPS/vehicle challenge, TNFα (Fig. 40a), MCP-1 and IL-6 (Fig. 40b) levels was significant increased in the plasma of WT and KO LPS-treated compared to vehicle-treated mice but no genotype-related differences were detectable. IL10 release was significantly increased in PTPH1-KO LPS-treated mice vs their vehicle control (Fig. 40a) (P_{KO} <0.05), while no modulation was recorded in WT mice group. No genotype-related effect on IL10 release was detectable between WT and KO mice.

LPS-treated mice vs their vehicle control (P_{KO} <0.05), while no modulation has been recorded in WT mice group (Fig. 40a). No genotype-related effect on IL10 release was detectable between WT and KO mice (Fig. 40a).

Fig. 40: CBA analysis on plasma from young PTPH1-WT and KO mice 180 minutes after 1mg/kg LPS injection. a) PTPH1-WT and KO mice displayed a LPS-induced increase in TNFα and IL10; **b)** MCP-1 and IL6 levels were significantly increased by LPS in both WT and KO mice; dot line indicates the detection limit of CBA kit, as reported by the supplier. 2way Anova followed by Bonferroni post test; *:p<0.05; **:p<0.01; ***:p<0.001.
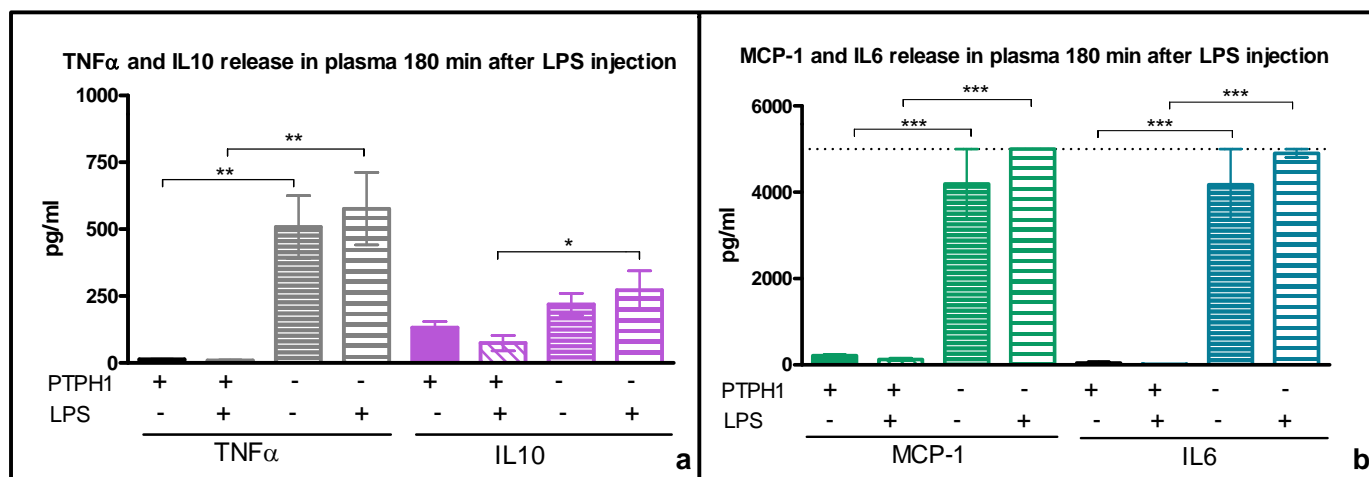
5.1.1.3. LPS-induced inflammation on aged mice – RT-PCR analysis

RT-PCR on cytokine-related genes

RT-PCR was performed on the same cytokine genes investigated in LPS experiments in young mice. IL-10, IL-2 and IL6 white cells expression levels were not significantly altered upon LPS challenge in both PTPH1-WT and KO aged mice (data not shown).

TNFα gene expression levels are not significantly increased in white cells from LPS-treated aged mice compared to veh-treated ones 30 minutes mpt in both genotypes (data not shown). At 60 mpt, significant TNFα mRNA increase was detected in PTPH1-KO mice group LPS *vs* vehicle treated (10.5 fold increase; $P_{KO\ 60mpt}<0.01$) (Fig. 41a). PTPH1-WT aged mice, LPS *vs* vehicle, displayed a trend in LPS-induced TNFα increase, but it is not statistically significant (Fig. 41a)..

At 180 mpt, both PTPH1-WT and KO LPS-treated mice showed a higher TNFα expression compared to their respective vehicle-treated animals (respectively a 4.9 and 7.3 fold increase; $P_{WT}<0.05$; $P_{KO}<0.05$) (Fig. 41b). No genotype-related effects in TNFα expression were recorded between WT and KO mice at the time points investigated (Fig. 41a, 41b).

Fig. 41: RT-PCR on white cells of LPS-treated WT and KO aged mice: TNFα gene. a) Trend in TNFα gene expression modulation in white cells of WT mice at 60 mpt; LPS-induced 10 fold increase in TNFα gene expression in KO aged mice at 180 mpt; **b)** Significant LPS-induced 5-6 fold increase in TNFα expression in both genotypes, LPS*vs*veh.
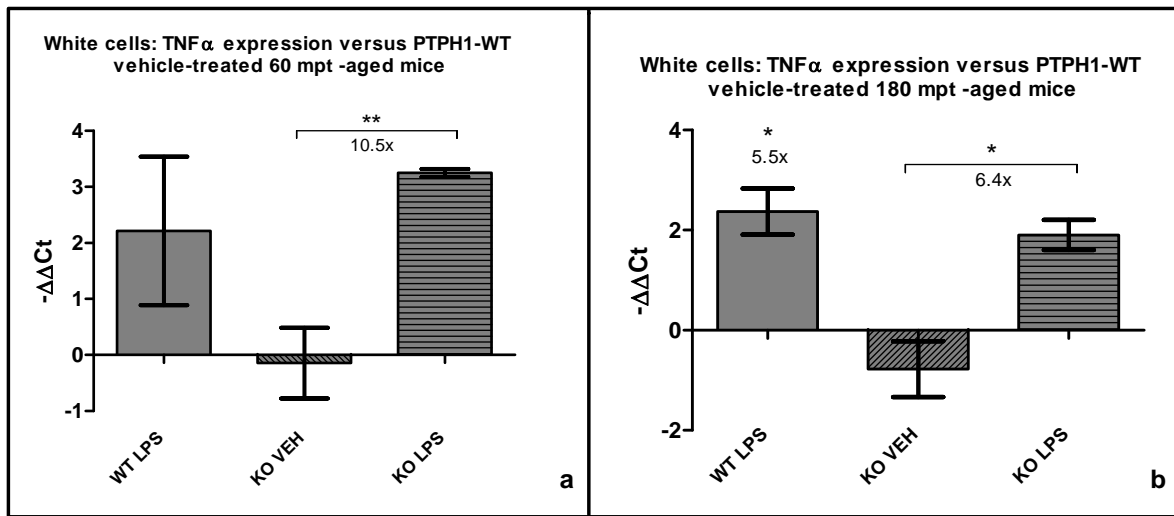
Ccl2 gene expression in white cells was not modulated at 30 mpt in both genotypes (data not shown) but at 60 mpt, a ccl2 10-fold upregulation was detectable in KO LPS-treated compared to vehicle treated aged mice (Fig. 42a). No LPS-induced modulation of ccl2 gene was detected in WT mice group at this time point (Fig. 42a). At 180 mpt, both PTPH1-WT and KO mice displayed LPS-induced ccl2 gene uperegulation in white cells, compared to their matched vehicle-treated aged animals (respectively 15 and 12-fold increase; Fig. 42b). No genotype-related differences in ccl2 expression were recorded between WT and KO mice at the time points investigated (Fig. 42a, 42b).

Fig. 42: RT-PCR on white cells of LPS-treated WT and KO aged mice: ccl2 gene. a) ccl2 gene expression is not modulated in WT white cell at 60 mpt while KO LPS-treated white cells display a 10-fold increase in ccl2 gene compared to veh-treated ones; **b)** at 180mpt both genotype show a LPS-induced increase in ccl2 gene expression. 2way Anova followed by T-test; *:p<0.05; **:p<0.01; ***:p<0.001.
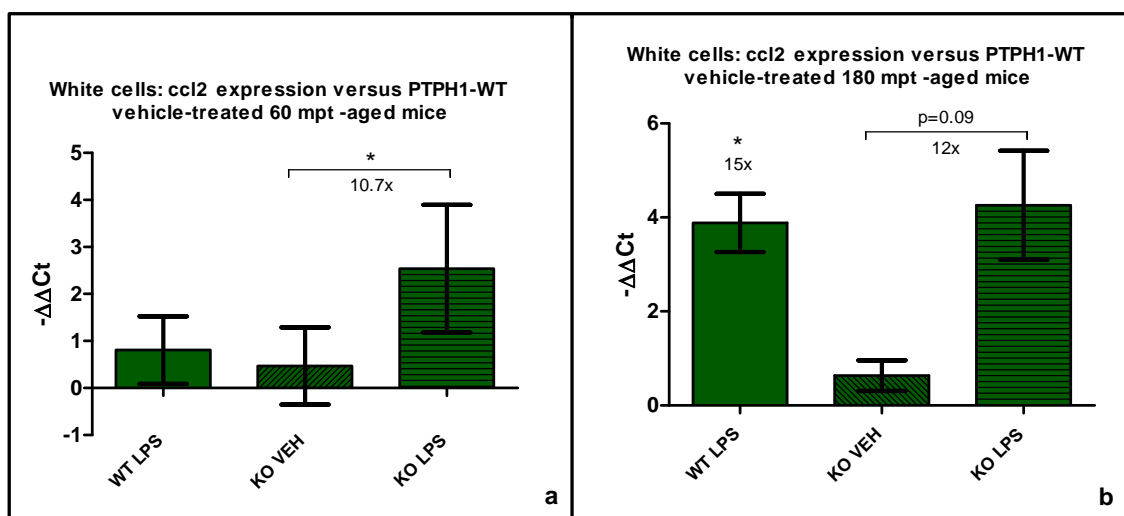
IL12a gene expression was not modulated in both WT and KO mice group at 30 (data not shown) and 60 mpt (Fig. 43a). At 60 mpt, no LPS-induced alteration in WT and KO mice was recorded but a genotype-related IL12a downregulation (4-fold) was present in LPS-treated KO mice ($P_{LPS}<0.05$) (Fig. 43a). At 180 mpt, IL12a gene was slightly significant upregulated (4-fold; $P_{LPS}<0.05$) in LPS-treated white cells of WT aged mice, but no modulation was detectable in KO mice (Fig. 43b).

Fig. 43: RT-PCR on white cells of LPS-treated WT and KO aged mice: cytokine-related genes. a) No LPS-induced modulation of IL12a gene in white cells of WT and KO mice at 60 mpt; at 60 mpt a genotype-related 4 fold decrease in IL12a gene was detectable in LPS-treated groups, KO*vs*WT; **b)** significant LPS-induced 4-fold increase in IL12a gene in WT white cells at 180 mpt; no modulation detectable in KO mice group. **c)** At 180mpt a genotype-related decrease in IL1β gene was detectable in LPS-treated groups KO*vs*WT. 2way Anova followed by T-test; *:p<0.05; **:p<0.01; ***:p<0.001.
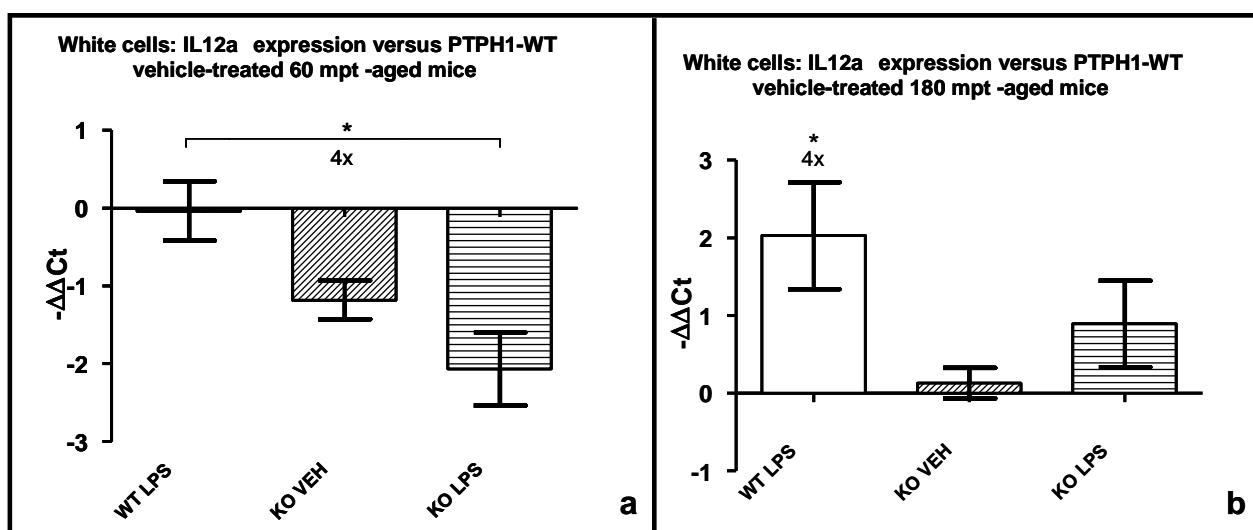
RT-PCR on PTPH1-related genes

RT-PCR has been carried out on the same PTPH1-related genes used in the "young mice experiment": Ghr, igf1, igf1r, adam17 and timp1.

No modulation of PTPH1-related genes as Ghr, igf1r, timp1, adam17 and igf1 (data not shown) has been detected in white cells extracted from old PTPH1-WT and KO female mice.

5.1.1.4. LPS-induced inflammation on aged mice – CBA analysis

The mouse inflammation CBA kit allows the analysis of 6 cytokines: TNFα, MCP-1, IL-6, IL-10, IFN-γ, IL-12p70.

IFN-γ and IL-12p70 release did not display a significant modulation in our mouse model at the time points investigated. Values recorded below detection limit were excluded from the final analysis.

- *30 minutes post treatment*

At 30 mpt, TNFα overall release was increased in the plasma of LPS-treated aged mice compared to vehicle-treated ones ($P_{2way\ LPS}$=0.0199), but Bonferroni's post hoc test revealed no significant differences in PTPH1-WT and KO group either due to treatment or to genotype (Fig. 44).

MCP-1 and IL10 plasma levels were not modulated either by LPS or by genotype at 30 mpt. At this time point, IL6 plasma release was significantly higher in WT LPS-treated compared to vehicle-treated (P_{WT}<0.05), while no modulation in IL6 release was detectable in KO mice, LPS *vs* vehicle. No genotype-related differences in cytokine release were recorded in LPS- treated WTvsKO aged animals 30 minutes post LPS injection (Fig. 44).

Fig. 44:CBA analysis on plasma 30 minutes after 1mg/kg LPS injection: aged mice. TNFα levels were slightly modulated in plasma of LPS-treated WT and KO mice, but not significantly; no LPS- or genotype-induced modulation of MCP-1 and IL10; IL6 release was slightly modulated in LPS-treated WT mice, but not in KO at 30 mpt. Dot line indicates the kit detetction limit. 2way Anova followed by Bonferroni post test; *:p<0.05; **:p<0.01; ***:p<0.001.

Cytokine release in plasma of LPS-induced inflammation model - aged mice - 30 mpt
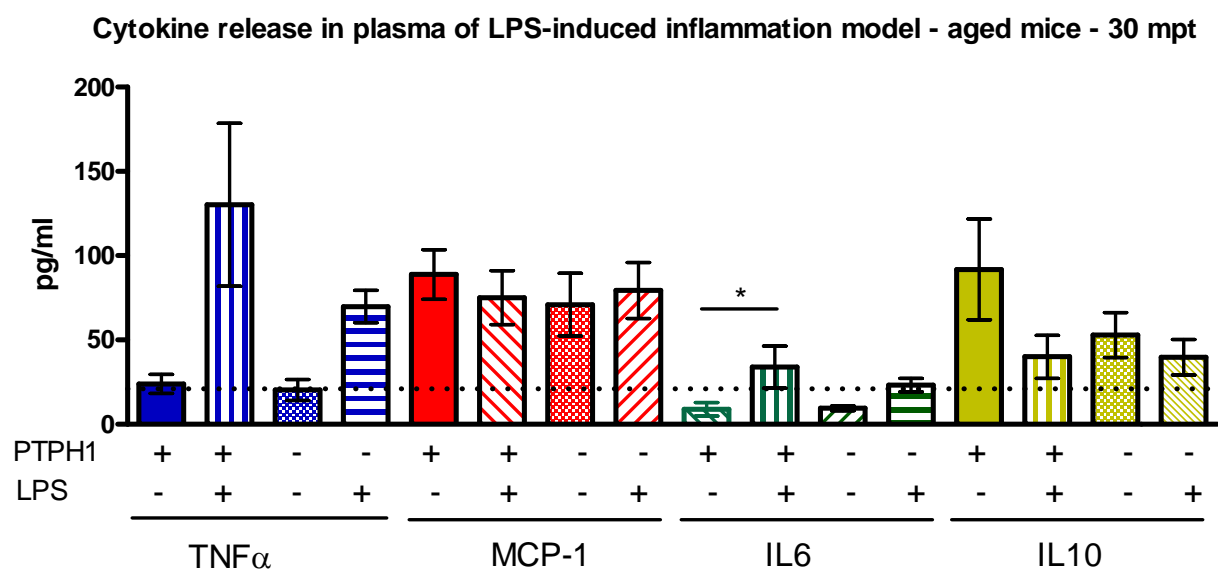
- *60 minutes post treatment*

At 60 minutes post treatment, a strong increase of LPS-induced TNFα, MCP-1, IL-6 and IL-10 release was detected in the plasma of LPS-treated compared to vehicle-treated aged mice in both

WT and KO group ($P_{LPSvsveh}$<0.001) (Fig. 45). Furthermore a genotype-related 40% decrease in MCP-1 plasma level was recorded in LPS-treated KOvsWT aged mice. At 60 mpt, no genotype-related differences were detected in TNFα, IL10 and IL-6 plasma release between PTPH1-WT and KO aged animals (Fig. 45).

Fig. 45: CBA analysis on plasma 60 minutes after 1mg/kg LPS injection: aged mice. Strong LPS-induced modulation of TNFα, MCP-1, IL6 and IL10 in both PTPH1-WT and KO aged mice at 60 mpt; a genotype-induced decrease of MCP-1 release was detectable in LPS-treated mice (WTvsKO). 2way Anova followed by Bonferroni post test; *:p<0.05; **:p<0.01; ***:p<0.001.
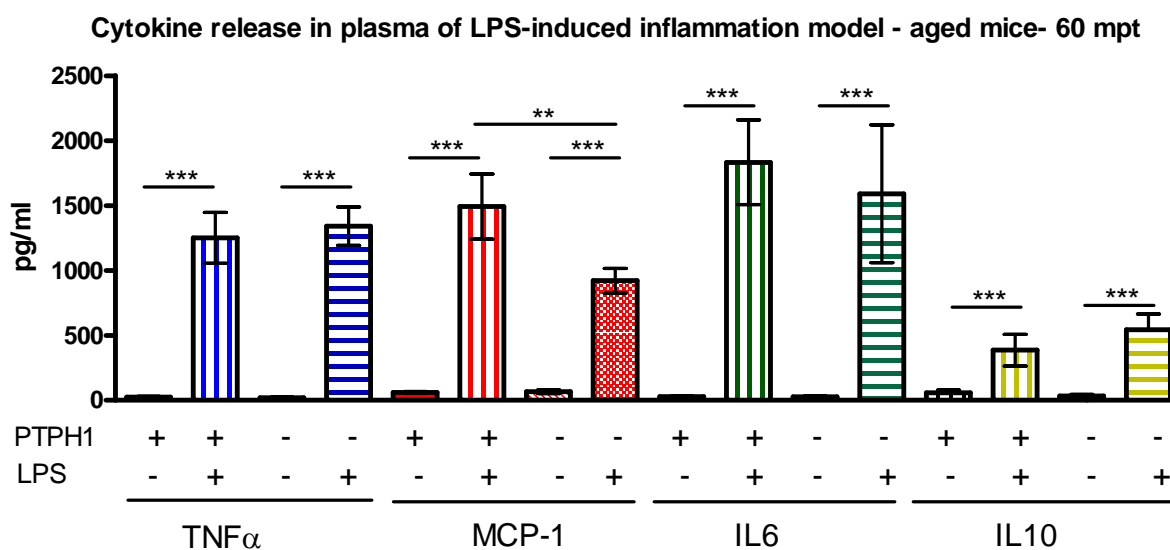
- *180 minutes post treatment*

At 180 minutes post treatment, a trend of increased LPS-induced TNFα release was detected in plasma of PTPH1-WT aged mice, while statistically significance was reached in PTPH1-KO aged mice (P_{KO}<0.05) (Fig. 46).

At this time point, MCP-1 and IL-6 release was significantly increased in the plasma of WT and KO LPS-treated compared to veh-treated mice (P_{WT}<0.001; P_{KO}<0.001) (Fig. 46).

IL10 plasma levels were significantly increased in PTPH1-KO LPS-treated mice vs their vehicle control (P_{KO}<0.001), while no modulation was recorded in WT aged mice. No genotype-related differences were detectable in cytokine release between WT and KO aged female mice at this late time point.

Fig. 46: CBA analysis on plasma 180 minutes after 1mg/kg LPS injection: aged mice. a) Strong LPS-induced modulation of MCP-1 and IL6 that reached the detection limit in both PTPH1-WT and KO aged mice; **b)** detail of LPS-induced modulation of TNFα and IL10 release in both genotype, it was statistically significant only in KO mice group. Dot line indicates the detection limit of the kit. 2way Anova followed by Bonferroni post test; *:p<0.05; **:p<0.01; ***:p<0.001.
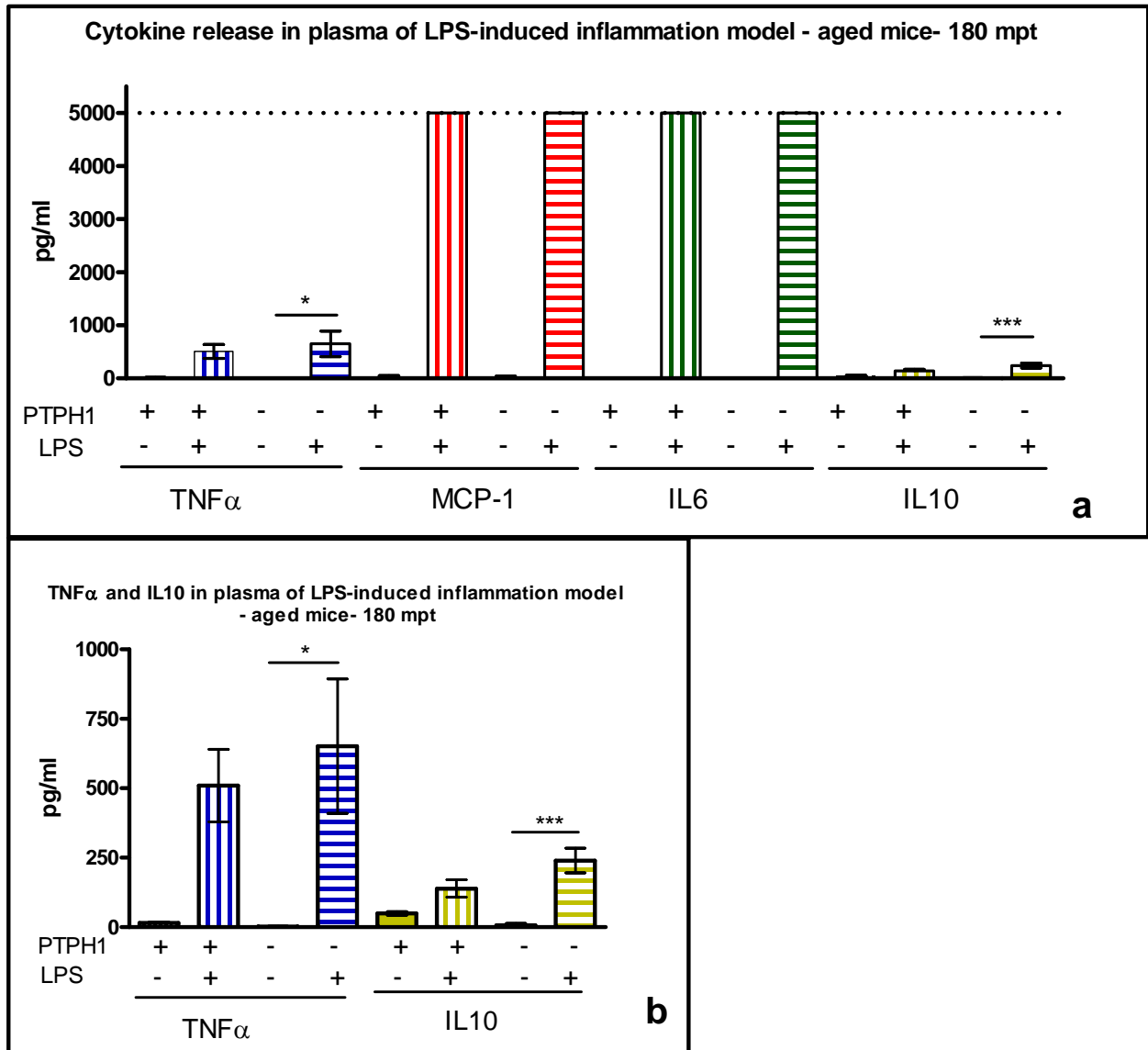
5.1.2. Carrageenan (CARR)-induced inflammation

No complication after injection of 2% carrageenan in the right paw of the mice was observed. All young and aged animals stayed alive until the end of the experiment.

5.1.2.1.Carrageenan (CARR)-induced inflammation on young mice

Paw thickness

A significantly higher paw thickness was measured by a precision caliper in the CARR-treated paws, compared to the controlateral vehicle treated one (Fig. 47). This modulation was statistically significant in both WT and KO groups and was detectable already after 1 hour from carrageenan injection. The edema was still present 24 hours post-injection (PTPH1-WT: $P_{1h}=0.0028$; $P_{3h}=0.0022$; $P_{1h}=0.0049$; $P_{1h}=0.0006$) (PTPH1-KO: $P_{1h}=0.0001$; $P_{3h}=0.0002$; $P_{1h}=0.0002$; $P_{1h}=0.0003$) (Fig. 47). No statistical differences in paw thickness were detected in PTPH1-WT versus PTPH1-KO animals.

Fig. 47: Carrageenan-induced paw edema in PTPH1-WT and KO young mice. Paw edema was detectable at 1h after treatment in both genotypes at the same intensity. This increase thickness of the paws was maintained till sacrifice, at 24h post CARR-injection. No genotype-related differences were detectable between WT and KO CARR-treated groups. 2way Anova followed by Paired T-test; *:p<0.05; **:p<0.01; ***:p<0.001. V-WT: vehicle-treated PTPH1-WT mice; C-WT: CARR-treated PTPH1-WT mice; V-KO: vehicle-treated PTPH1-KO mice; C-KO: CARR-treated PTPH1-KO mice..

Paw thickness
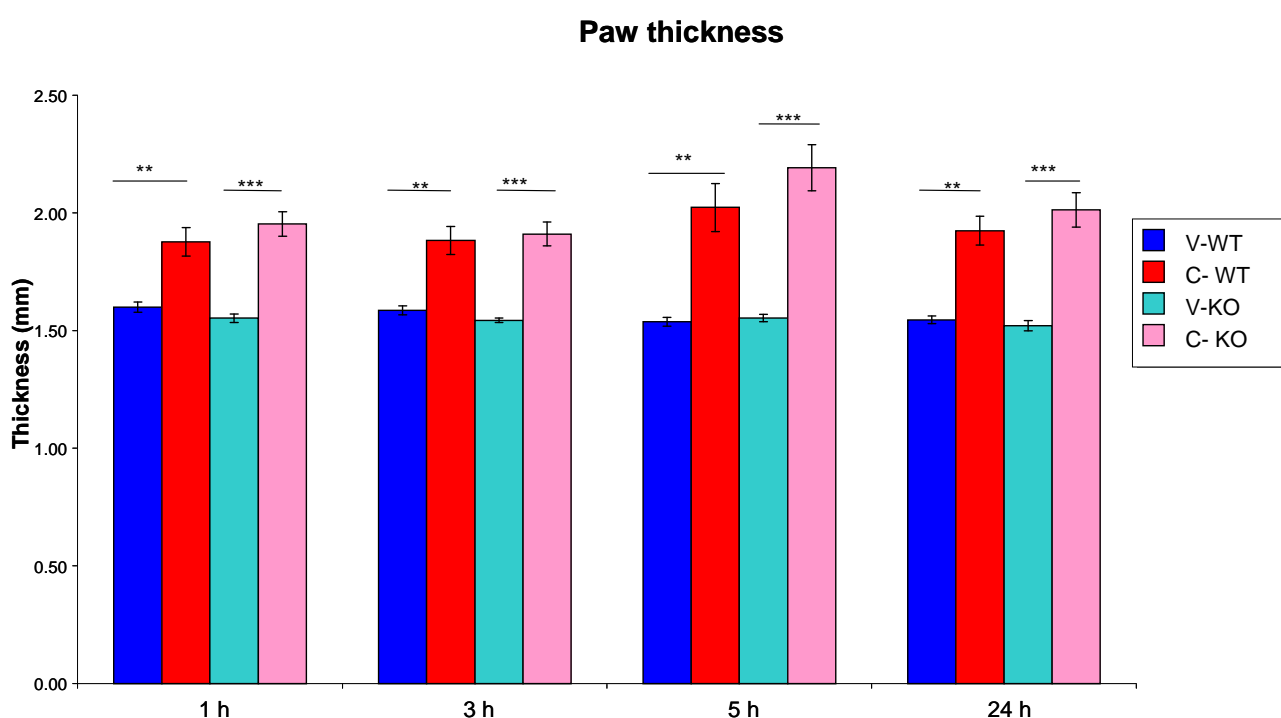
Behavioral Tests

Hargreaves's test

A significantly decreased response at the Hargreaves'test was detected in the CARR-treated paws compared to the controlateral vehicle treated ones (Fig. 48a). This decrease in withdrawal time was statistically significant in both WT and KO groups; it was detectable already at 1 hour after carrageenan injection through 24 h maintaining the same intensity (PTPH1-WT: $P_{1h}=0.00004$; $P_{3h}=0.0122$; $P_{1h}=0.0016$; $P_{1h}=0.0039$) (PTPH1-KO: $P_{1h}=0.0001$; $P_{3h}=0.00001$; $P_{1h}=0.0005$; $P_{1h}=0.0005$) (Fig. 35b). No statistical differences in withdrawal time were detected in PTPH1-WT versus PTPH1-KO animals.

Von Frey test

A significantly decreased response at the Von Frey test was detected in the CARR-treated paws compared to the controlateral vehicle treated ones (Fig. 48b). This decrease in withdrawal force was statistically significant in both WT and KO groups, it was detectable already at 1 hour after carrageenan injection through 24 h maintaining the same intensity till 24 hours post-injection (PTPH1-WT: $P_{1h}=0.017$; $P_{3h}=0.0002$; $P_{1h}=0.001621$; $P_{1h}=0.002458$) (PTPH1-KO: $P_{1h}=0.004$; $P_{3h}=0.00977$; $P_{1h}=0.001272$; $P_{1h}=0.007833$) (Fig. 35a). No statistical differences in withdrawal force were detected in PTPH1-WT versus PTPH1-KO animals.

CatWalk test

Intensity- The intensity parameter was not strongly modulated by CARR injection in both genotypes at 1 and 3 hours post-treatment (Fig. 49a). A trend of slight CARR-induced decrease in intensity was detectable in WT mice at 1 hour post-treatment.

At 5 and 24 hours after carrageenan injection, a significant decrease in intensity was recorded in the CARR-treated paws, compared to vehicle-treated ones in both WT and KO mice (PTPH1-WT: P_{5h}, P_{24h} <0.05) (PTPH1-KO: P_{5h}, P_{24h} <0.05). No genotype-related differences in the intensity parameter were detetcted (Fig. 49a).

Duty cycle- In the WT group, a slight significant decrease in duty cycle was detectable in the CARR-treated paws compared to the vehicle-treated ones already 1 hour after CARR-injection ($P_{WT\ 1h}$<0.05) (Fig. 49b). At this time point, no significant CARR-induced differences in duty cycle were disclosed in the PTPH1-KO mice group.

At 3 hours post CARR-injection, no differences were detectable in duty cycle due either to treatment or to genotype.

At 5 hours post treatment, PTPH1-KO CARR-treated paws displayed a significant decreased duty cycle compared to the controlateral vehicle-treated ones ($P_{KO\ 5h}$<0.01), but not compared to

WT CARR-treated. This difference was maintained in KO mice group, CARR *vs* vehicle, also 24 hours post-injection ($P_{KO\ 24h} < 0.05$) and it was detectable also in WT mice group (CARR*vs*vehicle $P_{WT\ 24h} < 0.05$) (Fig. 49b). No genotype-related differences in ducty cycle were detected at the time points investigated.

Fig. 48: Behavioral tests performed on CARR-treated PTPH1-WT and KO young mice. a) Withdrawal force measured at the Von Frey test was significantly decreased by CARR treatment in both WT and KO mice, starting 1 hour after CARR injection, till 24 hours. The peak was reached 5 hours after CARR treatment. **b)** The withdrawal time measured at Hargreaves' test was significantly decreased by CARR treatment in both WT and KO mice, starting 1 hour after CARR injection, till 24 hours. The peak of response was reached 5 hours after CARR treatment. No genotype-related differences were detectable between WT and KO CARR-treated groups at both tests. 2way Anova followed by Paired T-test *:p<0.05; **:p<0.01; ***:p<0.001. V-WT: vehicle-treated PTPH1-WT mice; C-WT: CARR-treated PTPH1-WT mice; V-KO: vehicle-treated PTPH1-KO mice; C-KO: CARR-treated PTPH1-KO mice.

Fig. 49: Catwalk analysis performed on CARR-treated PTPH1-WT and KO young mice. a) The intensity parameter was not strongly modulated by CARR injection in both genotypes at 1 and 3 hours post-treatment; a slight CARR-induced decrease in intensity was detectable in WT mice at 1 hour post-treatment. A significant CARR-induced modulation of gait analysis was detectable in both gentoypes. **b)** The duty cycle parameter was significantly altered by CARR injection in WT mice 1h post-treatment, but no difference has been detected in KO mice group. No CARR-induced or genotype-induced differences in duty cycle are detectable 3 hours after CARR treatment. A slight CARR-induced decrease duty cycle is detectable in WT group at 5 hours post-treatment while a strong dowregulation of this parameter is recorded in KO group. 24 hours after CARR-treatment both genotypes display a decrease percentage of duty cycle and no genotype-related differences are detectable between WT and KO CARR-treated groups. 2way Anova followed by Paired T-test *:p<0.05; **:p<0.01; ***:p<0.001.

Print area- No differences in print area due to either treatment or genotype were detectable at 1 and 3 hours post CARR-injection (Fig. 49).

At 5 and 24 hours post-injection KO CARR-treated paws showed a significant decreased print area compared to controlateral vehicle-treated paws ($P_{KO\ 5h} < 0.05$; $P_{KO\ 24h} < 0.05$). No differences were detected in WT CARR-treated *vs* vehicle treated paws at 5 hours post-injection, but a slight trend of genotype-related decreased print area was present between CARR-treated WT *vs* KO mice, at 24 hours time point ($P_{WT\ 24h} = 0.0642$) (Fig. 50).
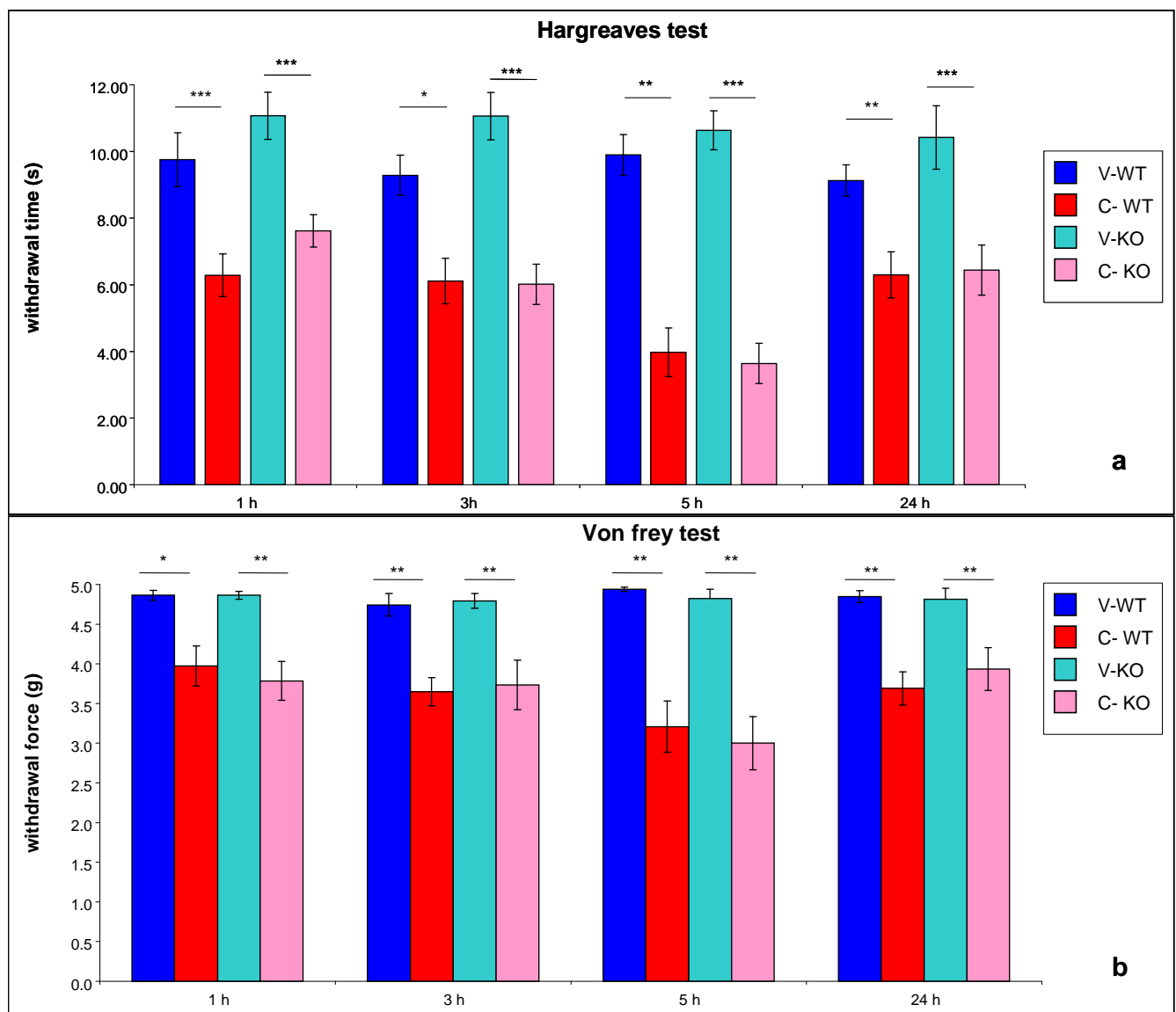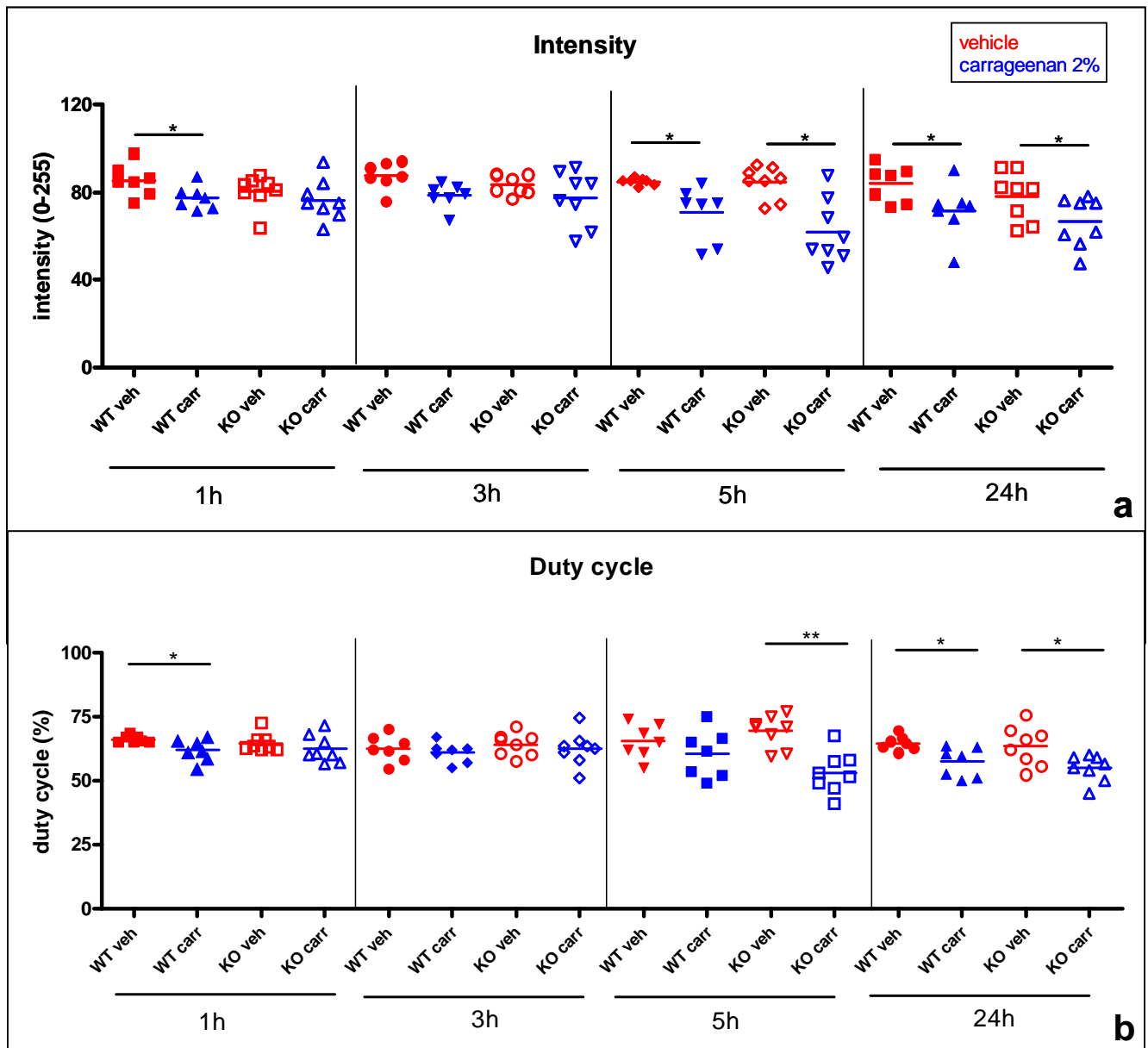
Fig. 50: Catwalk analysis performed on CARR-treated PTPH1-WT and KO young mice. a) The print area parameter was not modulated by CARR injection in both genotypes at 1 and 5 hours post-treatment; a slight CARR-induced decrease in print area was detectable in both genotypes at 5 and 24 hours post-treatment, and it was statistically significant only in KO mice group at both time points. A trend in genotype-related difference between CARR-treated animals (WT and KO) was recorded at 24h post- treatment. 2way Anova followed by Paired T-test *:p<0.05; **:p<0.01; ***:p<0.001.
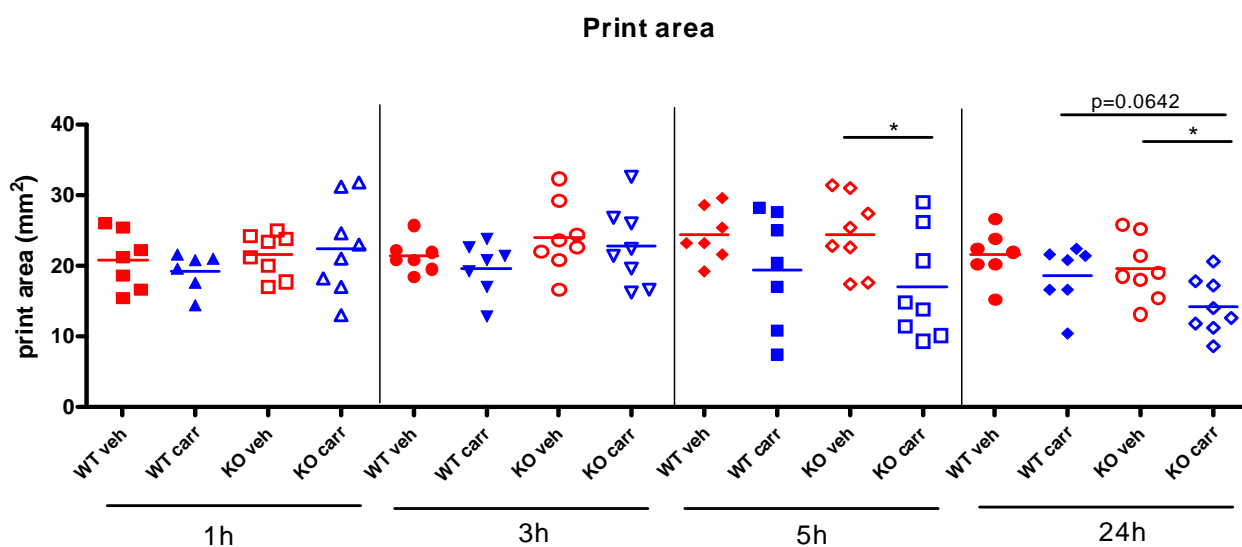
Cytokine Beads analysis

CBA analysis has been performed on the plasma of healthy (n=4 per genotype) and 2% carrageenan treated WT and KO female mice. No significant cytokine modulation has been detected in healthy and treated WT and KO mice 24 hours after carrageenan injection (data not shown).

Histological Analysis

Vehicle treatment did not induce any inflammatory signs and any significant changes in the paw architecture of both PTPH1-WT and KO mice (data not shown). Carrageenan treatment

induced a moderate to severe acute inflammation in the paws of both PTPH1-WT (Fig. 51a, 51b) and KO mice (Fig. 51d, 51e) compared to vehicle treatment. Neutrophil infiltration and hemorrhage, represented by red cells presence, were detected in CARR-treated mice 24 hours after injection (Fig. 51c, 51f). No genotype related differences were recorded by simple visual observation in the paws architecture or in cellular infiltration at this late time point.

Fig. 51: H&E staining on PTPH1-WT and KO paws. a) PTPH1-WT paws 24h post-CARR treatment display a strong inflammation (4x), **b)** severe cellular infiltration (10x) and **c)** also red cell presence, indicating hemorragia (40x). **d)** PTPH1-KO CARR-treated paws presents the same level of inflammation as matched WT paws (4x), **e)** with a strong presence of immune cells (10x) and **f)** red cells (40x).
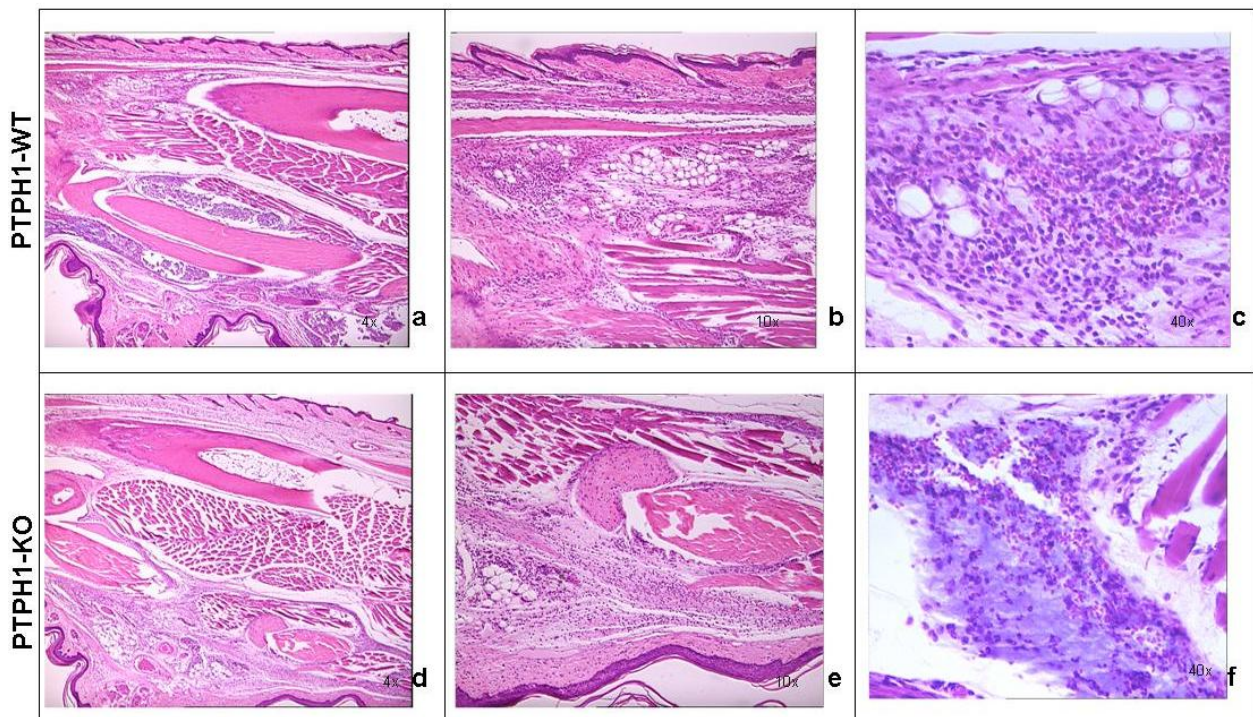
5.1.2.2. Carrageenan (CARR)-induced inflammation on aged mice

Paw thickness

A significantly higher paw thickness was measured by a precision caliper in the CARR-treated paws, compared to the controlateral vehicle treated one (Fig. 52). This modulation was statistically significant in both WT and KO groups and was detectable already after 1 hour from carrageenan injection. The edema was still present 24 hours post-injection (PTPH1-WT: $P_{1h-3h-5h}$=0.001; PTPH1-KO: $P_{1h-3h-5h}$=0.001) (Fig. 52). No statistical differences in paw thickness were detected in PTPH1-WT versus PTPH1-KO aged animals.

Fig. 52: Carrageenan-induced paw edema in PTPH1-WT and KO old mice. Paw edema was detectable at 1h after treatment in both genotypes at the same intensity. This increase thickness of the paws was maintained till sacrifice, at 5h post CARR-injection. No genotype-related differences were detectable between WT and KO CARR-treated groups. 2way Anova followed by Paired T-test *:p<0.05; **:p<0.01; ***:p<0.001.
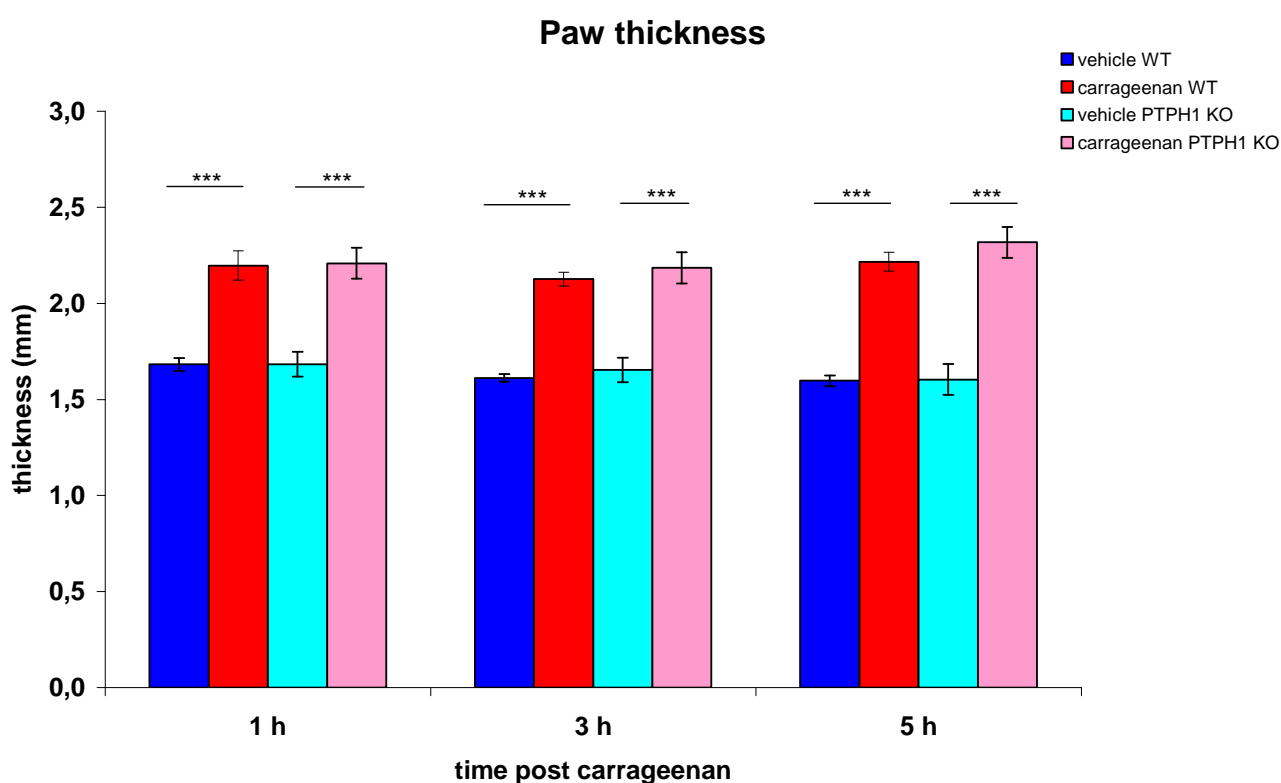
Behavioral Tests

Von Frey test- A significantly decreased response at the Von Frey test was detected in the CARR-treated paws compared to the controlateral vehicle-treated ones, in both WT and KO aged mice (Fig. 53). The decreased withdrawal force was detectable 1hour after carrageenan injection

onwards, maintaining the same intensity (PTPH1-WT: $P_{1h\text{-}3h\text{-}5h}$<0.001; PTPH1-KO: $P_{1h\text{-}3h\text{-}5h}$<0.001) (Fig. 53). No genotype-related modulation in withdrawal force was recorded between WT and KO aged mice.

Fig. 53: Von Frey test performed on CARR-treated PTPH1-WT and KO old mice. Withdrawal force measured at the Von Frey test was significantly decreased by CARR treatment in both WT and KO mice at 1h, 3h and 5h post injection. 2way Anova followed by Paired T-test *:p<0.05; **:p<0.01; ***:p<0.001.
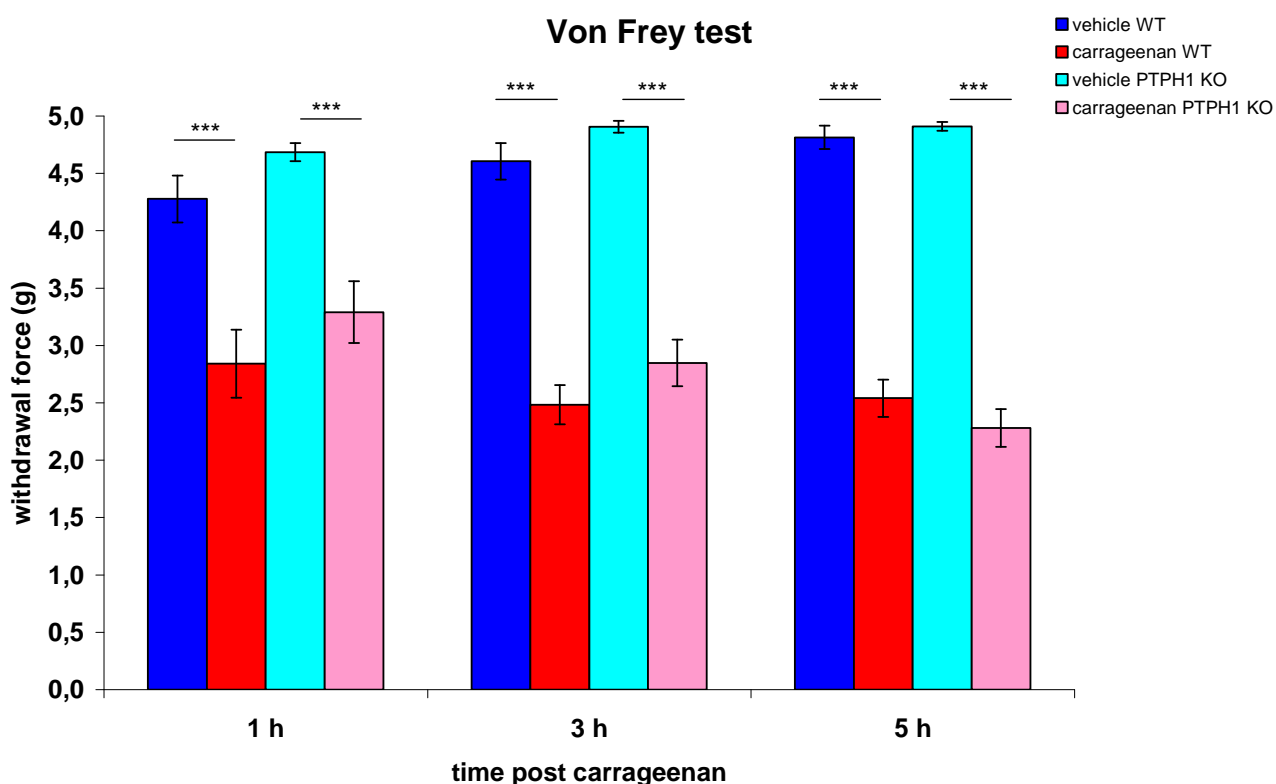
Histological Analysis

Vehicle treatment did not induce any inflammatory signs and any significant changes in the paw architecture of both PTPH1-WT and KO aged mice (data not shown). Edema was the major histopathological feature detectable 5 hours post-injection in both WT (Fig 54a, 54b) and KO (Fig 54d, 54e) CARR-treated paws. Neutrophil infiltration and hemorrhage were already present at this early time point in localized areas (Fig 54c, 54f). No genotype related differences were detetcted by simple visual observation in the paw architecture or in the edema extent between WT and KO aged female mice.

Fig. 54: H&E staining on PTPH1-WT and KO paws. a,d) PTPH1-WT and KO paws 5h post-CARR treatment displayed a strong edema (4x), **b,e)** with a few cells that were infiltrated (10x) but **c,f)** no hemorragia was present (40x). No major genotype-related differences was visible.
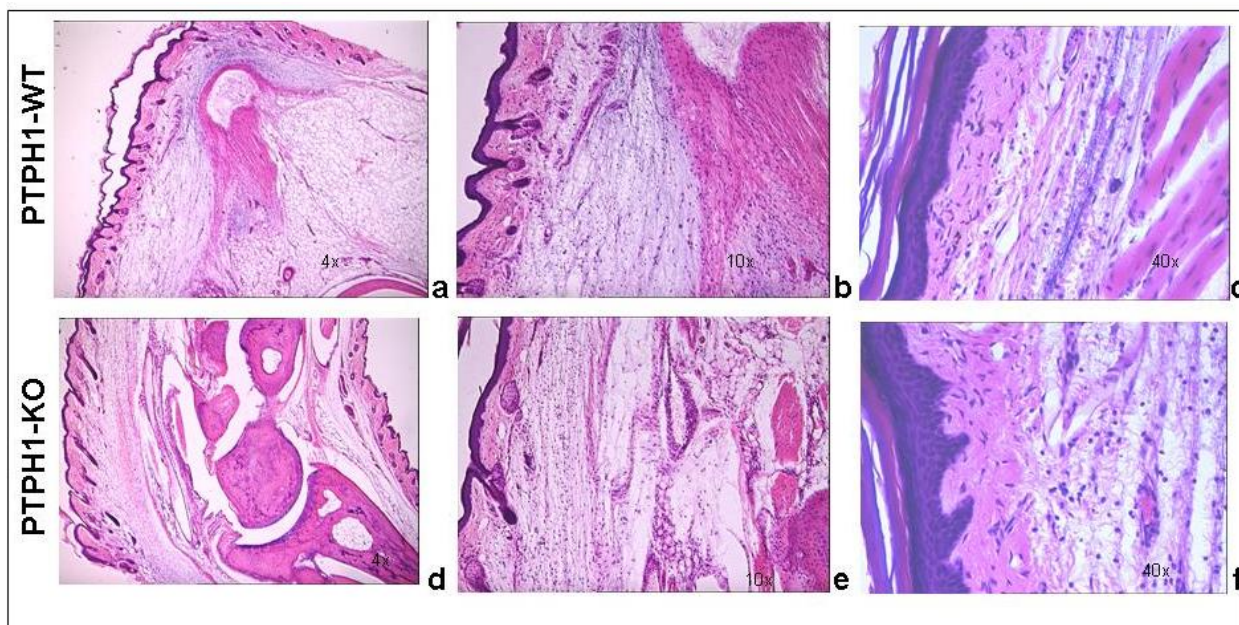
5.2. Discussion: PTPH1 role in inflammatory system

PTPH1 has been proposed to act as negative TCR regulator *in vitro*, interacting and dephosphorylating the TCRζ chain [47,82,83] but these results have not been confirmed by *ex vivo* studies on primary T cells [84,85]. Therefore we sought to ascertain whether PTPH1 has an effect on the immune response in the complex *in vivo* machinery. Two inflammatory mouse models have been used to test PTPH1 impact on the immune system: carrageenan- and LPS-induced inflammation.

Carrageenan λ is a sulfated polysaccharide derived from red seaweed that is able to activate the innate immune response. CARR interacts with TLR4 leading to increased Bcl10, to NFkB pathway activation and IL8 production [240,241]. CARR injection in the hind paw of the mouse is one of the most commonly used models of inflammation and inflammatory pain and it has a biphasic profile [242]. Recent studies point out an important role for prostaglandins, nitric oxide and TNFα in the CARR-induced inflammatory response [242-244]. In particular it has been shown that TNFα is involved in both phases of mouse carrageenan-induced edema. Thus TNFα has a strong relevance not only in inflammatory events, but also on nociceptive response and on neutrophils migration induced by carrageenan in mice [244]. Soluble TNFα is processed from its proprotein form by a specific sheddase called TACE [65,245] that is responsible for the processing

of other cytokines and cytokines receptors [72,246-248]. Interestingly PTPH1 is known to inhibits TACE expression and activity *in vitro* [52]. We therefore analyzed cytokines plasma levels in carrageenan treated WT and KO young and aged mice, but no modulation has been induced in both genotypes by this inflammatory agent (data not shown), in agreement with a previous CBA study on the rat carrageenan model [249]. We can conclude that peripheral 2% carrageenan stimulation has not been strong enough to reveal a phenotype in cytokine modulation in PTPH1-KO mice at plasma level and that hind paw and muscle cytokines concentrations should be analyzed in both genotypes to unravel PTPH1 role in local cytokine release.

As already mentioned, the CARR-induced model has a biphasic profile and it is characterized by an early development of edema that peaks at 6 and 72 h [242]. In the present study carrageenan injection induces a paw edema in PTPH1-WT and KO adult and aged mice detectable already 1 hour after injection and persistent till 24h (Fig. 52, 53), showing no differences in intensity between the genotypes and ages. Furthermore carrageenan challenge induces a marked neuthrophils migration at the site of injection that peaks at 6 h (Fig. 51, 54) [242]. Another hallmark of CARR stimulation is a long-lasting reduction in the threshold to nociceptive stimuli that is evident already after 1h and is sustained for up to 72h [242,250,251]. PTPH1-KO adult and aged mice do not show any significant differences in neutrophils infiltration or in pain behavior both at Von Frey's and Hargreaves' tests (only for adult mice) compared to WT littermates (Fig. 48, 53), suggesting that PTPH1 does not play a major role in the inflammatory-induced transmission and integration of the allodynic and painful stimuli. Comparatively Catwalk gait analysis shows an earlier onset (5h after injection) of spontaneous pain perception indicated as duty cycle (Fig. 49) and print area (Fig. 50) in PTPH1-KO adult mice, compared to matched WTs. These results might indicate a slight involvement of PTPH1 in the central or peripheral integration of the nociceptive stimulus that could occur at thalamic or cortical level [252-254], where PTPH1 is highly expressed [255].

As carrageenan, LPS challenge in rodents is frequently used as model to investigate the innate immune response mechanisms [96,97,256]. LPS is a major component of the outer membrane of Gram-negative bacteria and a critical player in the pathogesis of septic shock [98]. As carrageenan, LPS binds to MD2-TLR4 complex and activate both MyD88-dependent and independent (TRIF-dependent- TIR-domain-containing adapter-inducing interferon-β) pathways [34,96,108]. The MyD88-dependent pathway results in the activation of TRAF6 (TNF Receptor Associated Factor 6) and in the immediate activation of NFkB, MAPK and JNK pathways, leading to the early production of proinflammatory cytokines as TNFα, IL-1β, IL6 and MCP-1

[136,138,257]. MyD88-independent pathway results in rapid activation of the interferon regulatory factors (IRF) 3 and 7 that induce the production of IFNβ and consequently IFNα, nitric oxide production and delayed NFkB activation [136,138], leading to late cytokines production. LPS challenge on PTPH1-KO and WT mice aimed to understand the possible role of this phosphatase in the inflammatory process and in particular on cytokine expression and release. Thus, CBA analysis was performed on the plasma of LPS and vehicle treated WT and KO adult and aged female mice (IL-10, IL-12p70, TNFα, IL-6, MCP-1, IFN-γ).

IL10 is an immunomodulatory cytokine, whose production is rapidly induced by monocyte/macrophages upon LPS challenge [183]. IL10 treatment *in vitro* is known to negatively regulate LPS responses, in particular inhibiting the induction of pro-inflammatory cytokines like TNFα, IL12 [175, 176], IL-1α, and IL-6 [269][268]. Both PTPH1-WT and KO adult mice displayed significantly increased IL10 plasma level upon LPS challenge, but no significant reduction of IL-6, TNFα and thus MCP-1 plasma levels were detected in LPS-treated vs vehicle-treated PTPH1-WT and KO mice. Interestingly, IL10 levels were reduced in LPS-treated KO mice plasma compared to WTs at 30 and 60 minutes after challenge (Fig. 38, 39), but no increased MCP-1, TNFα, and IL6 plasma levels were detected in LPS-treated KO vs WT mice. Indeed, IL-10 has not an exclusive pro-inflammatory action [279] and it was demonstrated that in an LPS-model IL-10 release increases as MCP-1, IL-6 and TNFα [280]. Thus, our results on overall increased cytokines levels upon LPS treatment are in accordance with these studies. Comparatively an overall decrease in cytokines release was recorded at 30 and 60 minutes post challenge in LPS-treated PTPH1-KO vs WT mice (Fig. 38, 39).

Indeed IL10 up-regulates the expression of SOCS1 and 3 genes, which are able to block the IFNs-induced JAK/STAT pathway [91,258], and stimulates the expression of PTP1B [258]. It has been recently demonstrated that the production of IL10 by human Treg cells is enhanced by IL2 signaling via activation of STAT5 molecules [89,90]. PTPH1 is known to dephosphorylate STAT5b *in vitro* [19], and thus it appears controversial the IL10 reduction in PTPH1-KO plasma after 30 minutes and 1 hour post LPS injection. These data could indicate an alternative upstream target for PTPH1 possibly on the early MyD88-dependent pathway that acts on the overall pro and anti-inflammatory cytokines production.

In addition the present experiments demonstrate that endotoxin injection leads to a rapid increase of TNFα release at the same level in both PTPH1-WT and KO mice, 30 mpt (Fig. 38). TNFα is known to promote ccl2 gene expression, activating NFkB-inducing kinases and IkB kinases (IKK). In details, IKKs promote NFkB heterodimers translocation into the nucleus leading

to the transcription of targeted genes [140,141]. Several studies show that both NFkB and MAPK pathways are required for ccl2 induction, indeed transcription factor AP-1 and MAP kinase p38 contribute to TNFα–inducible expression of MCP-1 gene [140,259,260]. This regulatory mechanism might explain the reduction of both TNFα and MCP-1 gene expression and release in KO mice 1 hour post challenge (Fig. 36b, 37b, 39) (Table 8), when LPS induces the peak of TNFα plasma levels. Indeed LPS challenge fails to induce a full response, meant as TNFα expression and release, in PTPH1-KO mice leading to a lower stimulation of MCP-1 and possibly to a consequent reduced monocytes and macrophages recruitment 1 hour after injection. Cytokines levels in PTPH1-KO adult plasma are comparable to WT ones 3 hours after LPS injection (Fig. 40), suggesting that PTPH1 effect is temporally limited at the peak of TNFα release, or that some compensatory mechanisms might intervene later in the inflammatory process.

Table 8: Summary of the CBA and RT-PCR results in LPS-treated PTPH1-WT and KO mice at different time points (30, 60 and 180 minutes post- injection). = indicates no variation between WT and KO LPS-treated mice. – indicates a lower expression/release in LPS-treated KO compared to WT matched ones. – (ns) indicates a trend in lower expression/release in LPS-treated KO compared to WT matched ones. nn indicates non-performed.

LPS-treated KO*vs*WT						
	Minutes post-injection					
	30		60		180	
Cytokines	gene	protein	gene	protein	gene	protein
TNFα	=	=	-	-	=	=
MCP-1	=	-	- (ns)	-	=	=
IL6	=	- (ns)	=	- (ns)	=	=
IL12p70	=	-	=	=	=	=
IL 10	nn	-	nn	-	nn	=

A reduction in LPS-induced MCP-1 release was detectable also in PTPH1-KO aged mice compared to matched WTs at 60 mpt (Fig. 45). No significant TNFα modulation was detectable at 60mpt, but at a later time point, PTPH1-KO aged mice displayed significantly higher LPS-induced TNFα and IL10 plasma levels compared to vehicle-treated aged controls (Fig. 46b). This difference was lower and not significant in WT mice group. These data could suggest that inflammatory response, as cytokine release, is still ongoing in PTPH1-KO aged mice, while it is decaying in WT

mice. This hypothesis is partially supported by the gene expression analysis on white cells that showed a significantly 10-fold increase in TNFα expression 60 mpt in KO aged mice compared to matched WTs upon LPS stimulation (Fig. 41a). Moreover, our results point out a slight discrepancy of the CBA analysis between adult and aged mice. Indeed, ageing has a strong impact on inflammatory response [291][293]. Studies on aged mice demonstrate a functional decline of monocytes and macrophages, a low expression level of Toll-like receptors from activated splenic and peritoneal macrophages and an altered secretion of several chemokines and cytokines [291][290][292]. These data are in agreement with our findings on reduced cytokine release in WT and KO aged mice compared to matched young mice at the peak of LPS-induced inflammation (30 and 60 mpt) (Fig. 44, 45). Further targeted studies are needed to investigate the involvement of PTPH1 in the molecular mechanisms of ageing and inflammation.

Despite the fact that most proinflammatory cytokines are transcribed after NFkB activation, the overall control of production for several cytokines is more complex, and includes post-transcriptional and post-translational regulatory steps, which can be specific for certain cytokines. PTPH1 could act at one or more steps of this composite regulatory process. Proteolytic conversion of proproteins into the mature cytokine is a further level of control for cytokine production. TACE is involved in the ectodomain release of several cytokines, in particular of membrane-bound TNFα [64,65,261]. As already mentioned PTPH1 has been reported to be an inhibitor of TACE expression and activity *in vitro* [52]. Therefore TACE gene expression has been analyzed in white cells upon *in vivo* LPS challenge, but no gene modulations have been detected in both WT and KO cells (data not shown).

In summary, PTPH1-KO mice exhibit an increased spontaneous nociceptive perception in the CARR-induced inflammatory pain model. A decreased cytokine expression and release is detectable in PTPH1-KO mice in the early phases of LPS-induced inflammation. In conclusion the present study points out a potential role for PTPH1 in spontaneous pain sensitivity and indicates that this phosphatase might play a role in the positive regulation of the LPS-induced inflammatory response *in vivo*, in disagreement with previous reports indicating PTPH1 as potential negative regulator of immune response [47,82,83].

Chapter 6 - Conclusions

Summary

The dream of all patients and the goal of molecular biologists is the same: unraveling the complexity of signaling pathways in order to have a clear vision of the cellular machinery. To this end, thousands of researchers around the world are characterizing molecular and cellular signals that could be involved in disease pathogenesis. Over the last decades, tremendous progress has been made thank to new tecnologies such as Taqman, new generation antibodies and trangenic mice.

Tyrosine phosphorylation is one of the complex "tools" that a cell can use to regolate its numerous processes. In the past, researchers focused a major attention on one actor of this fine regulated mechanism, kinase. Recent studies pointed out that a very important role is played also by phosphatases, kinase counterpart. Thus, the substrates, mechanisms of regulation and implication in disease pathogenesis of PTPs have become an exiting and motivating topic for several laboratories and EU-founded committees (http://www.ich.ucl.ac.uk/ich/academicunits/PTPNET/Homepage).

The data presented in this manuscript provide a further piece of the puzzle represented by tyrosine phosphatase functions. These results contribute in giving new insights in phosphatase role in CNS functions, growth hormone signaling and innate immunity.

The emerging importance of PTP in CNS pathways has been widely described in Chapter 1. The generation of knock-out and knock-in animals has been the favourite tool used by researchers in order to understand the impact of a gene in the organism as a whole, *in toto*. The characterization of our PTPH1-KO mice allowed PTPH1 mapping in the brain and spinal cord and its behavioral phenotyping has revealed a functional meaning of PTPH1 expression. Furthermore, gene expression studies on PTPH1-KO mice have revealed a novel candidate substrate for PTPH1, CCKAR. For the first time, an extensive IHC study on PTPH1 and neurotransmitters (TH and GAD-67) expression has been performed, in order to understand whether PTPH1 silencing could affect neurotransmission. Histological evaluation allowed to identify GABAergic neurons as PTPH1-positive, but with a differential expression pattern throughtout the brain. These data provide a good starting point for further investigations on cognitive regulation and on phosphatases interplay in the CNS. Based on this manuscript, PTPH1 could be considered a target for possible future CNS interventions, in particular related to cognitive dysfunctions.

During the past decades, PTP role in GHR signaling has been deeply studied [12,15,19,23,151] and several phosphatase have been proposed as terapeutic targets for metabolic

diseases [231]. Unfortunately none of these promising targets has given the expected results so far, pointing out how intricated GHR regulation is and how less is still known in this field.

As other negative regulators [91,160], PTPH1-KO mice display enhanced body weight that is due to increased muscle portion rather than fat. These macroscopic features are releated to amplified GHR signaling that led to increased IGF1 expression in liver and release in serum. A further analysis should be performed on IGF1 release upon PTPH1 silencing, in order to understand whether increased IGF1 expression is limited to the liver. The next questions to be answered should be "Is PTPH1 regulating GHR signaling and consequently IGF1 release in a cell type-dependent manner?" and "Is PTPH1 acting on GH-IGF1 axis in disease conditions e.g. model of inflammation?". Furthermore, PTPH1-induced CCKAR modulation in the pancreatic tissue should be considered, in order to evaluate whether cholecystokinin receptor could be involved in the enhanced body weight displayed by PTPH1-KO mice.

The present manuscript has also given new insights on PTPs role in innate immunity, in particular in cytokine release, deepening the knowledge of PTPH1 impact on two models of induced inflammation. As already mentioned, in the past decade the increasing interest in PTPs-immunity interaction has led to amazing findings in immune response regulation [22,87,97,149,256,262]. In general, negative regulators of inflammatory response have become challenging targets for several immune-related diseases as autoimmune disorders. Several PTP inhibitors have been proposed as potential drugs in the treatment of MS, SLE, RA[25,145,185,263]. Anyway a deeper knowledge of the mechanisms of action of PTPs in basal and diseased conditions is essential to prevent and overcome possible side effects. We demonstrated that PTPH1-KO mice diplayed reduced and delayed the acute inflammatory cytokine response *in vivo* upon LPS challenge, suggesting a possible new therapeutical target for the anti-inflammatory strategies in controlling inflammatory events.

Significance and future directions

The present dissertation fully characterizes the first PTPH1-KO mice lacking both the catalytic and PDZ domains. Our deep analysis of behavioral phenotype allowed the identification of slight modulation of cognitive aspects related to PTPH1 absence [255]. These results could not be replicated by others possibly because of difference in the genetic background and genetic construct of the KO mice [85].

The future experiments could be driven to investigate PTPH1 role in CNS pathologies, possibly through the administration of antipsychotic drugs. This challenge could reveal minor effects of PTPH1 that were not detectable in basal conditions.

PTPH1-KO mice analysis also allowed confirming the *in vitro* observation of PTPH1 role in dephosphorylating GHR [19,183]. Indeed PTPH1-KO mice display enhanced body weight and increased IGF1 liver expression. These data could suggest a possible use of PTPH1 inhibitor in metabolic diseases. A further challenge of PTPH1-KO animals with a targeted disease-inducing agent could allow identifying other potential impacts of this phosphatase in metabolic disorders and could allow using these KO mice as animal model for these pathologies.

Furthermore the secondary phenotyping of PTPH1-KO revealed for the first time an *in vivo* impact of PTPH1 in cytokine release and a slight PTPH1 involvement in spontaneous pain perception that is not related to immune cells infiltration.

Taken together, all the data concerning PTPH1 role in CNS, in IGF1 secretion and in the immune system could be the starting point for a new hypothesis and the basis for a new dissertation. Indeed it would be worthy to investigate PTPH1 role in neuroprotection, in particular in stroke model, considering the relevance of immune regulation and IGF1 in this pathology and their modulation in our KO mice.

In humans, PTPH1 has been often related to cancer and tumor susceptibility. PTPH1 is a candidate tumor suppressor for gastro-intestinal carcinoma, but it is still far from being considered a biomarker for these diseases. The translation of these data into human is the final step to be achieved, in order to give them a clinical relevance.

List of Pubblications

Pilecka I., Patrignani C., Pescini R., Curchod ML., Perrin D., Xue Y., Yasenchak J., Clarck A., Magnone MC., Zaratin PF., Rommel C. and van Huijsduijnen RH: ***"Protein-tyrosine phosphatase H1 controls growth hormone receptor signaling and systemic growth",*** *J. Biol. Chem. 2007 Nov 30;282(48):35405-15.*

Patrignani C., Magnone MC., Tavano P., Ardizzone M., Muzio V., Greco B. and Zaratin PF: ***"Knockout mice reveal a role for protein tyrosine phosphatase H1 in cognition "****, Behav. Brain Funct 2008 Aug 12; 4: 36.*

Carboni S., Dati G., Patrignani C., Lafont D., Gotteland JP., Greco B., Zaratin PF.; ***"Modulation of post-ischemic immunoreactions through c-JUN N-terminal kinase (JNK) inhibition: a novel target for neuroprotection"*** *in submission, 2009.*

Patrignani C., Lafont DT, Muzio V., Greco B and Zaratin PF: ***"Characterization of protein tyrosine phosphatase H1 knockout mice in animal models of local and systemic inflammation"****, in submission to J. Inflamm, 2009.*

References

1. Alonso A, Sasin J, Bottini N, Friedberg I, Friedberg I, Osterman A *et al.*: **Protein tyrosine phosphatases in the human genome.** *Cell* 2004, **117:** 699-711.

2. Hunter T, Sefton BM: **Transforming gene product of Rous sarcoma virus phosphorylates tyrosine.** *Proc Natl Acad Sci U S A* 1980, **77:** 1311-1315.

3. Tonks NK: **Protein tyrosine phosphatases: from genes, to function, to disease.** *Nat Rev Mol Cell Biol* 2006, **7:** 833-846.

4. Stoker AW: **Protein tyrosine phosphatases and signalling.** *J Endocrinol* 2005, **185:** 19-33.

5. Ostman A, Hellberg C, Bohmer FD: **Protein-tyrosine phosphatases and cancer.** *Nat Rev Cancer* 2006, **6:** 307-320.

6. Pawson T: **Specificity in signal transduction: from phosphotyrosine-SH2 domain interactions to complex cellular systems.** *Cell* 2004, **116:** 191-203.

7. Gil-Henn H, Volohonsky G, Elson A: **Regulation of protein-tyrosine phosphatases alpha and epsilon by calpain-mediated proteolytic cleavage.** *J Biol Chem* 2001, **276:** 31772-31779.

8. Aicher B, Lerch MM, Muller T, Schilling J, Ullrich A: **Cellular redistribution of protein tyrosine phosphatases LAR and PTPsigma by inducible proteolytic processing.** *J Cell Biol* 1997, **138:** 681-696.

9. Meng K, Rodriguez-Pena A, Dimitrov T, Chen W, Yamin M, Noda M *et al.*: **Pleiotrophin signals increased tyrosine phosphorylation of beta beta-catenin through inactivation of the intrinsic catalytic activity of the receptor-type protein tyrosine phosphatase beta/zeta.** *Proc Natl Acad Sci U S A* 2000, **97:** 2603-2608.

10. Jiang G, den HJ, Su J, Noel J, Sap J, Hunter T: **Dimerization inhibits the activity of receptor-like protein-tyrosine phosphatase-alpha.** *Nature* 1999, **401:** 606-610.

11. Meng TC, Buckley DA, Galic S, Tiganis T, Tonks NK: **Regulation of insulin signaling through reversible oxidation of the protein-tyrosine phosphatases TC45 and PTP1B.** *J Biol Chem* 2004, **279:** 37716-37725.

12. Meng TC, Fukada T, Tonks NK: **Reversible oxidation and inactivation of protein tyrosine phosphatases in vivo.** *Mol Cell* 2002, **9:** 387-399.

13. Argetsinger LS, Campbell GS, Yang X, Witthuhn BA, Silvennoinen O, Ihle JN *et al.*: **Identification of JAK2 as a growth hormone receptor-associated tyrosine kinase.** *Cell* 1993, **74:** 237-244.

14. Miquet JG, Sotelo AI, Bartke A, Turyn D: **Suppression of growth hormone (GH) Janus tyrosine kinase 2/signal transducer and activator of transcription 5 signaling pathway in transgenic mice overexpressing bovine GH.** *Endocrinology* 2004, **145:** 2824-2832.

15. Kim SO, Jiang J, Yi W, Feng GS, Frank SJ: **Involvement of the Src homology 2-containing tyrosine phosphatase SHP-2 in growth hormone signaling.** *J Biol Chem* 1998, **273:** 2344-2354.

16. ten HJ, de J, I, Fu Y, Zhu W, Tremblay M, David M *et al.*: **Identification of a nuclear Stat1 protein tyrosine phosphatase.** *Mol Cell Biol* 2002, **22:** 5662-5668.

17. Gu F, Dube N, Kim JW, Cheng A, Ibarra-Sanchez MJ, Tremblay ML *et al.*: **Protein tyrosine phosphatase 1B attenuates growth hormone-mediated JAK2-STAT signaling.** *Mol Cell Biol* 2003, **23:** 3753-3762.

18. Hackett RH, Wang YD, Sweitzer S, Feldman G, Wood WI, Larner AC: **Mapping of a cytoplasmic domain of the human growth hormone receptor that regulates rates of inactivation of Jak2 and Stat proteins.** *J Biol Chem* 1997, **272:** 11128-11132.

19. Pasquali C, Curchod ML, Walchli S, Espanel X, Guerrier M, Arigoni F *et al.*: **Identification of protein tyrosine phosphatases with specificity for the ligand-activated growth hormone receptor.** *Mol Endocrinol* 2003, **17:** 2228-2239.

20. Aoki N, Matsuda T: **A nuclear protein tyrosine phosphatase TC-PTP is a potential negative regulator of the PRL-mediated signaling pathway: dephosphorylation and deactivation of signal transducer and activator of transcription 5a and 5b by TC-PTP in nucleus.** *Mol Endocrinol* 2002, **16:** 58-69.

21. Umeda S, Beamer WG, Takagi K, Naito M, Hayashi S, Yonemitsu H *et al.*: **Deficiency of SHP-1 protein-tyrosine phosphatase activity results in heightened osteoclast function and decreased bone density.** *Am J Pathol* 1999, **155:** 223-233.

22. Tsui HW, Siminovitch KA, de SL, Tsui FW: **Motheaten and viable motheaten mice have mutations in the haematopoietic cell phosphatase gene.** *Nat Genet* 1993, **4:** 124-129.

23. Kozlowski M, Mlinaric-Rascan I, Feng GS, Shen R, Pawson T, Siminovitch KA: **Expression and catalytic activity of the tyrosine phosphatase PTP1C is severely impaired in motheaten and viable motheaten mice.** *J Exp Med* 1993, **178:** 2157-2163.

24. Saxton TM, Ciruna BG, Holmyard D, Kulkarni S, Harpal K, Rossant J *et al.*: **The SH2 tyrosine phosphatase shp2 is required for mammalian limb development.** *Nat Genet* 2000, **24:** 420-423.

25. Heinonen KM, Nestel FP, Newell EW, Charette G, Seemayer TA, Tremblay ML *et al.*: **T-cell protein tyrosine phosphatase deletion results in progressive systemic inflammatory disease.** *Blood* 2004, **103:** 3457-3464.

26. Elchebly M, Payette P, Michaliszyn E, Cromlish W, Collins S, Loy AL *et al.*: **Increased insulin sensitivity and obesity resistance in mice lacking the protein tyrosine phosphatase-1B gene.** *Science* 1999, **283:** 1544-1548.

27. Klaman LD, Boss O, Peroni OD, Kim JK, Martino JL, Zabolotny JM *et al.*: **Increased energy expenditure, decreased adiposity, and tissue-specific insulin sensitivity in protein-tyrosine phosphatase 1B-deficient mice.** *Mol Cell Biol* 2000, **20:** 5479-5489.

28. Stepanek L, Stoker AW, Stoeckli E, Bixby JL: **Receptor tyrosine phosphatases guide vertebrate motor axons during development.** *J Neurosci* 2005, **25:** 3813-3823.

29. Wallace MJ, Batt J, Fladd CA, Henderson JT, Skarnes W, Rotin D: **Neuronal defects and posterior pituitary hypoplasia in mice lacking the receptor tyrosine phosphatase PTPsigma.** *Nat Genet* 1999, **21:** 334-338.

30. Elchebly M, Wagner J, Kennedy TE, Lanctot C, Michaliszyn E, Itie A *et al.*: **Neuroendocrine dysplasia in mice lacking protein tyrosine phosphatase sigma.** *Nat Genet* 1999, **21:** 330-333.

31. Meathrel K, Adamek T, Batt J, Rotin D, Doering LC: **Protein tyrosine phosphatase sigma-deficient mice show aberrant cytoarchitecture and structural abnormalities in the central nervous system.** *J Neurosci Res* 2002, **70:** 24-35.

32. Wansink DG, Peters W, Schaafsma I, Sutmuller RP, Oerlemans F, Adema GJ *et al.*: **Mild impairment of motor nerve repair in mice lacking PTP-BL tyrosine phosphatase activity.** *Physiol Genomics* 2004, **19:** 50-60.

33. Hironaka K, Umemori H, Tezuka T, Mishina M, Yamamoto T: **The protein-tyrosine phosphatase PTPMEG interacts with glutamate receptor delta 2 and epsilon subunits.** *J Biol Chem* 2000, **275:** 16167-16173.

34. Akira S, Takeda K: **Toll-like receptor signalling.** *Nat Rev Immunol* 2004, **4:** 499-511.

35. Mustelin T, Tasken K: **Positive and negative regulation of T-cell activation through kinases and phosphatases.** *Biochem J* 2003, **371:** 15-27.

36. Mustelin T, Vang T, Bottini N: **Protein tyrosine phosphatases and the immune response.** *Nat Rev Immunol* 2005, **5:** 43-57.

37. Qu CK, Nguyen S, Chen J, Feng GS: **Requirement of Shp-2 tyrosine phosphatase in lymphoid and hematopoietic cell development.** *Blood* 2001, **97:** 911-914.

38. Tartaglia M, Niemeyer CM, Fragale A, Song X, Buechner J, Jung A *et al.*: **Somatic mutations in PTPN11 in juvenile myelomonocytic leukemia, myelodysplastic syndromes and acute myeloid leukemia.** *Nat Genet* 2003, **34:** 148-150.

39. Feng GS: **Shp-2 tyrosine phosphatase: signaling one cell or many.** *Exp Cell Res* 1999, **253:** 47-54.

40. An H, Zhao W, Hou J, Zhang Y, Xie Y, Zheng Y *et al.*: **SHP-2 phosphatase negatively regulates the TRIF adaptor protein-dependent type I interferon and proinflammatory cytokine production.** *Immunity* 2006, **25:** 919-928.

41. Tsui FW, Martin A, Wang J, Tsui HW: **Investigations into the regulation and function of the SH2 domain-containing protein-tyrosine phosphatase, SHP-1.** *Immunol Res* 2006, **35:** 127-136.

42. Hasegawa K, Martin F, Huang G, Tumas D, Diehl L, Chan AC: **PEST domain-enriched tyrosine phosphatase (PEP) regulation of effector/memory T cells.** *Science* 2004, **303:** 685-689.

43. Huber A, Menconi F, Corathers S, Jacobson EM, Tomer Y: **Joint genetic susceptibility to type 1 diabetes and autoimmune thyroiditis: from epidemiology to mechanisms.** *Endocr Rev* 2008, **29:** 697-725.

44. Begovich AB, Carlton VE, Honigberg LA, Schrodi SJ, Chokkalingam AP, Alexander HC *et al.*: **A missense single-nucleotide polymorphism in a gene encoding a protein**

tyrosine phosphatase (PTPN22) is associated with rheumatoid arthritis. *Am J Hum Genet* 2004, **75:** 330-337.

45. Terszowski G, Jankowski A, Hendriks WJ, Rolink AG, Kisielow P: **Within the hemopoietic system, LAR phosphatase is a T cell lineage-specific adhesion receptor-like protein whose phosphatase activity appears dispensable for T cell development, repertoire selection and function.** *Eur J Immunol* 2001, **31:** 832-840.

46. Young JA, Becker AM, Medeiros JJ, Shapiro VS, Wang A, Farrar JD *et al*.: **The protein tyrosine phosphatase PTPN4/PTP-MEG1, an enzyme capable of dephosphorylating the TCR ITAMs and regulating NF-kappaB, is dispensable for T cell development and/or T cell effector functions.** *Mol Immunol* 2008, **45:** 3756-3766.

47. Gjorloff-Wingren A, Saxena M, Han S, Wang X, Alonso A, Renedo M *et al*.: **Subcellular localization of intracellular protein tyrosine phosphatases in T cells.** *Eur J Immunol* 2000, **30:** 2412-2421.

48. Yang Q, Tonks NK: **Isolation of a cDNA clone encoding a human protein-tyrosine phosphatase with homology to the cytoskeletal-associated proteins band 4.1, ezrin, and talin.** *Proc Natl Acad Sci U S A* 1991, **88:** 5949-5953.

49. Zhang SH, Eckberg WR, Yang Q, Samatar AA, Tonks NK: **Biochemical characterization of a human band 4.1-related protein-tyrosine phosphatase, PTPH1.** *J Biol Chem* 1995, **270:** 20067-20072.

50. Zhang SH, Kobayashi R, Graves PR, Piwnica-Worms H, Tonks NK: **Serine phosphorylation-dependent association of the band 4.1-related protein-tyrosine phosphatase PTPH1 with 14-3-3beta protein.** *J Biol Chem* 1997, **272:** 27281-27287.

51. Zhang SH, Liu J, Kobayashi R, Tonks NK: **Identification of the cell cycle regulator VCP (p97/CDC48) as a substrate of the band 4.1-related protein-tyrosine phosphatase PTPH1.** *J Biol Chem* 1999, **274:** 17806-17812.

52. Zheng Y, Schlondorff J, Blobel CP: **Evidence for regulation of the tumor necrosis factor alpha-convertase (TACE) by protein-tyrosine phosphatase PTPH1.** *J Biol Chem* 2002, **277:** 42463-42470.

53. Jespersen T, Gavillet B, van Bemmelen MX, Cordonier S, Thomas MA, Staub O *et al*.: **Cardiac sodium channel Na(v)1.5 interacts with and is regulated by the protein tyrosine phosphatase PTPH1.** *Biochem Biophys Res Commun* 2006, **348:** 1455-1462.

54. van Hemert MJ, Steensma HY, van Heusden GP: **14-3-3 proteins: key regulators of cell division, signalling and apoptosis.** *Bioessays* 2001, **23:** 936-946.

55. Berg D, Holzmann C, Riess O: **14-3-3 proteins in the nervous system.** *Nat Rev Neurosci* 2003, **4:** 752-762.

56. Kong L, Lv Z, Chen J, Nie Z, Wang D, Shen H *et al*.: **Expression analysis and tissue distribution of two 14-3-3 proteins in silkworm (Bombyx mori).** *Biochim Biophys Acta* 2007, **1770:** 1598-1604.

57. Kilani RT, Medina A, Aitken A, Jalili RB, Carr M, Ghahary A: **Identification of different isoforms of 14-3-3 protein family in human dermal and epidermal layers.** *Mol Cell Biochem* 2008, **314:** 161-169.

58. Fu H, Subramanian RR, Masters SC: **14-3-3 proteins: structure, function, and regulation.** *Annu Rev Pharmacol Toxicol* 2000, **40:** 617-647.

59. Lavoie C, Chevet E, Roy L, Tonks NK, Fazel A, Posner BI *et al*.: **Tyrosine phosphorylation of p97 regulates transitional endoplasmic reticulum assembly in vitro.** *Proc Natl Acad Sci U S A* 2000, **97:** 13637-13642.

60. Bar-Nun S: **The role of p97/Cdc48p in endoplasmic reticulum-associated degradation: from the immune system to yeast.** *Curr Top Microbiol Immunol* 2005, **300:** 95-125.

61. Vij N: **AAA ATPase p97/VCP: cellular functions, disease and therapeutic potential.** *J Cell Mol Med* 2008, **12:** 2511-2518.

62. Madeo F, Schlauer J, Zischka H, Mecke D, Frohlich KU: **Tyrosine phosphorylation regulates cell cycle-dependent nuclear localization of Cdc48p.** *Mol Biol Cell* 1998, **9:** 131-141.

63. Huovila AP, Turner AJ, Pelto-Huikko M, Karkkainen I, Ortiz RM: **Shedding light on ADAM metalloproteinases.** *Trends Biochem Sci* 2005, **30:** 413-422.

64. Edwards DR, Handsley MM, Pennington CJ: **The ADAM metalloproteinases.** *Mol Aspects Med* 2008, **29:** 258-289.

65. Black RA, Rauch CT, Kozlosky CJ, Peschon JJ, Slack JL, Wolfson MF *et al*.: **A metalloproteinase disintegrin that releases tumour-necrosis factor-alpha from cells.** *Nature* 1997, **385:** 729-733.

66. Boissy P, Lenhard TR, Kirkegaard T, Peschon JJ, Black RA, Delaisse JM *et al*.: **An assessment of ADAMs in bone cells: absence of TACE activity prevents osteoclast recruitment and the formation of the marrow cavity in developing long bones.** *FEBS Lett* 2003, **553:** 257-261.

67. Buxbaum JD, Liu KN, Luo Y, Slack JL, Stocking KL, Peschon JJ *et al*.: **Evidence that tumor necrosis factor alpha converting enzyme is involved in regulated alpha-secretase cleavage of the Alzheimer amyloid protein precursor.** *J Biol Chem* 1998, **273:** 27765-27767.

68. Zhao J, Chen H, Peschon JJ, Shi W, Zhang Y, Frank SJ *et al*.: **Pulmonary hypoplasia in mice lacking tumor necrosis factor-alpha converting enzyme indicates an indispensable role for cell surface protein shedding during embryonic lung branching morphogenesis.** *Dev Biol* 2001, **232:** 204-218.

69. Delwig A, Rand MD: **Kuz and TACE can activate Notch independent of ligand.** *Cell Mol Life Sci* 2008, **65:** 2232-2243.

70. Deng X, Lu J, Lehman-McKeeman LD, Malle E, Crandall DL, Ganey PE *et al*.: **p38 mitogen-activated protein kinase-dependent tumor necrosis factor-alpha-converting enzyme is important for liver injury in hepatotoxic interaction between lipopolysaccharide and ranitidine.** *J Pharmacol Exp Ther* 2008, **326:** 144-152.

71. Zhan M, Jin B, Chen SE, Reecy JM, Li YP: **TACE release of TNF-alpha mediates mechanotransduction-induced activation of p38 MAPK and myogenesis.** *J Cell Sci* 2007, **120:** 692-701.

72. Peschon JJ, Slack JL, Reddy P, Stocking KL, Sunnarborg SW, Lee DC *et al.*: **An essential role for ectodomain shedding in mammalian development.** *Science* 1998, **282:** 1281-1284.

73. Ling Wu KNJGHaQW: **Localization of Nav1.5 sodium channel protein in the mouse brain.** *Neuroreport* 2002, **13**.

74. Ratcliffe CF, Qu Y, McCormick KA, Tibbs VC, Dixon JE, Scheuer T *et al.*: **A sodium channel signaling complex: modulation by associated receptor protein tyrosine phosphatase beta.** *Nat Neurosci* 2000, **3:** 437-444.

75. Ahern CA, Zhang JF, Wookalis MJ, Horn R: **Modulation of the cardiac sodium channel NaV1.5 by Fyn, a Src family tyrosine kinase.** *Circ Res* 2005, **96:** 991-998.

76. Sahin M, Slaugenhaupt SA, Gusella JF, Hockfield S: **Expression of PTPH1, a rat protein tyrosine phosphatase, is restricted to the derivatives of a specific diencephalic segment.** *Proc Natl Acad Sci U S A* 1995, **92:** 7859-7863.

77. Walton KM, Martell KJ, Kwak SP, Dixon JE, Largent BL: **A novel receptor-type protein tyrosine phosphatase is expressed during neurogenesis in the olfactory neuroepithelium.** *Neuron* 1993, **11:** 387-400.

78. Salinas PC, Nusse R: **Regional expression of the Wnt-3 gene in the developing mouse forebrain in relationship to diencephalic neuromeres.** *Mech Dev* 1992, **39:** 151-160.

79. Daugherty RL, Gottardi CJ: **Phospho-regulation of Beta-catenin adhesion and signaling functions.** *Physiology (Bethesda)* 2007, **22:** 303-309.

80. Arpin M, Algrain M, Louvard D: **Membrane-actin microfilament connections: an increasing diversity of players related to band 4.1.** *Curr Opin Cell Biol* 1994, **6:** 136-141.

81. Flores-Morales A, Greenhalgh CJ, Norstedt G, Rico-Bautista E: **Negative regulation of growth hormone receptor signaling.** *Mol Endocrinol* 2006, **20:** 241-253.

82. Han S, Williams S, Mustelin T: **Cytoskeletal protein tyrosine phosphatase PTPH1 reduces T cell antigen receptor signaling.** *Eur J Immunol* 2000, **30:** 1318-1325.

83. Sozio MS, Mathis MA, Young JA, Walchli S, Pitcher LA, Wrage PC *et al.*: **PTPH1 is a predominant protein-tyrosine phosphatase capable of interacting with and dephosphorylating the T cell receptor zeta subunit.** *J Biol Chem* 2004, **279:** 7760-7769.

84. Bauler TJ, Hughes ED, Arimura Y, Mustelin T, Saunders TL, King PD: **Normal TCR signal transduction in mice that lack catalytically active PTPN3 protein tyrosine phosphatase.** *J Immunol* 2007, **178:** 3680-3687.

85. Bauler TJ, Hendriks WJ, King PD: **The FERM and PDZ domain-containing protein tyrosine phosphatases, PTPN4 and PTPN3, are both dispensable for T cell receptor signal transduction.** *PLoS ONE* 2008, **3:** e4014.

86. Janeway CA, Jr., Medzhitov R: **Introduction: the role of innate immunity in the adaptive immune response.** *Semin Immunol* 1998, **10:** 349-350.

87. Medzhitov R, Janeway CA, Jr.: **Innate immune recognition and control of adaptive immune responses.** *Semin Immunol* 1998, **10:** 351-353.

88. Medzhitov R, Janeway CA, Jr.: **An ancient system of host defense.** *Curr Opin Immunol* 1998, **10:** 12-15.

89. Tsuji-Takayama K, Suzuki M, Yamamoto M, Harashima A, Okochi A, Otani T *et al.*: **The production of IL-10 by human regulatory T cells is enhanced by IL-2 through a STAT5-responsive intronic enhancer in the IL-10 locus.** *J Immunol* 2008, **181:** 3897-3905.

90. Tsuji-Takayama K, Suzuki M, Yamamoto M, Harashima A, Okochi A, Otani T *et al.*: **IL-2 activation of STAT5 enhances production of IL-10 from human cytotoxic regulatory T cells, HOZOT.** *Exp Hematol* 2008, **36:** 181-192.

91. Yoshimura A, Naka T, Kubo M: **SOCS proteins, cytokine signalling and immune regulation.** *Nat Rev Immunol* 2007, **7:** 454-465.

92. Ma X, Trinchieri G: **Regulation of interleukin-12 production in antigen-presenting cells.** *Adv Immunol* 2001, **79:** 55-92.

93. Trinchieri G, Pflanz S, Kastelein RA: **The IL-12 family of heterodimeric cytokines: new players in the regulation of T cell responses.** *Immunity* 2003, **19:** 641-644.

94. Trinchieri G: **Interleukin-12 and the regulation of innate resistance and adaptive immunity.** *Nat Rev Immunol* 2003, **3:** 133-146.

95. Kibe Y, Takenaka H, Kishimoto S: **Spatial and temporal expression of basic fibroblast growth factor protein during wound healing of rat skin.** *Br J Dermatol* 2000, **143:** 720-727.

96. Roger T, Froidevaux C, Le RD, Reymond MK, Chanson AL, Mauri D *et al.*: **Protection from lethal Gram-negative bacterial sepsis by targeting Toll-like receptor 4.** *Proc Natl Acad Sci U S A* 2009.

97. Salojin K, Oravecz T: **Regulation of innate immunity by MAPK dual-specificity phosphatases: knockout models reveal new tricks of old genes.** *J Leukoc Biol* 2007, **81:** 860-869.

98. Beutler B, Rietschel ET: **Innate immune sensing and its roots: the story of endotoxin.** *Nat Rev Immunol* 2003, **3:** 169-176.

99. Schletter J, Heine H, Ulmer AJ, Rietschel ET: **Molecular mechanisms of endotoxin activity.** *Arch Microbiol* 1995, **164:** 383-389.

100. Schletter J, Brade H, Brade L, Kruger C, Loppnow H, Kusumoto S *et al.*: **Binding of lipopolysaccharide (LPS) to an 80-kilodalton membrane protein of human cells is mediated by soluble CD14 and LPS-binding protein.** *Infect Immun* 1995, **63:** 2576-2580.

101. Galanos C, Luderitz O, Rietschel ET, Westphal O, Brade H, Brade L *et al.*: **Synthetic and natural Escherichia coli free lipid A express identical endotoxic activities.** *Eur J Biochem* 1985, **148:** 1-5.

102. Golenbock DT, Hampton RY, Raetz CR, Wright SD: **Human phagocytes have multiple lipid A-binding sites.** *Infect Immun* 1990, **58:** 4069-4075.

103. Schumann RR, Leong SR, Flaggs GW, Gray PW, Wright SD, Mathison JC *et al.*: **Structure and function of lipopolysaccharide binding protein.** *Science* 1990, **249:** 1429-1431.

104. Wright SD, Ramos RA, Tobias PS, Ulevitch RJ, Mathison JC: **CD14, a receptor for complexes of lipopolysaccharide (LPS) and LPS binding protein.** *Science* 1990, **249:** 1431-1433.

105. Fenton MJ, Golenbock DT: **LPS-binding proteins and receptors.** *J Leukoc Biol* 1998, **64:** 25-32.

106. Janeway CA, Jr., Medzhitov R: **Innate immune recognition.** *Annu Rev Immunol* 2002, **20:** 197-216.

107. Akira S, Takeda K: **Functions of toll-like receptors: lessons from KO mice.** *C R Biol* 2004, **327:** 581-589.

108. Kawai T, Akira S: **Toll-like receptor downstream signaling.** *Arthritis Res Ther* 2005, **7:** 12-19.

109. Poltorak A, Smirnova I, He X, Liu MY, Van HC, McNally O *et al.*: **Genetic and physical mapping of the Lps locus: identification of the toll-4 receptor as a candidate gene in the critical region.** *Blood Cells Mol Dis* 1998, **24:** 340-355.

110. Rock FL, Hardiman G, Timans JC, Kastelein RA, Bazan JF: **A family of human receptors structurally related to Drosophila Toll.** *Proc Natl Acad Sci U S A* 1998, **95:** 588-593.

111. Smirnova I, Poltorak A, Chan EK, McBride C, Beutler B: **Phylogenetic variation and polymorphism at the toll-like receptor 4 locus (TLR4).** *Genome Biol* 2000, **1:** RESEARCH002.

112. Juan TS, Hailman E, Kelley MJ, Busse LA, Davy E, Empig CJ *et al.*: **Identification of a lipopolysaccharide binding domain in CD14 between amino acids 57 and 64.** *J Biol Chem* 1995, **270:** 5219-5224.

113. Juan TS, Kelley MJ, Johnson DA, Busse LA, Hailman E, Wright SD *et al.*: **Soluble CD14 truncated at amino acid 152 binds lipopolysaccharide (LPS) and enables cellular response to LPS.** *J Biol Chem* 1995, **270:** 1382-1387.

114. da Silva CJ, Ulevitch RJ: **MD-2 and TLR4 N-linked glycosylations are important for a functional lipopolysaccharide receptor.** *J Biol Chem* 2002, **277:** 1845-1854.

115. Sultzer BM: **Endotoxin-induced resistance to a staphylococcal infection: cellular and humoral responses compared in two mouse strains.** *J Infect Dis* 1968, **118:** 340-348.

116. Coutinho A, Meo T, Watanabe T: **Independent segregation of two functional markers expressed on the same B-cell subset in the mouse: the Mls determinants and LPS receptors.** *Scand J Immunol* 1977, **6:** 1005-1013.

117. Qureshi ST, Gros P, Malo D: **The Lps locus: genetic regulation of host responses to bacterial lipopolysaccharide.** *Inflamm Res* 1999, **48:** 613-620.

118. Qureshi ST, Lariviere L, Leveque G, Clermont S, Moore KJ, Gros P *et al.*: **Endotoxin-tolerant mice have mutations in Toll-like receptor 4 (Tlr4).** *J Exp Med* 1999, **189:** 615-625.

119. Hoshino K, Takeuchi O, Kawai T, Sanjo H, Ogawa T, Takeda Y *et al.*: **Cutting edge: Toll-like receptor 4 (TLR4)-deficient mice are hyporesponsive to lipopolysaccharide: evidence for TLR4 as the Lps gene product.** *J Immunol* 1999, **162:** 3749-3752.

120. Rhee SH, Hwang D: **Murine TOLL-like receptor 4 confers lipopolysaccharide responsiveness as determined by activation of NF kappa B and expression of the inducible cyclooxygenase.** *J Biol Chem* 2000, **275:** 34035-34040.

121. Faure E, Equils O, Sieling PA, Thomas L, Zhang FX, Kirschning CJ *et al.*: **Bacterial lipopolysaccharide activates NF-kappaB through toll-like receptor 4 (TLR-4) in cultured human dermal endothelial cells. Differential expression of TLR-4 and TLR-2 in endothelial cells.** *J Biol Chem* 2000, **275:** 11058-11063.

122. Muzio M, Mantovani A: **Toll-like receptors.** *Microbes Infect* 2000, **2:** 251-255.

123. Laflamme N, Rivest S: **Toll-like receptor 4: the missing link of the cerebral innate immune response triggered by circulating gram-negative bacterial cell wall components.** *FASEB J* 2001, **15:** 155-163.

124. Fusunyan RD, Nanthakumar NN, Baldeon ME, Walker WA: **Evidence for an innate immune response in the immature human intestine: toll-like receptors on fetal enterocytes.** *Pediatr Res* 2001, **49:** 589-593.

125. Frantz S, Kobzik L, Kim YD, Fukazawa R, Medzhitov R, Lee RT *et al.*: **Toll4 (TLR4) expression in cardiac myocytes in normal and failing myocardium.** *J Clin Invest* 1999, **104:** 271-280.

126. Kleeberger SR, Reddy S, Zhang LY, Jedlicka AE: **Genetic susceptibility to ozone-induced lung hyperpermeability: role of toll-like receptor 4.** *Am J Respir Cell Mol Biol* 2000, **22:** 620-627.

127. Kleeberger SR, Reddy SP, Zhang LY, Cho HY, Jedlicka AE: **Toll-like receptor 4 mediates ozone-induced murine lung hyperpermeability via inducible nitric oxide synthase.** *Am J Physiol Lung Cell Mol Physiol* 2001, **280:** L326-L333.

128. Nomura F, Akashi S, Sakao Y, Sato S, Kawai T, Matsumoto M *et al.*: **Cutting edge: endotoxin tolerance in mouse peritoneal macrophages correlates with down-regulation of surface toll-like receptor 4 expression.** *J Immunol* 2000, **164:** 3476-3479.

129. Iwami KI, Matsuguchi T, Masuda A, Kikuchi T, Musikacharoen T, Yoshikai Y: **Cutting edge: naturally occurring soluble form of mouse Toll-like receptor 4 inhibits lipopolysaccharide signaling.** *J Immunol* 2000, **165:** 6682-6686.

130. Rehli M, Poltorak A, Schwarzfischer L, Krause SW, Andreesen R, Beutler B: **PU.1 and interferon consensus sequence-binding protein regulate the myeloid expression of the human Toll-like receptor 4 gene.** *J Biol Chem* 2000, **275:** 9773-9781.

131. Fan J, Kapus A, Marsden PA, Li YH, Oreopoulos G, Marshall JC *et al.*: **Regulation of Toll-like receptor 4 expression in the lung following hemorrhagic shock and lipopolysaccharide.** *J Immunol* 2002, **168:** 5252-5259.

132. Tobias PS, Soldau K, Gegner JA, Mintz D, Ulevitch RJ: **Lipopolysaccharide binding protein-mediated complexation of lipopolysaccharide with soluble CD14.** *J Biol Chem* 1995, **270:** 10482-10488.

133. Ulevitch RJ, Tobias PS: **Receptor-dependent mechanisms of cell stimulation by bacterial endotoxin.** *Annu Rev Immunol* 1995, **13:** 437-457.

134. Su GL, Klein RD, Aminlari A, Zhang HY, Steinstraesser L, Alarcon WH *et al.*: **Kupffer cell activation by lipopolysaccharide in rats: role for lipopolysaccharide binding protein and toll-like receptor 4.** *Hepatology* 2000, **31:** 932-936.

135. Byrd-Leifer CA, Block EF, Takeda K, Akira S, Ding A: **The role of MyD88 and TLR4 in the LPS-mimetic activity of Taxol.** *Eur J Immunol* 2001, **31:** 2448-2457.

136. Takeda K, Akira S: **TLR signaling pathways.** *Semin Immunol* 2004, **16:** 3-9.

137. Medzhitov R, Preston-Hurlburt P, Kopp E, Stadlen A, Chen C, Ghosh S *et al.*: **MyD88 is an adaptor protein in the hToll/IL-1 receptor family signaling pathways.** *Mol Cell* 1998, **2:** 253-258.

138. Zughaier SM, Zimmer SM, Datta A, Carlson RW, Stephens DS: **Differential induction of the toll-like receptor 4-MyD88-dependent and -independent signaling pathways by endotoxins.** *Infect Immun* 2005, **73:** 2940-2950.

139. Muzio M, Polntarutti N, Bosisio D, Prahladan MK, Mantovani A: **Toll like receptor family (TLT) and signalling pathway.** *Eur Cytokine Netw* 2000, **11:** 489-490.

140. Goebeler M, Gillitzer R, Kilian K, Utzel K, Brocker EB, Rapp UR *et al.*: **Multiple signaling pathways regulate NF-kappaB-dependent transcription of the monocyte chemoattractant protein-1 gene in primary endothelial cells.** *Blood* 2001, **97:** 46-55.

141. Karin M: **The beginning of the end: IkappaB kinase (IKK) and NF-kappaB activation.** *J Biol Chem* 1999, **274:** 27339-27342.

142. Ulevitch RJ: **Therapeutics targeting the innate immune system.** *Nat Rev Immunol* 2004, **4:** 512-520.

143. Zhang G, Ghosh S: **Toll-like receptor-mediated NF-kappaB activation: a phylogenetically conserved paradigm in innate immunity.** *J Clin Invest* 2001, **107:** 13-19.

144. Lee MS, Kim YJ: **Signaling pathways downstream of pattern-recognition receptors and their cross talk.** *Annu Rev Biochem* 2007, **76:** 447-480.

145. Aikawa Y, Yamamoto M, Yamamoto T, Morimoto K, Tanaka K: **An anti-rheumatic agent T-614 inhibits NF-kappaB activation in LPS- and TNF-alpha-stimulated THP-1 cells without interfering with IkappaBalpha degradation.** *Inflamm Res* 2002, **51:** 188-194.

146. Yamamoto M, Sato S, Hemmi H, Sanjo H, Uematsu S, Kaisho T *et al.*: **Essential role for TIRAP in activation of the signalling cascade shared by TLR2 and TLR4.** *Nature* 2002, **420:** 324-329.

147. Kaisho T, Takeuchi O, Kawai T, Hoshino K, Akira S: **Endotoxin-induced maturation of MyD88-deficient dendritic cells.** *J Immunol* 2001, **166:** 5688-5694.

148. Kawai T, Takeuchi O, Fujita T, Inoue J, Muhlradt PF, Sato S *et al.*: **Lipopolysaccharide stimulates the MyD88-independent pathway and results in activation of IFN-regulatory factor 3 and the expression of a subset of lipopolysaccharide-inducible genes.** *J Immunol* 2001, **167:** 5887-5894.

149. Liew FY, Xu D, Brint EK, O'Neill LA: **Negative regulation of toll-like receptor-mediated immune responses.** *Nat Rev Immunol* 2005, **5:** 446-458.

150. Baum HB, Biller BM, Katznelson L, Oppenheim DS, Clemmons DR, Cannistraro KB *et al.*: **Assessment of growth hormone (GH) secretion in men with adult-onset GH deficiency compared with that in normal men--a clinical research center study.** *J Clin Endocrinol Metab* 1996, **81:** 84-92.

151. Eden EB, Burman P, Holdstock C, Karlsson FA: **Effects of growth hormone (GH) on ghrelin, leptin, and adiponectin in GH-deficient patients.** *J Clin Endocrinol Metab* 2003, **88:** 5193-5198.

152. Aberg ND, Brywe KG, Isgaard J: **Aspects of growth hormone and insulin-like growth factor-I related to neuroprotection, regeneration, and functional plasticity in the adult brain.** *ScientificWorldJournal* 2006, **6:** 53-80.

153. Touw IP, de Koning JP, Ward AC, Hermans MH: **Signaling mechanisms of cytokine receptors and their perturbances in disease.** *Mol Cell Endocrinol* 2000, **160:** 1-9.

154. Johansson AG: **Gender difference in growth hormone response in adults.** *J Endocrinol Invest* 1999, **22:** 58-60.

155. Schneider HJ, Pagotto U, Stalla GK: **Central effects of the somatotropic system.** *Eur J Endocrinol* 2003, **149:** 377-392.

156. Wells JA: **Binding in the growth hormone receptor complex.** *Proc Natl Acad Sci U S A* 1996, **93:** 1-6.

157. Herrington J, Carter-Su C: **Signaling pathways activated by the growth hormone receptor.** *Trends Endocrinol Metab* 2001, **12:** 252-257.

158. Herrington J, Smit LS, Schwartz J, Carter-Su C: **The role of STAT proteins in growth hormone signaling.** *Oncogene* 2000, **19:** 2585-2597.

159. Stofega MR, Herrington J, Billestrup N, Carter-Su C: **Mutation of the SHP-2 binding site in growth hormone (GH) receptor prolongs GH-promoted tyrosyl phosphorylation of GH receptor, JAK2, and STAT5B.** *Mol Endocrinol* 2000, **14:** 1338-1350.

160. Krebs DL, Hilton DJ: **SOCS: physiological suppressors of cytokine signaling.** *J Cell Sci* 2000, **113 (Pt 16):** 2813-2819.

161. Carter-Su C, Rui L, Herrington J: **Role of the tyrosine kinase JAK2 in signal transduction by growth hormone.** *Pediatr Nephrol* 2000, **14:** 550-557.

162. Naka T, Narazaki M, Hirata M, Matsumoto T, Minamoto S, Aono A *et al.*: **Structure and function of a new STAT-induced STAT inhibitor.** *Nature* 1997, **387:** 924-929.

163. Yasukawa H, Misawa H, Sakamoto H, Masuhara M, Sasaki A, Wakioka T *et al.*: **The JAK-binding protein JAB inhibits Janus tyrosine kinase activity through binding in the activation loop.** *EMBO J* 1999, **18:** 1309-1320.

164. Hansen JA, Lindberg K, Hilton DJ, Nielsen JH, Billestrup N: **Mechanism of inhibition of growth hormone receptor signaling by suppressor of cytokine signaling proteins.** *Mol Endocrinol* 1999, **13:** 1832-1843.

165. Gebert CA, Park SH, Waxman DJ: **Termination of growth hormone pulse-induced STAT5b signaling.** *Mol Endocrinol* 1999, **13:** 38-56.

166. Valenzuela DM, Murphy AJ, Frendewey D, Gale NW, Economides AN, Auerbach W *et al.*: **High-throughput engineering of the mouse genome coupled with high-resolution expression analysis.** *Nat Biotechnol* 2003, **21:** 652-659.

167. Ramboz S, Oosting R, Amara DA, Kung HF, Blier P, Mendelsohn M *et al.*: **Serotonin receptor 1A knockout: an animal model of anxiety-related disorder.** *Proc Natl Acad Sci U S A* 1998, **95:** 14476-14481.

168. Lister RG: **The use of a plus-maze to measure anxiety in the mouse.** *Psychopharmacology (Berl)* 1987, **92:** 180-185.

169. Jones BJ, Roberts DJ: **The quantiative measurement of motor inco-ordination in naive mice using an acelerating rotarod.** *J Pharm Pharmacol* 1968, **20:** 302-304.

170. Pettibone DJ, Hess JF, Hey PJ, Jacobson MA, Leviten M, Lis EV *et al.*: **The effects of deleting the mouse neurotensin receptor NTR1 on central and peripheral responses to neurotensin.** *J Pharmacol Exp Ther* 2002, **300:** 305-313.

171. Bontekoe CJ, McIlwain KL, Nieuwenhuizen IM, Yuva-Paylor LA, Nellis A, Willemsen R *et al.*: **Knockout mouse model for Fxr2: a model for mental retardation.** *Hum Mol Genet* 2002, **11:** 487-498.

172. Hikosaka O, Nakamura K, Sakai K, Nakahara H: **Central mechanisms of motor skill learning.** *Curr Opin Neurobiol* 2002, **12:** 217-222.

173. Rustay NR, Wahlsten D, Crabbe JC: **Influence of task parameters on rotarod performance and sensitivity to ethanol in mice.** *Behav Brain Res* 2003, **141:** 237-249.

174. Holcomb LA, Gordon MN, Jantzen P, Hsiao K, Duff K, Morgan D: **Behavioral changes in transgenic mice expressing both amyloid precursor protein and presenilin-1 mutations: lack of association with amyloid deposits.** *Behav Genet* 1999, **29:** 177-185.

175. Mogil JS, Richards SP, O'Toole LA, Helms ML, Mitchell SR, Belknap JK: **Genetic sensitivity to hot-plate nociception in DBA/2J and C57BL/6J inbred mouse strains: possible sex-specific mediation by delta2-opioid receptors.** *Pain* 1997, **70:** 267-277.

176. Livak KJ, Schmittgen TD: **Analysis of relative gene expression data using real-time quantitative PCR and the 2(-Delta Delta C(T)) Method.** *Methods* 2001, **25:** 402-408.

177. Hargreaves K, Dubner R, Brown F, Flores C, Joris J: **A new and sensitive method for measuring thermal nociception in cutaneous hyperalgesia.** *Pain* 1988, **32:** 77-88.

178. Moller KA, Berge OG, Hamers FP: **Using the CatWalk method to assess weight-bearing and pain behaviour in walking rats with ankle joint monoarthritis induced by carrageenan: Effects of morphine and rofecoxib.** *J Neurosci Methods* 2008, **174:** 1-9.

179. Gabriel AF, Marcus MA, Honig WM, Walenkamp GH, Joosten EA: **The CatWalk method: a detailed analysis of behavioral changes after acute inflammatory pain in the rat.** *J Neurosci Methods* 2007, **163:** 9-16.

180. Vrinten DH, Hamers FF: **'CatWalk' automated quantitative gait analysis as a novel method to assess mechanical allodynia in the rat; a comparison with von Frey testing.** *Pain* 2003, **102:** 203-209.

181. Vrinten DH, Hamers FF: **'CatWalk' automated quantitative gait analysis as a novel method to assess mechanical allodynia in the rat; a comparison with von Frey testing.** *Pain* 2003, **102:** 203-209.

182. Franklin K.B.J, Paxinos G: **The mouse brain in stereotaxic coordinates.** *Academic Press* 1997.

183. Pilecka I, Patrignani C, Pescini R, Curchod ML, Perrin D, Xue Y *et al.*: **Protein-tyrosine Phosphatase H1 Controls Growth Hormone Receptor Signaling and Systemic Growth.** *J Biol Chem* 2007, **282:** 35405-35415.

184. Allen Institute for Brain Science. http://mouse.brain-map.org/brain/Cckar.html. 2009. Ref Type: Generic

185. Bialy L, Waldmann H: **Inhibitors of protein tyrosine phosphatases: next-generation drugs?** *Angew Chem Int Ed Engl* 2005, **44:** 3814-3839.

186. Arpin M, Algrain M, Louvard D: **Membrane-actin microfilament connections: an increasing diversity of players related to band 4.1.** *Curr Opin Cell Biol* 1994, **6:** 136-141.

187. Vollmer JY, Clerc RG: **Homeobox genes in the developing mouse brain.** *J Neurochem* 1998, **71:** 1-19.

188. Huang X, Cheng HJ, Tessier-Lavigne M, Jin Y: **MAX-1, a novel PH/MyTH4/FERM domain cytoplasmic protein implicated in netrin-mediated axon repulsion.** *Neuron* 2002, **34:** 563-576.

189. Cooper BG, Mizumori SJ: **Temporary inactivation of the retrosplenial cortex causes a transient reorganization of spatial coding in the hippocampus.** *J Neurosci* 2001, **21:** 3986-4001.

190. Miro-Bernie N, Ichinohe N, Perez-Clausell J, Rockland KS: **Zinc-rich transient vertical modules in the rat retrosplenial cortex during postnatal development.** *Neuroscience* 2006, **138:** 523-535.

191. Vann SD, Aggleton JP: **Testing the importance of the retrosplenial guidance system: effects of different sized retrosplenial cortex lesions on heading direction and spatial working memory.** *Behav Brain Res* 2004, **155:** 97-108.

192. Jinno S, Klausberger T, Marton LF, Dalezios Y, Roberts JD, Fuentealba P *et al.*: **Neuronal diversity in GABAergic long-range projections from the hippocampus.** *J Neurosci* 2007, **27:** 8790-8804.

193. Otani S, Connor JA, Levy WB: **Long-term potentiation and evidence for novel synaptic association in CA1 stratum oriens of rat hippocampus.** *Learn Mem* 1995, **2:** 101-106.

194. Gaskin S, White NM: **Cooperation and competition between the dorsal hippocampus and lateral amygdala in spatial discrimination learning.** *Hippocampus* 2006, **16:** 577-585.

195. White NM, Gaskin S: **Dorsal hippocampus function in learning and expressing a spatial discrimination.** *Learn Mem* 2006, **13:** 119-122.

196. Wolff M, Gibb SJ, Dalrymple-Alford JC: **Beyond spatial memory: the anterior thalamus and memory for the temporal order of a sequence of odor cues.** *J Neurosci* 2006, **26:** 2907-2913.

197. Komura Y, Tamura R, Uwano T, Nishijo H, Kaga K, Ono T: **Retrospective and prospective coding for predicted reward in the sensory thalamus.** *Nature* 2001, **412:** 546-549.

198. Maxwell WL, Pennington K, MacKinnon MA, Smith DH, McIntosh TK, Wilson JT *et al.*: **Differential responses in three thalamic nuclei in moderately disabled, severely disabled and vegetative patients after blunt head injury.** *Brain* 2004, **127:** 2470-2478.

199. Mitchell KJ, Johnson MK, Raye CL, Greene EJ: **Prefrontal cortex activity associated with source monitoring in a working memory task.** *J Cogn Neurosci* 2004, **16:** 921-934.

200. Warburton EC, Baird A, Morgan A, Muir JL, Aggleton JP: **The conjoint importance of the hippocampus and anterior thalamic nuclei for allocentric spatial learning: evidence from a disconnection study in the rat.** *J Neurosci* 2001, **21:** 7323-7330.

201. Van Groen T, Wyss JM: **Projections from the anterodorsal and anteroventral nucleus of the thalamus to the limbic cortex in the rat.** *J Comp Neurol* 1995, **358:** 584-604.

202. Conde F, Maire-Lepoivre E, Audinat E, Crepel F: **Afferent connections of the medial frontal cortex of the rat. II. Cortical and subcortical afferents.** *J Comp Neurol* 1995, **352:** 567-593.

203. Kunzle H: **The hippocampal continuation (indusium griseum): its connectivity in the hedgehog tenrec and its status within the hippocampal formation of higher vertebrates.** *Anatomy and Embryology* 2004, **208:** 183-213.

204. McLaughlin DF, Juliano SL: **Disruption of layer 4 development alters laminar processing in ferret somatosensory cortex.** *Cereb Cortex* 2005, **15:** 1791-1803.

205. Noctor SC, Palmer SL, McLaughlin DF, Juliano SL: **Disruption of layers 3 and 4 during development results in altered thalamocortical projections in ferret somatosensory cortex.** *J Neurosci* 2001, **21:** 3184-3195.

206. Jones EG: **The thalamic matrix and thalamocortical synchrony.** *Trends Neurosci* 2001, **24:** 595-601.

207. Thomson AM, Bannister AP: **Interlaminar connections in the neocortex.** *Cereb Cortex* 2003, **13:** 5-14.

208. McCormick DA, Thompson RF: **Neuronal responses of the rabbit cerebellum during acquisition and performance of a classically conditioned nictitating membrane-eyelid response.** *J Neurosci* 1984, **4:** 2811-2822.

209. Boyden ES, Katoh A, Raymond JL: **Cerebellum-dependent learning: the role of multiple plasticity mechanisms.** *Annu Rev Neurosci* 2004, **27:** 581-609.

210. Edmondson SR, Werther GA, Russell A, LeRoith D, Roberts CT, Jr., Beck F: **Localization of growth hormone receptor/binding protein messenger ribonucleic acid (mRNA) during rat fetal development: relationship to insulin-like growth factor-I mRNA.** *Endocrinology* 1995, **136:** 4602-4609.

211. Carro E, Nunez A, Busiguina S, Torres-Aleman I: **Circulating insulin-like growth factor I mediates effects of exercise on the brain.** *J Neurosci* 2000, **20:** 2926-2933.

212. Frago LM, Paneda C, Dickson SL, Hewson AK, Argente J, Chowen JA: **Growth hormone (GH) and GH-releasing peptide-6 increase brain insulin-like growth factor-I**

expression and activate intracellular signaling pathways involved in neuroprotection. *Endocrinology* 2002, **143:** 4113-4122.

213. Le Greves M, Le Greves P, Nyberg F: **Age-related effects of IGF-1 on the NMDA-, GH- and IGF-1-receptor mRNA transcripts in the rat hippocampus.** *Brain Res Bull* 2005, **65:** 369-374.

214. Svensson J, Diez M, Engel J, Wass C, Tivesten A, Jansson JO *et al.*: **Endocrine, liver-derived IGF-I is of importance for spatial learning and memory in old mice.** *J Endocrinol* 2006, **189:** 617-627.

215. Bondanelli M, Ambrosio MR, Margutti A, Franceschetti P, Zatelli MC, degli Uberti EC: **Activation of the somatotropic axis by testosterone in adult men: evidence for a role of hypothalamic growth hormone-releasing hormone.** *Neuroendocrinology* 2003, **77:** 380-387.

216. Veldhuis JD, Metzger DL, Martha PM, Jr., Mauras N, Kerrigan JR, Keenan B *et al.*: **Estrogen and testosterone, but not a nonaromatizable androgen, direct network integration of the hypothalamo-somatotrope (growth hormone)-insulin-like growth factor I axis in the human: evidence from pubertal pathophysiology and sex-steroid hormone replacement.** *J Clin Endocrinol Metab* 1997, **82:** 3414-3420.

217. Giustina A, Veldhuis JD: **Pathophysiology of the neuroregulation of growth hormone secretion in experimental animals and the human.** *Endocr Rev* 1998, **19:** 717-797.

218. Murphy LJ, Friesen HG: **Differential effects of estrogen and growth hormone on uterine and hepatic insulin-like growth factor I gene expression in the ovariectomized hypophysectomized rat.** *Endocrinology* 1988, **122:** 325-332.

219. Donahue CP, Kosik KS, Shors TJ: **Growth hormone is produced within the hippocampus where it responds to age, sex, and stress.** *Proc Natl Acad Sci U S A* 2006, **103:** 6031-6036.

220. Shors TJ, Chua C, Falduto J: **Sex differences and opposite effects of stress on dendritic spine density in the male versus female hippocampus.** *J Neurosci* 2001, **21:** 6292-6297.

221. Shors TJ, Falduto J, Leuner B: **The opposite effects of stress on dendritic spines in male vs. female rats are NMDA receptor-dependent.** *Eur J Neurosci* 2004, **19:** 145-150.

222. Wood GE, Beylin AV, Shors TJ: **The contribution of adrenal and reproductive hormones to the opposing effects of stress on trace conditioning in males versus females.** *Behav Neurosci* 2001, **115:** 175-187.

223. Bi S, Scott KA, Kopin AS, Moran TH: **Differential roles for cholecystokinin a receptors in energy balance in rats and mice.** *Endocrinology* 2004, **145:** 3873-3880.

224. Bi S, Chen J, Behles RR, Hyun J, Kopin AS, Moran TH: **Differential body weight and feeding responses to high-fat diets in rats and mice lacking cholecystokinin 1 receptors.** *Am J Physiol Regul Integr Comp Physiol* 2007, **293:** R55-R63.

225. Cooper SJ, Dourish CT, Clifton PG: **CCK antagonists and CCK-monoamine interactions in the control of satiety.** *Am J Clin Nutr* 1992, **55:** 291S-295S.

226. Gibbs J, Young RC, Smith GP: **Cholecystokinin decreases food intake in rats.** *J Comp Physiol Psychol* 1973, **84:** 488-495.

227. Shimokata H, Ando F, Niino N, Miyasaka K, Funakoshi A: **Cholecystokinin A receptor gene promoter polymorphism and intelligence.** *Ann Epidemiol* 2005, **15:** 196-201.

228. Nomoto S, Miyake M, Ohta M, Funakoshi A, Miyasaka K: **Impaired learning and memory in OLETF rats without cholecystokinin (CCK)-A receptor.** *Physiol Behav* 1999, **66:** 869-872.

229. Sullivan JM: **Cellular and molecular mechanisms underlying learning and memory impairments produced by cannabinoids.** *Learn Mem* 2000, **7:** 132-139.

230. Walchli S, Espanel X, Harrenga A, Rossi M, Cesareni G, Hooft van HR: **Probing protein-tyrosine phosphatase substrate specificity using a phosphotyrosine-containing phage library.** *J Biol Chem* 2004, **279:** 311-318.

231. Hooft van HR, Walchli S, Ibberson M, Harrenga A: **Protein tyrosine phosphatases as drug targets: PTP1B and beyond.** *Expert Opin Ther Targets* 2002, **6:** 637-647.

232. Eden EB, Karlsson FA, Naessen T, Gillberg P, Wide L: **Ambulatory morning growth hormone concentrations increase in men and decrease in women with age.** *Scand J Clin Lab Invest* 2002, **62:** 25-31.

233. Eden EB, Burman P, Johansson AG, Wide L, Karlsson FA: **Effects of short-term administration of growth hormone in healthy young men, women, and women taking oral contraceptives.** *J Intern Med* 2000, **247:** 570-578.

234. Ayling CM, Moreland BH, Zanelli JM, Schulster D: **Human growth hormone treatment of hypophysectomized rats increases the proportion of type-1 fibres in skeletal muscle.** *J Endocrinol* 1989, **123:** 429-435.

235. Katsumata M, Cattaneo D, White P, Burton KA, Dauncey MJ: **Growth hormone receptor gene expression in porcine skeletal and cardiac muscles is selectively regulated by postnatal undernutrition.** *J Nutr* 2000, **130:** 2482-2488.

236. Blair ER, Hoffman HE, Bishop AC: **Engineering non-natural inhibitor sensitivity in protein tyrosine phosphatase H1.** *Bioorg Med Chem* 2006, **14:** 464-471.

237. Ikuta S, Itoh F, Hinoda Y, Toyota M, Makiguchi Y, Imai K *et al.*: **Expression of cytoskeletal-associated protein tyrosine phosphatase PTPH1 mRNA in human hepatocellular carcinoma.** *J Gastroenterol* 1994, **29:** 727-732.

238. Jing M, Bohl J, Brimer N, Kinter M, Vande Pol SB: **Degradation of tyrosine phosphatase PTPN3 (PTPH1) by association with oncogenic human papillomavirus E6 proteins.** *J Virol* 2007, **81:** 2231-2239.

239. Hsu EC, Lin YC, Hung CS, Huang CJ, Lee MY, Yang SC *et al.*: **Suppression of hepatitis B viral gene expression by protein-tyrosine phosphatase PTPN3.** *J Biomed Sci* 2007, **14:** 731-744.

240. Bhattacharyya S, Dudeja PK, Tobacman JK: **Carrageenan-induced NFkappaB activation depends on distinct pathways mediated by reactive oxygen species and Hsp27 or by Bcl10.** *Biochim Biophys Acta* 2008, **1780:** 973-982.

241. Bhattacharyya S, Gill R, Chen ML, Zhang F, Linhardt RJ, Dudeja PK *et al.*: **Toll-like receptor 4 mediates induction of the Bcl10-NFkappaB-interleukin-8 inflammatory pathway by carrageenan in human intestinal epithelial cells.** *J Biol Chem* 2008, **283:** 10550-10558.

242. Posadas I, Bucci M, Roviezzo F, Rossi A, Parente L, Sautebin L *et al*.: **Carrageenan-induced mouse paw oedema is biphasic, age-weight dependent and displays differential nitric oxide cyclooxygenase-2 expression.** *Br J Pharmacol* 2004, **142:** 331-338.

243. Bucci M, Roviezzo F, Posadas I, Yu J, Parente L, Sessa WC *et al*.: **Endothelial nitric oxide synthase activation is critical for vascular leakage during acute inflammation in vivo.** *Proc Natl Acad Sci U S A* 2005, **102:** 904-908.

244. Rocha AC, Fernandes ES, Quintao NL, Campos MM, Calixto JB: **Relevance of tumour necrosis factor-alpha for the inflammatory and nociceptive responses evoked by carrageenan in the mouse paw.** *Br J Pharmacol* 2006, **148:** 688-695.

245. Moss ML, Jin SL, Milla ME, Bickett DM, Burkhart W, Carter HL *et al*.: **Cloning of a disintegrin metalloproteinase that processes precursor tumour-necrosis factor-alpha.** *Nature* 1997, **385:** 733-736.

246. Rio C, Buxbaum JD, Peschon JJ, Corfas G: **Tumor necrosis factor-alpha-converting enzyme is required for cleavage of erbB4/HER4.** *J Biol Chem* 2000, **275:** 10379-10387.

247. Borrell-Pages M, Rojo F, Albanell J, Baselga J, Arribas J: **TACE is required for the activation of the EGFR by TGF-alpha in tumors.** *EMBO J* 2003, **22:** 1114-1124.

248. Sunnarborg SW, Hinkle CL, Stevenson M, Russell WE, Raska CS, Peschon JJ *et al*.: **Tumor necrosis factor-alpha converting enzyme (TACE) regulates epidermal growth factor receptor ligand availability.** *J Biol Chem* 2002, **277:** 12838-12845.

249. Loram LC, Fuller A, Fick LG, Cartmell T, Poole S, Mitchell D: **Cytokine profiles during carrageenan-induced inflammatory hyperalgesia in rat muscle and hind paw.** *J Pain* 2007, **8:** 127-136.

250. Nantel F, Denis D, Gordon R, Northey A, Cirino M, Metters KM *et al*.: **Distribution and regulation of cyclooxygenase-2 in carrageenan-induced inflammation.** *Br J Pharmacol* 1999, **128:** 853-859.

251. Beloeil H, Asehnoune K, Moine P, Benhamou D, Mazoit JX: **Bupivacaine's action on the carrageenan-induced inflammatory response in mice: cytokine production by leukocytes after ex-vivo stimulation.** *Anesth Analg* 2005, **100:** 1081-1086.

252. Monconduit L, Bourgeais L, Bernard JF, Le BD, Villanueva L: **Ventromedial thalamic neurons convey nociceptive signals from the whole body surface to the dorsolateral neocortex.** *J Neurosci* 1999, **19:** 9063-9072.

253. Monconduit L, Villanueva L: **The lateral ventromedial thalamic nucleus spreads nociceptive signals from the whole body surface to layer I of the frontal cortex.** *Eur J Neurosci* 2005, **21:** 3395-3402.

254. Price DD: **Central neural mechanisms that interrelate sensory and affective dimensions of pain.** *Mol Interv* 2002, **2:** 392-403, 339.

255. Patrignani C, Magnone MC, Tavano P, Ardizzone M, Muzio V, Greco B *et al*.: **Knockout mice reveal a role for protein tyrosine phosphatase H1 in cognition.** *Behav Brain Funct* 2008, **4:** 36.

256. Salojin KV, Owusu IB, Millerchip KA, Potter M, Platt KA, Oravecz T: **Essential role of MAPK phosphatase-1 in the negative control of innate immune responses.** *J Immunol* 2006, **176:** 1899-1907.

257. Takeuchi O, Akira S: **[Roles of Toll-like receptor in host defense and the mechanism of its signal transduction].** *Nippon Saikingaku Zasshi* 2004, **59:** 523-529.

258. Grutz G: **New insights into the molecular mechanism of interleukin-10-mediated immunosuppression.** *J Leukoc Biol* 2005, **77:** 3-15.

259. Martin T, Cardarelli PM, Parry GC, Felts KA, Cobb RR: **Cytokine induction of monocyte chemoattractant protein-1 gene expression in human endothelial cells depends on the cooperative action of NF-kappa B and AP-1.** *Eur J Immunol* 1997, **27:** 1091-1097.

260. Park SK, Yang WS, Han NJ, Lee SK, Ahn H, Lee IK *et al.*: **Dexamethasone regulates AP-1 to repress TNF-alpha induced MCP-1 production in human glomerular endothelial cells.** *Nephrol Dial Transplant* 2004, **19:** 312-319.

261. Kirkegaard T, Naresh A, Sabine VS, Tovey SM, Edwards J, Dunne B *et al.*: **Expression of tumor necrosis factor alpha converting enzyme in endocrine cancers.** *Am J Clin Pathol* 2008, **129:** 735-743.

262. Holmlund U, Cebers G, Dahlfors AR, Sandstedt B, Bremme K, Ekstrom ES *et al.*: **Expression and regulation of the pattern recognition receptors Toll-like receptor-2 and Toll-like receptor-4 in the human placenta.** *Immunology* 2002, **107:** 145-151.

263. Haziot A, Ferrero E, Kontgen F, Hijiya N, Yamamoto S, Silver J *et al.*: **Resistance to endotoxin shock and reduced dissemination of gram-negative bacteria in CD14-deficient mice.** *Immunity* 1996, **4:** 407-414.